480
10/17/79

DR. 229

DOE/JPL/954607-4

DEVELOPMENT AND TESTING OF SHINGLE-TYPE SOLAR CELL MODULES

Final Report

By
N. F. Shepard

February 28, 1979

Work Performed Under Contract No. NAS-7-100-954607

General Electric Company
Valley Forge Space Center
Philadelphia, Pennsylvania

U.S. Department of Energy

Solar Energy

DISCLAIMER

NOTICE

DOE/JPL/954607-4
Distribution Category UC-63b

FINAL REPORT

DEVELOPMENT AND TESTING OF SHINGLE-TYPE SOLAR CELL MODULES

JPL CONTRACT NO. 954607

PREPARED BY: N. F. SHEPARD

REPORT DATE: FEBRUARY 28, 1979

The JPL Low-Cost Solar Array Project is sponsored by the U.S. Department of Energy and forms part of the Solar Photovoltaic Conversion Program to initiate a major effort toward the development of low-cost solar arrays. This work was performed for the Jet Propulsion Laboratory, California Institute of Technology by Agreement between NASA and DOE.

GENERAL ELECTRIC
SPACE DIVISION
Valley Forge Space Center
P. O. Box 8555 • Philadelphia, Penna. 19101

ACKNOWLEDGEMENT

The author wishes to gratefully acknowledge the contributions of Messrs. W. C. Yager and T. S. Chan in the preparation of this document. Mr. Yager developed the analytical model for the zero depth concentrator which is reported in Appendix A and Mr. Chan was responsible for writing the FORTRAN coding for the model.

ABSTRACT

The design, development, fabrication and testing of a shingle-type terrestrial solar cell module which produces 98 watts/m^2 of exposed module area at 1 kW/m^2 insolation and 61^{o}C are reported. These modules make it possible to easily incorporate photovoltaic power generation into the sloping roofs of residential or commercial buildings by simply nailing the modules to the plywood roof sheathing.

This design consists of nineteen series-connected 53 mm diameter solar cells arranged in a closely packed hexagon configuration. These cells are individually bonded to the embossed surface of a 3 mm thick thermally tempered hexagon-shaped piece of ASG SUNADEX glass. Monsanto SAFLEX polyvinyl butyral is used as the laminating adhesive. RTVII functions as the encapsulant between the underside of the glass superstrate and a rear protective sheet of 0.8 mm thick TEXTOLITE. The semi-flexible portion of each shingle module is a composite laminate construction consisting of outer layers of B. F. Goodrich FLEXSEAL and an epichlorohydrin closed cell foam core.

The module design has satisfactorily survived the JPL - defined qualification testing program which includes 50 thermal cycles between -40 and +90^{o}C, a seven day temperature - humidity exposure test and a mechanical integrity test consisting of a bidirectional cyclic loading at 2390 Pa (50 lb/ft^2) which is intended to simulate loads due to a 45 m/s (100 mph) wind.

TABLE OF CONTENTS

LIST OF ILLUSTRATIONS

LIST OF TABLES

SECTION 1
SUMMARY

The shingle-type solar cell module shown in Figure 1-1 has been designed and developed during the one year period covered by this final report. A total of 50 modules have been fabricated for delivery to JPL. Six of these have been subjected to an environmental testing program consisting of 50 thermal cycles between -40 to +90°C, a one week temperature-humidity exposure, and a 100 cycle bidirectional mechanical integrity test to simulate snow and wind loading at 2390 Pa (50 lb/ft^2). This module design sandwiches the interconnected solar cells between a sheet of tempered SUNADEX glass on the front surface and a sheet of fiberglass/epoxy on the rear side. The 19 series-connected solar cells are bonded to the embossed surface of this glass with polyvinyl butyral (PVB) film and the space between the covers is filled with RTVII which functions as the primary encapsulant. The semi-flexible portion of each module is a laminate constructed of B. F. Goodrich FLEXSEAL outer skins and an epichlorohydrin closed cell foam core. A two-sided printed wiring board, which is sandwiched within this laminate, provides the connection between the ends of the solar cell circuit string and the four output terminals of the module. These terminals overlap, negative on positive, and are interconnected with a machine screw/flat washer to produce the shingle installation shown in Figure 1-2.

An average module electrical performance of 5.79 watts was measured at 100 mW/cm^2 insolation and at 28°C using JPL-supplied Terrestrial Secondary Standard No. 025 as the reference. This represents an overall module efficiency of 11.4 percent based on the exposed module area. If this performance is reflected to the calculated Nominal Operating Cell Temperature (NOCT) of 61°C, the resulting module output yields an areal specific power output of 98 watts/m^2 of exposed module area at 100 mW/cm^2 insolation and at the NOCT.

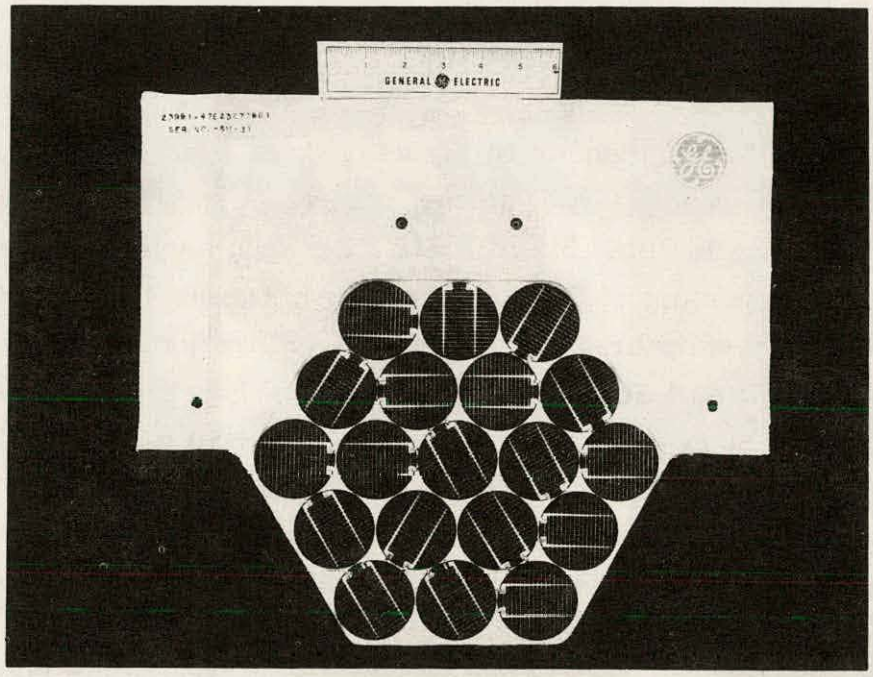

(a) Front (Photo No. VF 78-278A)

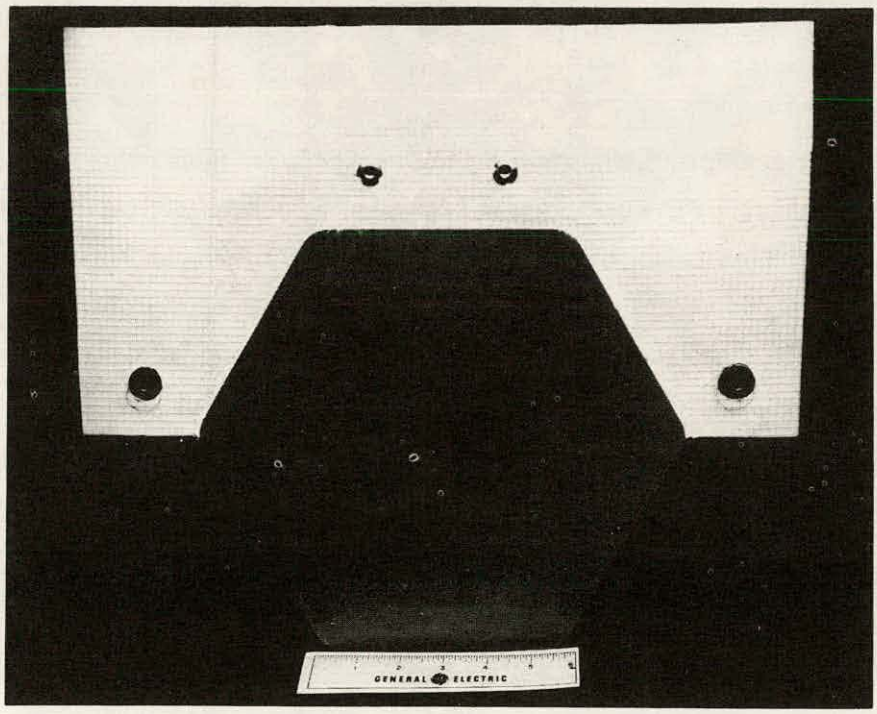

(b) Back (VF Photo No. 77-557A)
Figure 1-1. Photographs of Shingle Solar Cell Module

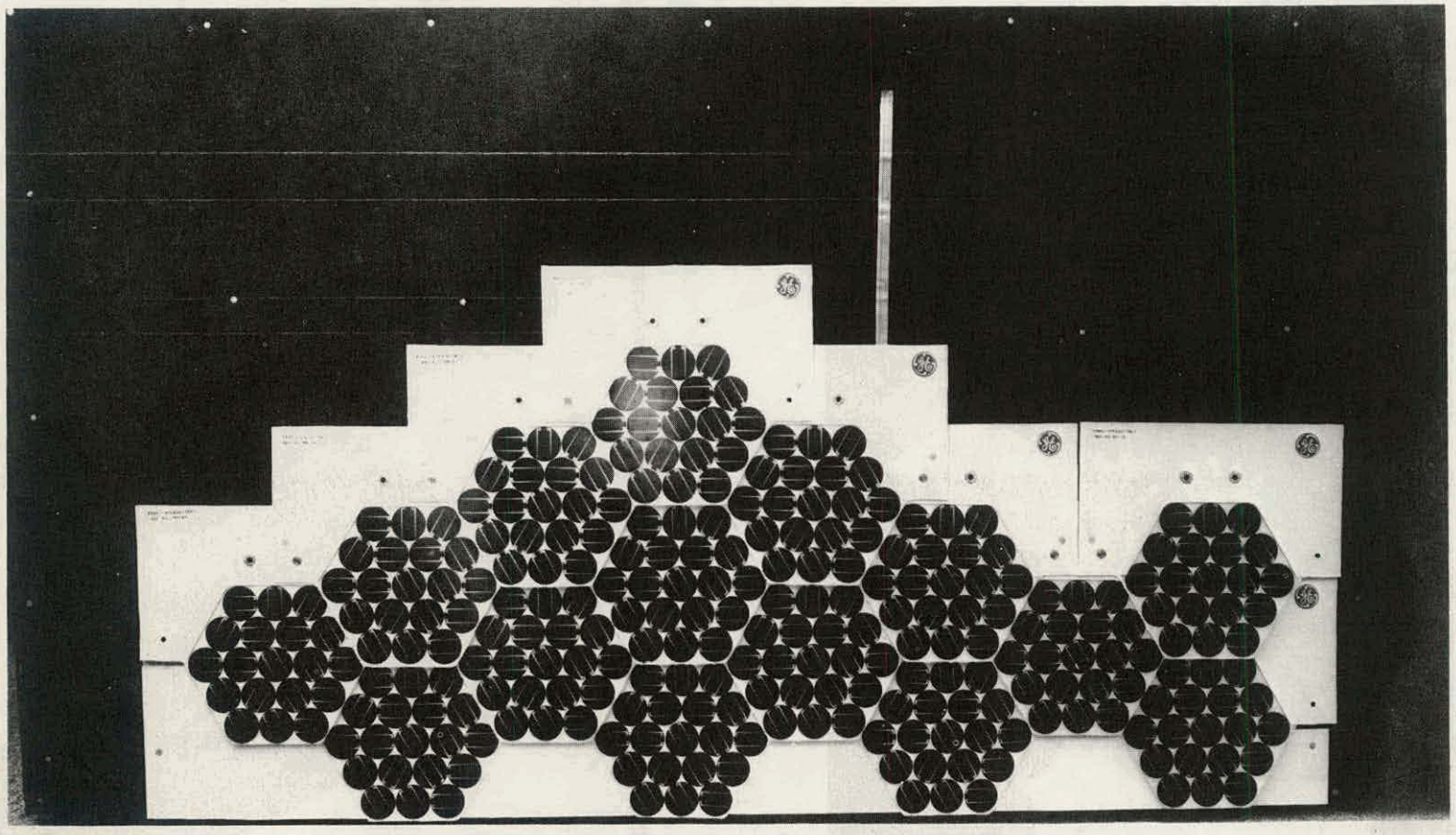

Figure 1-2. Arrangement of Modules on Simulated Roof Structure
(Photo No. VF 78-237B)

SECTION 2
INTRODUCTION

The general scope of work under this contract involves the design, development, fabrication and testing of a solar cell module which is suitable for use in place of shingles on the sloping roofs of residential or commercial buildings. Modules of this type employ a semi-flexible substrate which is suitable for mounting on an independent rigid surface such as plywood roof sheathing. As specified in the contract statement of work, these modules shall be capable of producing an electrical power output of 80 W/m^2 of installed module area at a module temperature of 60^oC with an insolation of 1 kW/m^2. The installed weight of these shingle-type modules shall not exceed 250 kg/kW of peak power output. As a design goal these modules shall be designed for a service life of at least 15 years. An implicit requirement is that the shingle not sustain damage during the normal handling associated with installation on a roof. The vulnerability to the localized bearing loads associated with walking or kneeling on the installed shingles does not constitute a design requirement but will be assessed as part of this development effort. The program is organized into seven major tasks as given below.

Task No.	Description
1	Substrate Evaluation and Testing
2	Solar Cell Tray Evaluation and Testing
3	Module Interconnection and Testing
4	Shingle Module Design
5	Fabrication and Acceptance Testing of Modules
6	Qualification Testing of Modules
7	Analytical Model of a Zero Depth Solar Photovoltaic Concentrator

During the initial phases of the program, the activities on Tasks 1, 2 and 3 involved the investigation of a variety of shingle module implementation approaches.

Considerable effort was expended in an attempt to develop an approach which used methyl methacrylate (MMA) as the sole solar cell encapsulant. This proved to be

impractical because the relatively high modulus MMA could not elastically accommodate the strains at the specified low temperature extreme of -40°C. Attempts to buffer the solar cells with a transparent silicone conformal coating prior to embedding within MMA also proved to be unsuccessful.

This activity, as well as the evaluation of various module-to-module interconnection concepts, has been reported in the first two quarterly reports published under this contract. These results will not be repeated here, but rather the emphasis of this final report will be on the design, fabrication, and testing of the tempered glass covered shingle module.

Task 7 was added after the completion of the initial contract effort. The results of this additional task activity, which involved the development of an analytical model of a zero depth solar photovoltaic concentrator, are reported in Appendix A to this document.

Fifty shingle solar cell modules were delivered to JPL on May 19, 1978. Forty of these modules were mounted on a simulated roof structure and have been undergoing outdoor exposure testing at the JPL Field Test Site since October 17, 1978.

SECTION 3
TECHNICAL DISCUSSION

3.1 DESCRIPTION OF SELECTED DESIGN

3.1.1 GENERAL DESCRIPTION

The selected design for the shingle solar cell module is represented by the assembly drawing shown in Figure 3-1. This module consists of two basic functional parts: an exposed rigid portion which contains the solar cell assembly, and a flexible portion which is overlapped by the higher courses of the roof installation. The design of the shingle module provides a closely-packed array of 19 series-connected solar cells. A minimum separation of 0.5 mm (0.020 inch) is maintained between adjacent cells by assembly tooling which positions the cells prior to bonding to the glass coverplate. The position of the four output terminals of the module has been established to permit the connection of the negative terminals of one course on the roof directly to the positive terminals of the course below. The method of connection, which uses a machine screw and flat washer, is discussed in Section 3.1.6.

As shown in Sections C-C and D-D of Figure 3-1, the top substrate FLEXSEAL skin overlaps, and is bonded to, the glass coverplate to form a weather-tight joint around the upper three sides of the hexagon. The bottom skin and printed wiring board are sandwiched between the glass coverplate and the bottom fiberglass/epoxy cover to produce a similar seal around these three edges on the bottom. The exposed edges of the glass coverplate are sealed with a bead of RTV102 which is applied between the coverplate and the bottom fiberglass/epoxy cover as shown in Section F-F.

The key features of this shingle module design are summarized in Table 3-1. The calculated module output of 4.95 watts at the Standard Operating Conditions (SOC) which include a calculated NOCT of 61°C, yields an areal specific output of 98 watts/m^2 of exposed module area. This is 23 percent better than the minimum requirement of the contract. The specific weight of the module is 202 kg/kW of peak power output at SOC as compared to a maximum specified value of 250 kg/kW.

Table 3-1. Key Features of Shingle Module Design

Parameter	Value
Total Solar Cell Area	419.2 cm^2
Exposed Module Area	507.0 cm^2
Packing Factor	0.827
Electrical Power Output at the Maximum Power Point	
At 1 kW/m^2 and 28°C	5.79 Watts*
At Standard Operating Conditions	4.95 Watts
Module Weight	1.00 kg*

* Average of 50 modules delivered

3.1.2 SUBSTRATE CONFIGURATION

The semi-flexible substrate portion of the shingle is of laminar construction as shown in Figure 3-2. The two outer-skins of this substrate are FLEXSEAL polyester scrim reinforced HYPALON. This material is white in color and provides the weather-resistance properties required to meet the 15 year service life goals. A center core of closed cell epichlorohydrin foam (Rubatex No. R-473-E) provides a low-density, high-temperature resistant filler material to achieve a nearly uniform thickness of the entire surface area of the shingle. The substrate also affords protection to the flexible printed wiring board which is sandwiched between the bottom skin and the core. This double sided printed wiring board, which carries both the positive and negative terminations for the module, is made from material identified by GE designation FLGF 0.006 C 2/2 which consists of 2 oz/ft^2 copper foil on both sides of a 0.006 inch thick fiberglass/epoxy substrate. This copper is etched away to form the bus strip patterns. The calculated series resistance of this copper bus network is the 4.6 m Ω at 20°C, which represents a negligible power loss.

The entire composite substrate is bonded together with the B.F. Goodrich adhesive system described in Table 3-2. This contact adhesive and associated primers are traditionally used as part of the FLEXSEAL roofing system. Two different primers have been specified depending upon the nature of the surface to be bonded. In either case the

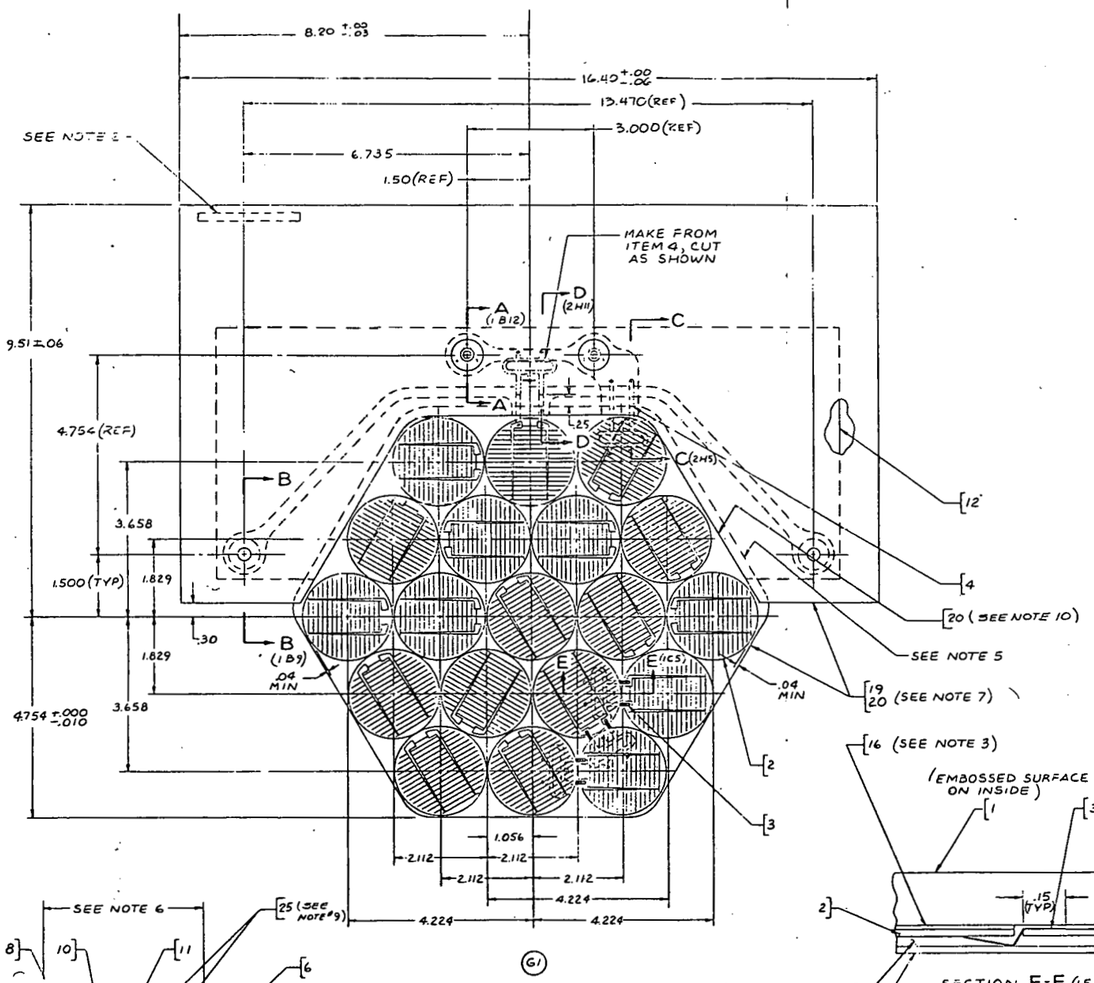

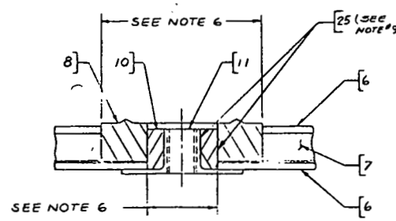

SECTION A-A (1H9)
TYPICAL BOTH POSITIVE TERMINALS
SCALE: 5/1

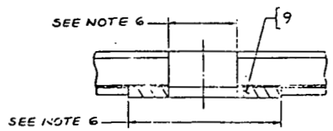

SECTION B-B (1F11)
TYPICAL BOTH NEGATIVE TERMINALS
SCALE: 5/1

SECTION E-E (1F8)
TYPICAL INTERCONNECTION BETWEEN SOLAR CELLS (17 PLACES)
SCALE: 5/1

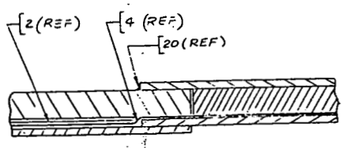

SECTION C-C (1G8)
TYPICAL BOTH POSITIVE FEEDTHROUGH
SCALE: 5/1

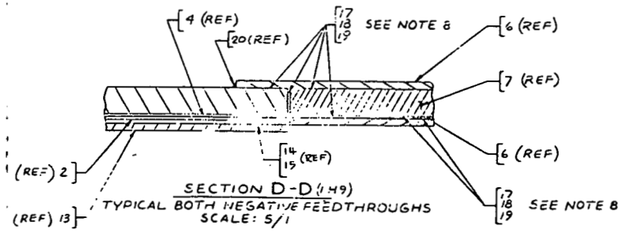

SECTION D-D (1H9)
TYPICAL BOTH NEGATIVE FEEDTHROUGHS
SCALE: 5/1

NOTES:

1. INTERPRETATION OF DRAWING TERMS AND TOLERANCES PER S 3C009.
2. MARK PART "2399I-47E232779G_" AS APPLICABLE PER 11BA1526 CL 21E.
3. HEAT SEAL SOLAR CELLS (ITEM 2) TO EMBOSSED SURFACE OF GLASS COVERPLATE (ITEM 1) USING ITEM 16. THE ENTIRE CELL SURFACE MUST BE BONDED TO THE GLASS. ITEM 16 SHALL NOT PROJECT MORE THAN .010 RADIUS BEYOND THE CELL CIRCUMFERENCE.
4. FILL VOID BETWEEN ITEMS 1 AND 13 WITH ITEM 14. PRIME SURFACES OF ITEMS 1,2,6 AND 13 WITH ITEM 15. AFTER CURING, TRIM ITEM 14 AROUND EDGES OF GLASS COVERPLATE.
5. CUT ITEM 7 TO MATCH GLASS COVERPLATE (ITEM 1) AT FINAL ASSEMBLY.
6. CUT HOLES IN ITEM 6 TO MATCH CORRESPONDING DIAMETERS OF ITEMS 8 AND 9.
7. FOLLOWING FINAL TRIMMING OF OVERALL DIMENSIONS, COAT EXTERIOR EDGES OF SUBSTRATE AND GLASS COVERPLATE WITH ITEMS 19 AND 20. (REFER TO PIR 1R30-588 FOR BONDING INSTRUCTIONS).
8. BOND ITEMS 1 TO 6, 12 TO 1, 6 TO 7, 7 TO 1, 21 TO 23, 22 TO 24 12 TO 6, AND 12 TO 7 USING ITEM 19. PRIME SURFACES OF ITEMS 1 & 12 WITH ITEM 17 AND SURFACE OF ITEMS 6, 7, 21, 22, 23 AND 24 WITH ITEM 18. (REFER TO PIR 1R30-588 FOR BONDING INSTRUCTIONS).
9. BOND ITEMS 8 TO 10, AND 10 TO 11 USING ITEM 25.
10. RUN A FILLET OF ITEM 20 ALONG THE INTERFACE BETWEEN ITEMS 1 AND 6.

Figure 3-1. Assembly Drawing of Shingle Solar Cell Module

primer is applied in a very thin coating and allowed to dry thoroughly prior to the application of the contact adhesive to both surfaces to be joined. The edge sealer (A1436-B) is applied to the outer edges of the substrate to seal the exposed foam core material.

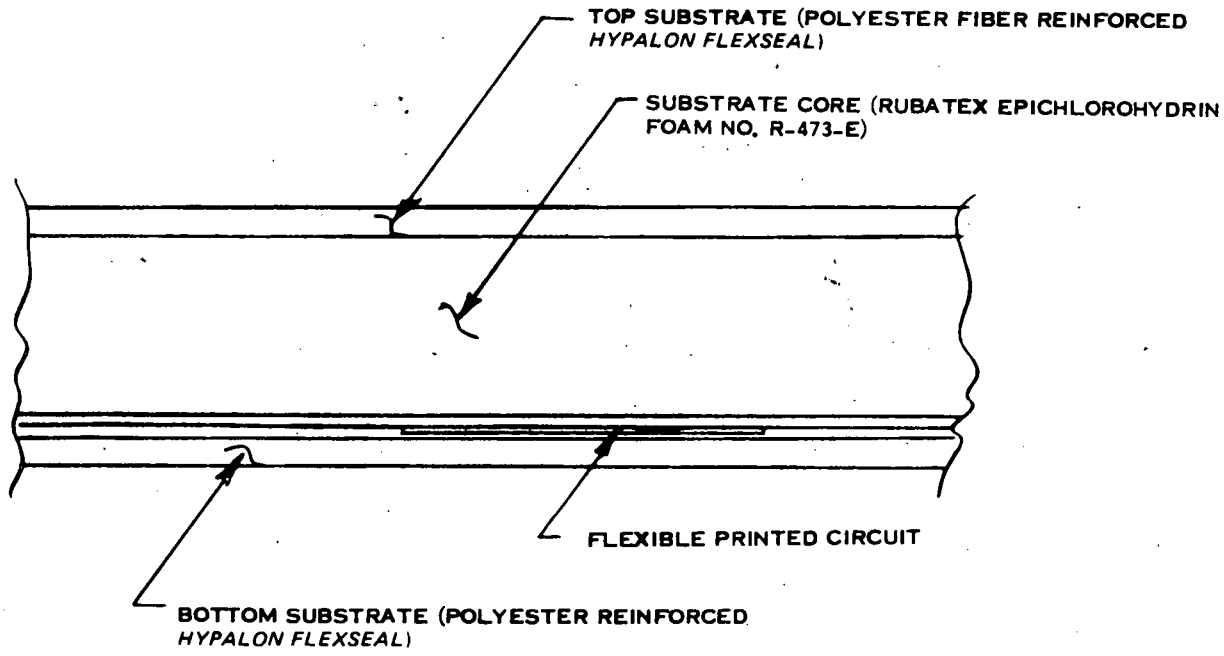

Figure 3-2. Section Through Shingle Module Substrate

Table 3-2. Substrate Adhesive System

Identification No. *	Description/Application
A 1104-B	Primer for Non-porous Surfaces
A 178-B	Primer for Porous Surfaces
CA-1056	Contact Adhesive (all surfaces)
A 1436-B	Edge Sealer

* B. F. Goodrich Co.
General Products Division
Solon, Ohio 44139

A load-deflection test was performed on a segment of the substrate consisting of a top and bottom skin of polyester scrim reinforced FLEXSEAL bonded to a cord of epichlorohydrin foam. The resulting load-deflection curve with a 14.3 mm (0.563 inch) diameter bearing surface is as given in Figure 3-3. The use of these data in the determination of module-to-module interconnection joint contact force will be discussed later.

3.1.3 SOLAR CELL SELECTION

A Spectrolab solar cell was selected for use in this module design on the basic of the lowest specific cost of the delivered power output. The distribution of the electrical output of the cells received from Spectrolab is given in Table 3-3. As measured by Spectrolab these cells have an average electrical output of 569 mA at 0.475 volts when measured at 1 kW/m^2 insolation and 28°C. A random sample of 66 cells from this group yielded an average performance of 595 mA at 0.475 volts under these same test conditions when measured by GE using the Large Area Pulse Solar Simulator (LAPSS) with JPL - supplied Terrestrial Secondary Standard No. 025 as the reference.

Scanning electron micrographs of the front and rear contacts of these cells are shown in Figures 3-4 and 3-5, respectively. These micrographs clearly reveal the nature of the printed contact surface.

3.1.4 SOLAR CELL INTERCONNECTOR

The solar cell interconnector shown in Figure 3-6 is fabricated from nominal 50 μm (0.002 inch) thick soft copper foil (Alloy No. 110) which is subsequently solder plated to a thickness of 13 to 18 μm (0.0005 to 0.0007 inch) on both surfaces. The resistance of this interconnector measured between the two "N" joints and the three "P" joints is 1.67 mΩ at 25°C. At 60°C this series resistance loss amounts to 0.3 percent of the cell maximum power output. Figure 3-7 shows a typical "N" contact solder-joint which was made by reflowing the solder plating on the interconnector with a hand soldering iron.

3.1.5 MODULE ENCAPUSLATION

The details of the encapsulation surrounding the solar cell assembly are shown in Figure 3-8. The solar cells are individually bonded to the underside of the glass coverplate with disks of Monsanto SAFLEX SR-10 PVB film. This glass coverplate is fabricated from 3 mm thick ASG SUNADEX low-iron glass (0.01% iron-oxide content) which is cut to the hexagon shape and then thermally tempered to provide the flexual strength required to

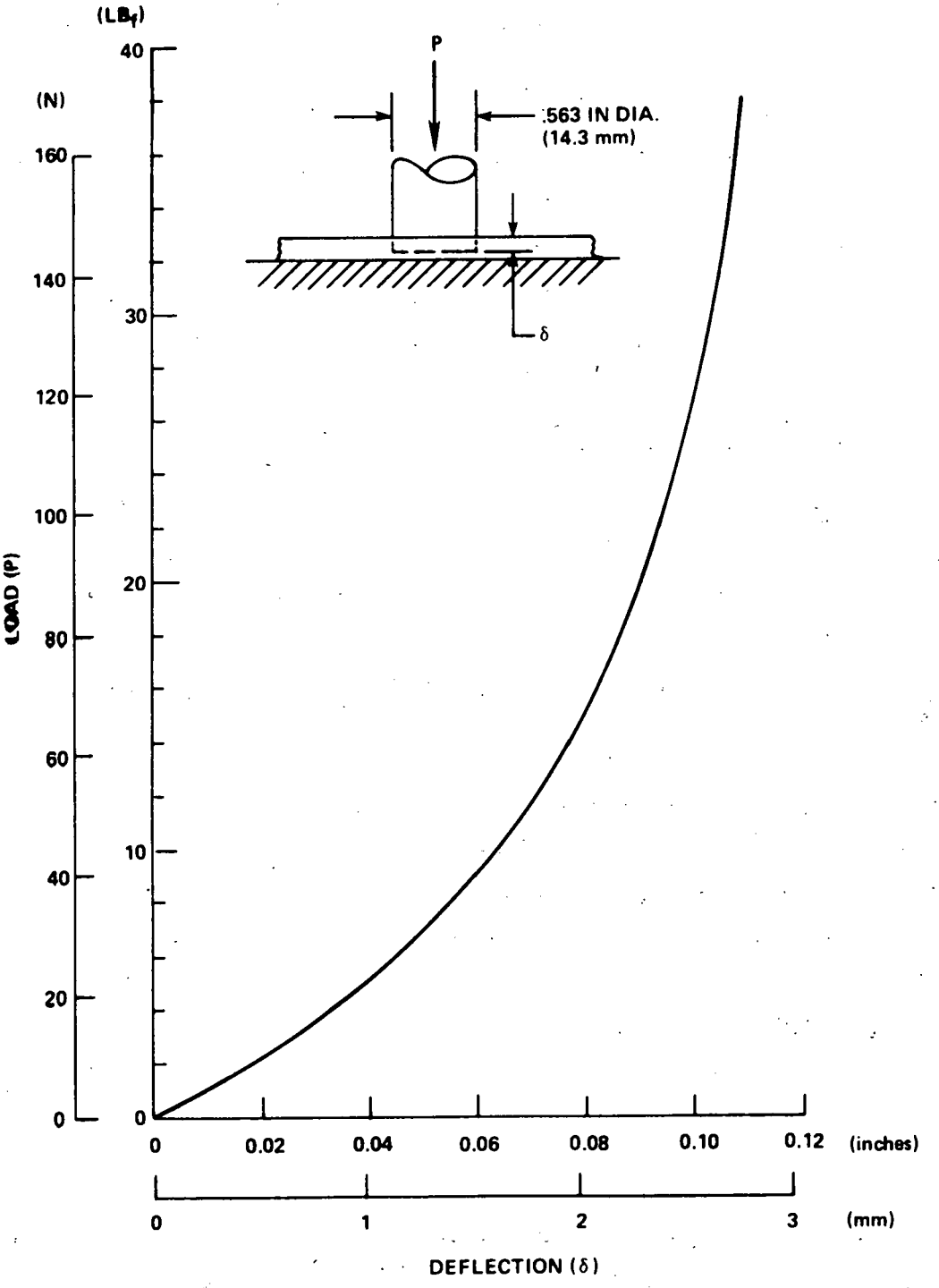

Figure 3-3. Local Bearing Load-Deflection Curve for Substrate

Table 3-3. Electrical Performance of Production Solar Cells as Measured by Spectrolab

Range of Output Current Group (mA at 0.475 V)	Quantity of Solar Cells In Group
510 - 519	69
520 - 529	95
530 - 539	108
540 - 549	115
550 - 559	120
560 - 569	127
570 - 579	164
580 - 589	147
590 - 599	146
600 - 609	97
610 - 619	72
620 - 629	27
630 - 639	13

sustain the bearing loads associated with walking or kneeling. The transmission of this glass is compared with that of ASG LO-IRON (0.05% iron-oxide content) in Figure 3-9. These data do not indicate a clear transmittance advantage associated with the use of the SUNADEX glass, but this selection was made because of the embossed surface texture of this glass and its influence on the enhanced output of the module as discussed in Section 3.4.

The primary encapsulation around the solar cells is provided by RTV 11, which is a white pourable conformal coating. This dimethyl silicone compound fills the space surrounding the solar cells and interconnectors and bonds the front glass coverplate to the rear protective sheet of fiberglass/epoxy. This rear sheet is required to prevent damage to the module from sharp objects such as nails which are everpresent during the installation of a shingle roof. The adhesion of the RTV 11 to both the glass coverplate and the rear TEXTOLITE sheet is increased by the use of GE primer number SS-4044 followed by a thin coating of RTV 108 (10 to 20 percent by weight mixed with heptane).

3.1.6 MODULE-TO-MODULE INTERCONNECTION

The module-to-module interconnection is accomplished as shown in Figure 3-10. This basic concept relies on the development of high contact pressure under three conical projections, which are part of solder plated copper bosses within each mating shingle, to achieve a low-resistance, environmental stable connection.

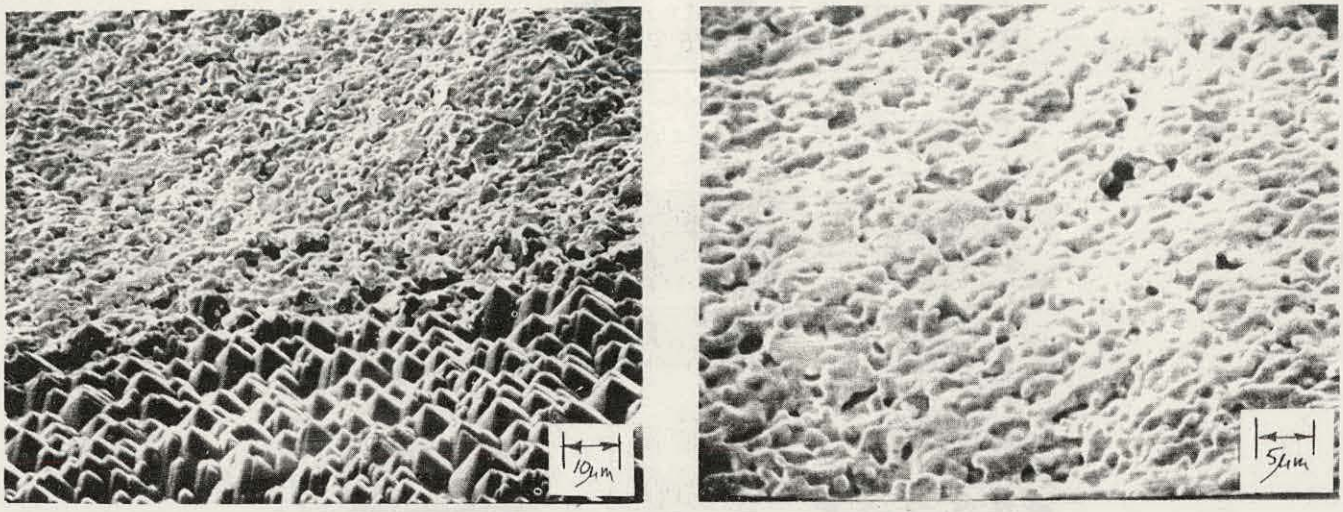

(a) Front Contact Interface With Active Area

(b) Front Contact

Figure 3-4. Scanning Electron Micrographs of Solar Cell Front Contact

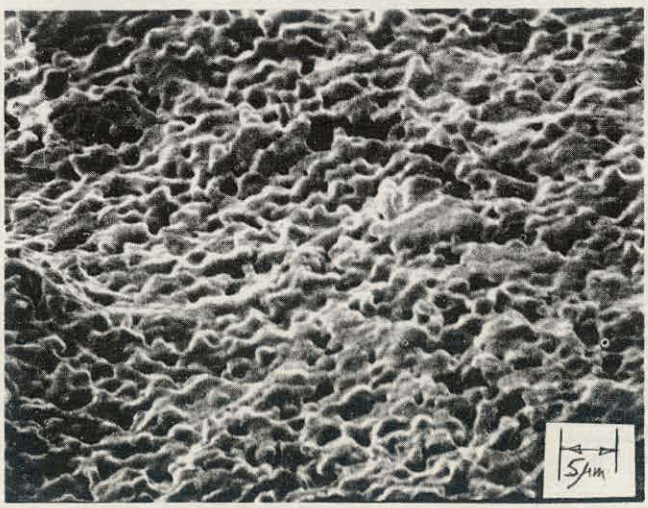

Figure 3-5. Scanning Electron Micrograph of Solar Cell Back Contact

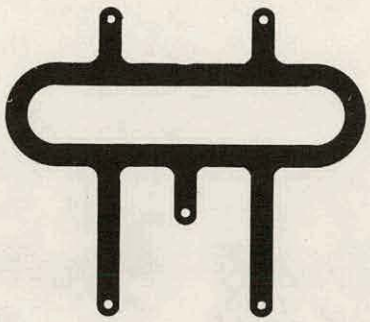

Figure 3-6. Solar Cell Interconnector

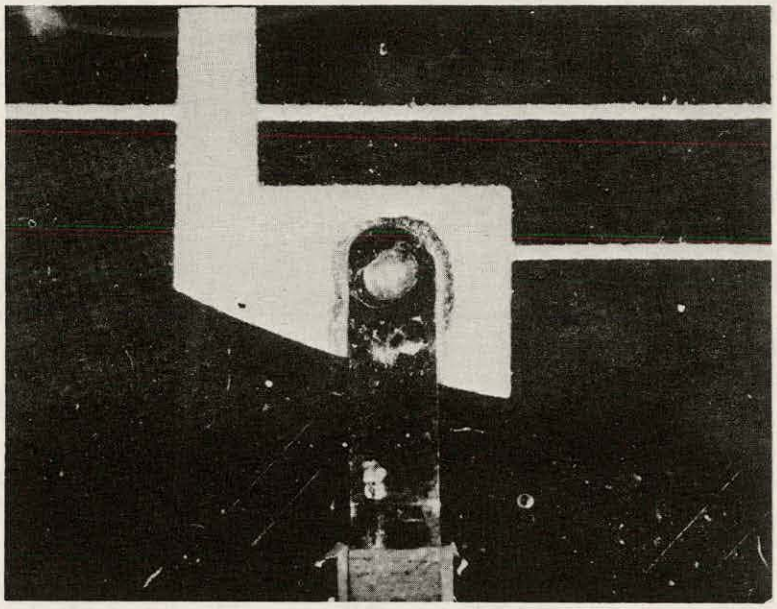

Figure 3-7. Typical "N" Contact Solder Joint

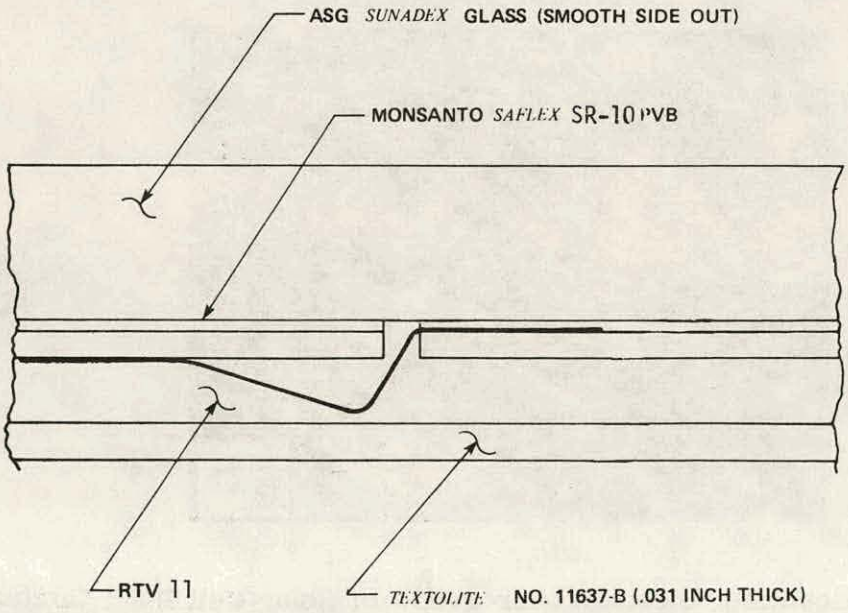

Figure 3-8. Module Encapsulation

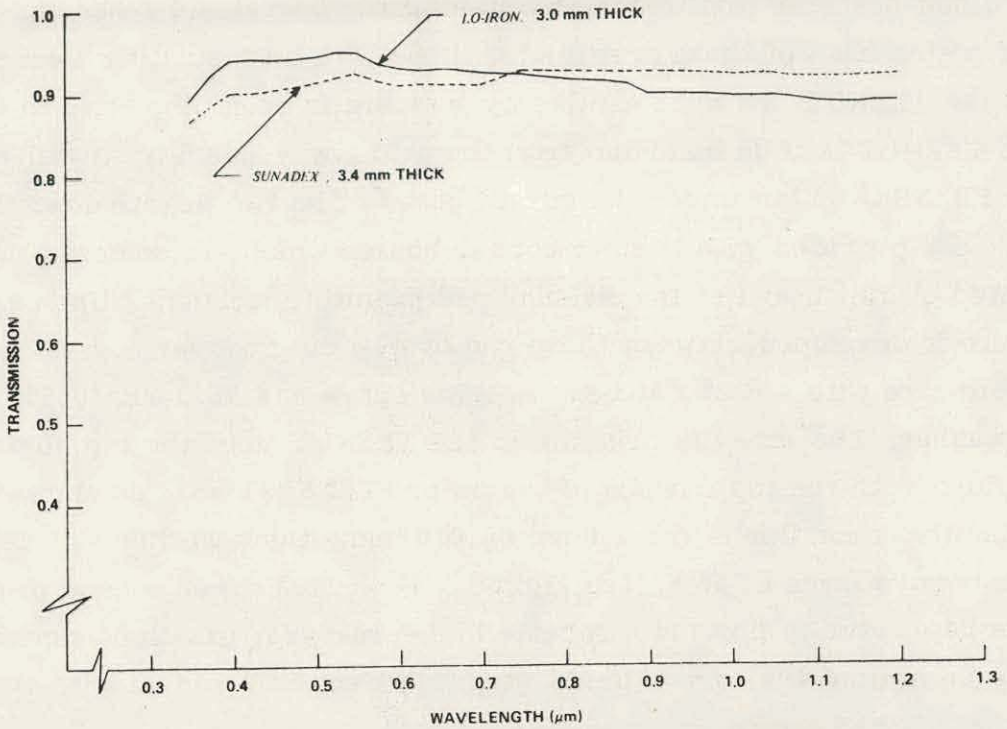

Figure 3-9. Transmission of ASG Low-Iron Soda-Lime Glasses Without Anti-Reflection Coating

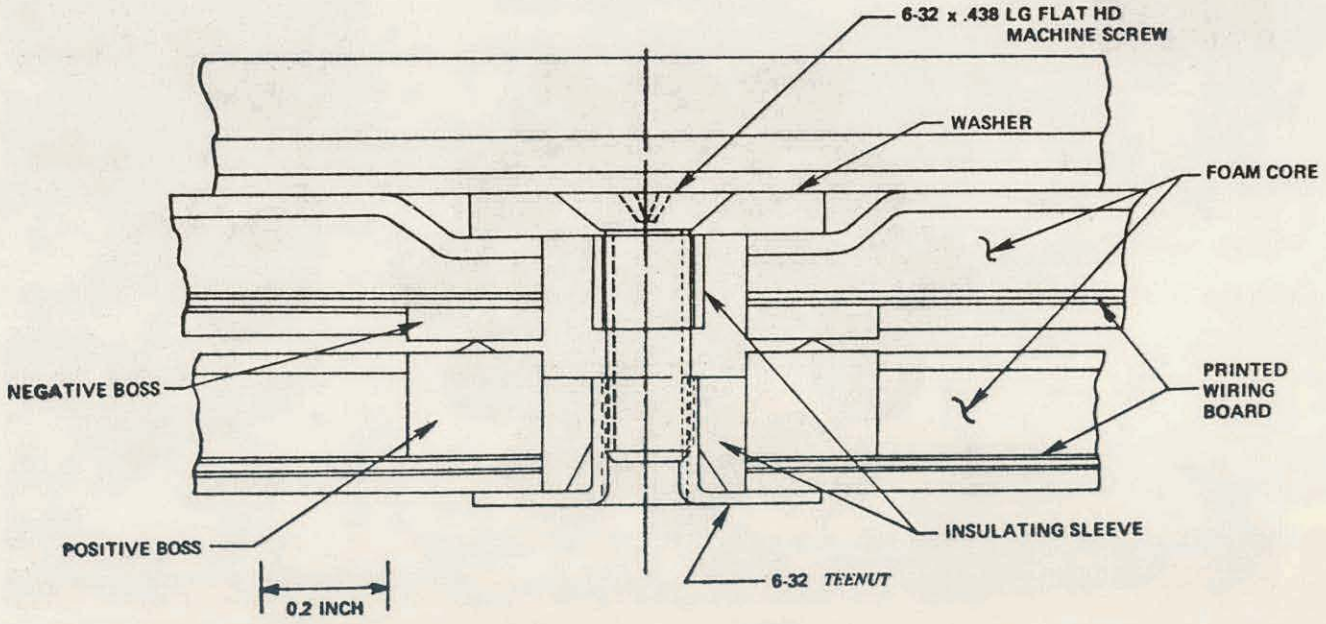

Figure 3-10. Module-to-Module Interconnection

The two positive terminals of each shingle are provided with these copper bosses which are soldered to the circular pads on the top of the printed circuit board. A 6-32 TENNUT, which has been modified by shortening the barrel and removing the prongs, is centered within each of these positive terminals with an insulating sleeve. Both this sleeve and the TEENUT are made captive by bonding to each other and to the copper boss. The TEENUT is thus insulated from the positive terminal by the sleeve and by the bottom FLEXSEAL skin under the circuit board. The two negative terminals of each module are provided with thinner copper bosses which are soldered to the bottom of the printed circuit board at the circular pad mounting locations. Upon assembly, contact pressure is developed between these two overlapping copper bosses by compressing the substrate core with a 6-32 flat head machine screw and 16.5 mm (0.650 inch) diameter flat washer. The screw is driven into the TEENUT until the top surface of the washer is flush with the top surface of the outer FLEXSEAL skin as shown in Figure 3-11. Under these conditions the 1.8 mm (0.070 inch) thick washer will have developed a total compressive force of 52 N (see Figure 3-4) or 17.3 N per conical projection. This is adequate force to provide a reliable high-pressure, gas-tight contact. The insulating sleeve around the screw thread prevents electrical contact with the negative

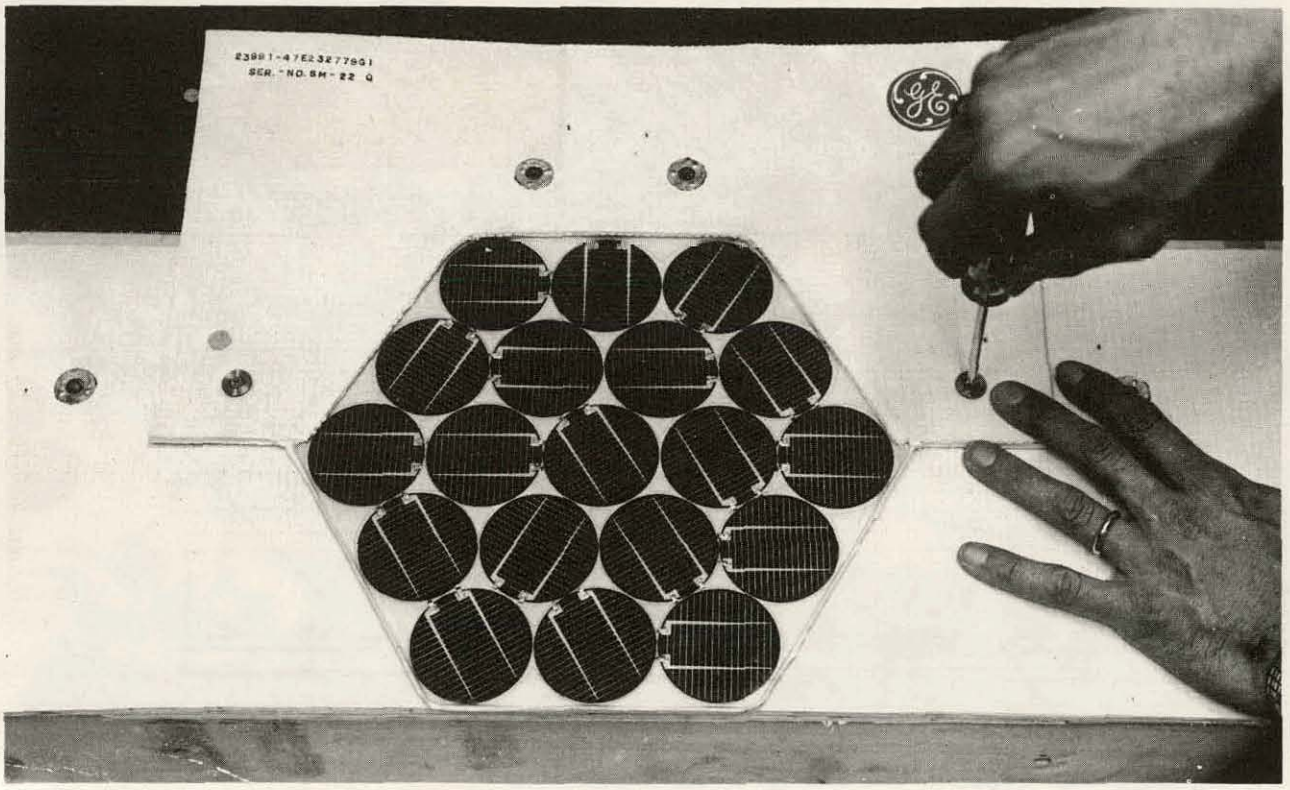

Figure 3-11. Installation of Module-to-Module Interconnector

terminal of the module so that the exposed screw head/washer/TEENUT are electrically neutral after installation. This interconnector design concept is also capable of accommodating up to 1.8 mm (0.07 inch) of misregistration between the centerlines of overlapping terminal bosses.

3.2 SYSTEM INSTALLATION CONSIDERATIONS

The shingle modules described above are installed by overlapping in the manner shown in Figures 3-12 and 3-13. The four electrical terminals of each module are interconnected as previously described using a flat-head machine screw and washer to apply the contact force. The shingles are attached to the roof sheathing by nailing through the substrate at two places per shingle with ordinary roofing nails as shown in Figure 3-14. The module-to-module interconnectors between overlapping layers form a series/parallel matrix of interconnected modules, as shown in Figure 3-15, with the current increasing as modules are added in the parallel direction across the length of the roof from gable-to-gable and voltage increasing as modules are added in the series direction along the slant height of the roof from eave-to-ridge. At both the positive and negative terminations of each solar cell circuit it is necessary to attach conductors to carry the current

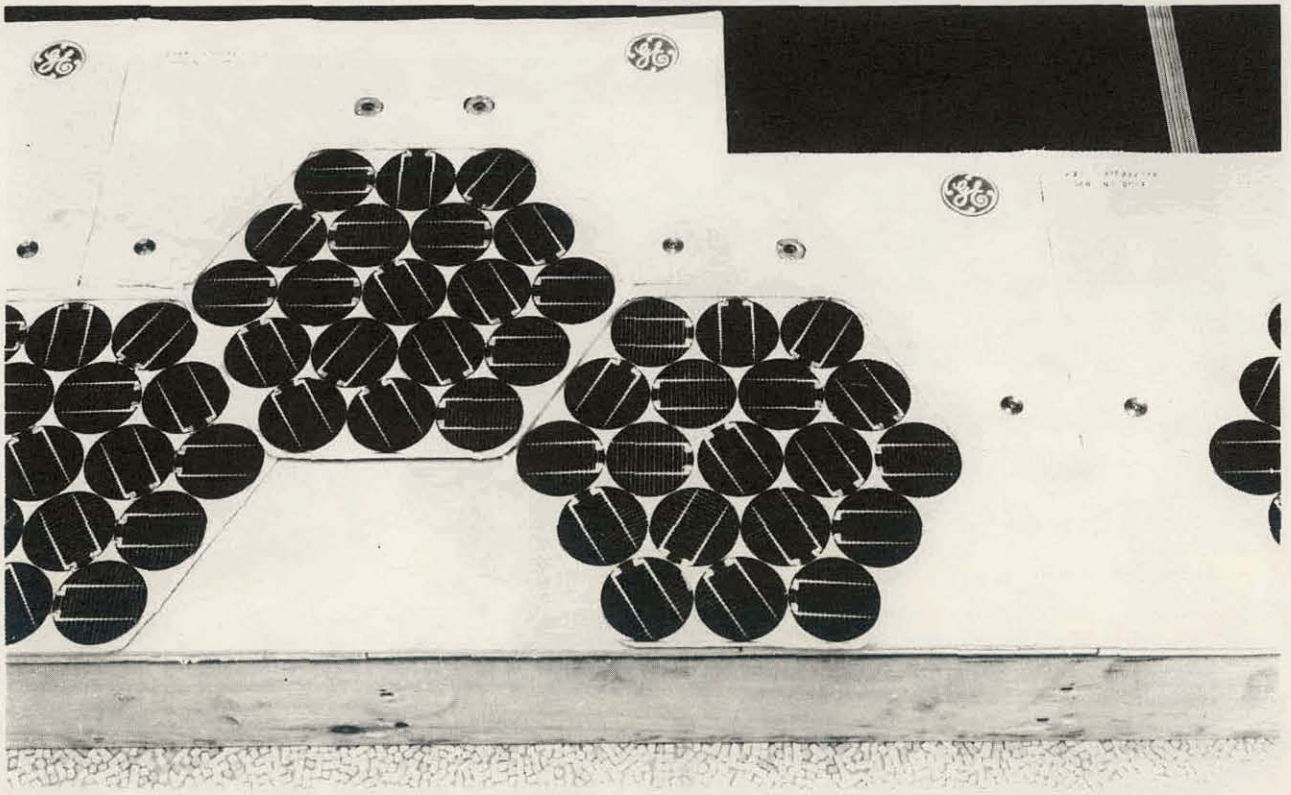

Figure 3-12. Typical Overlap Between Courses

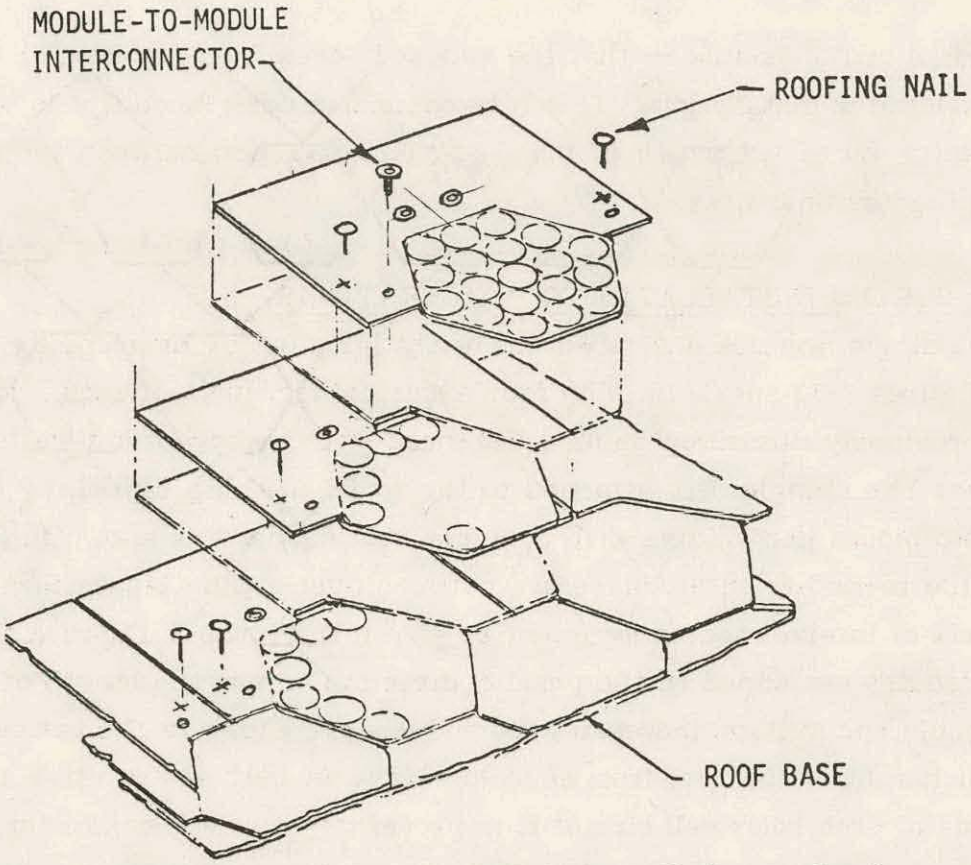

Figure 3-13. Exploded View of Shingle Module Installation on Roof

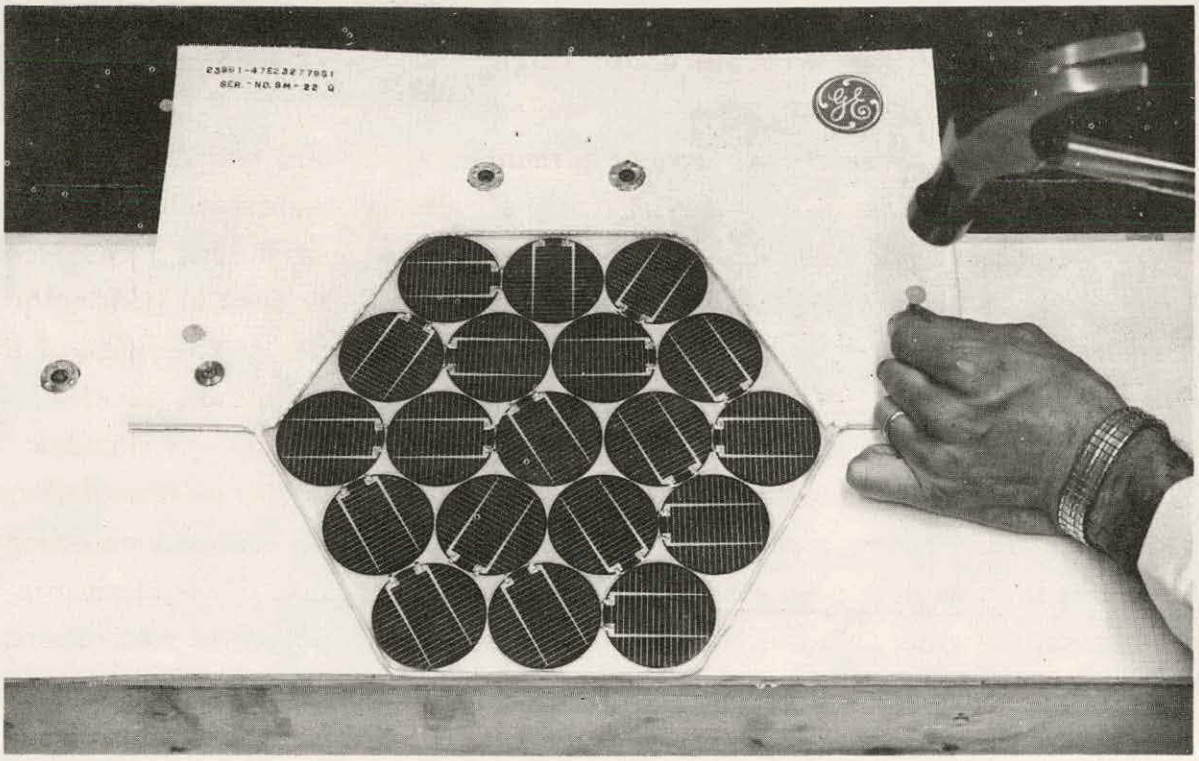

Figure 3-14. Nailing of Shingle Module to Roof Sheathing

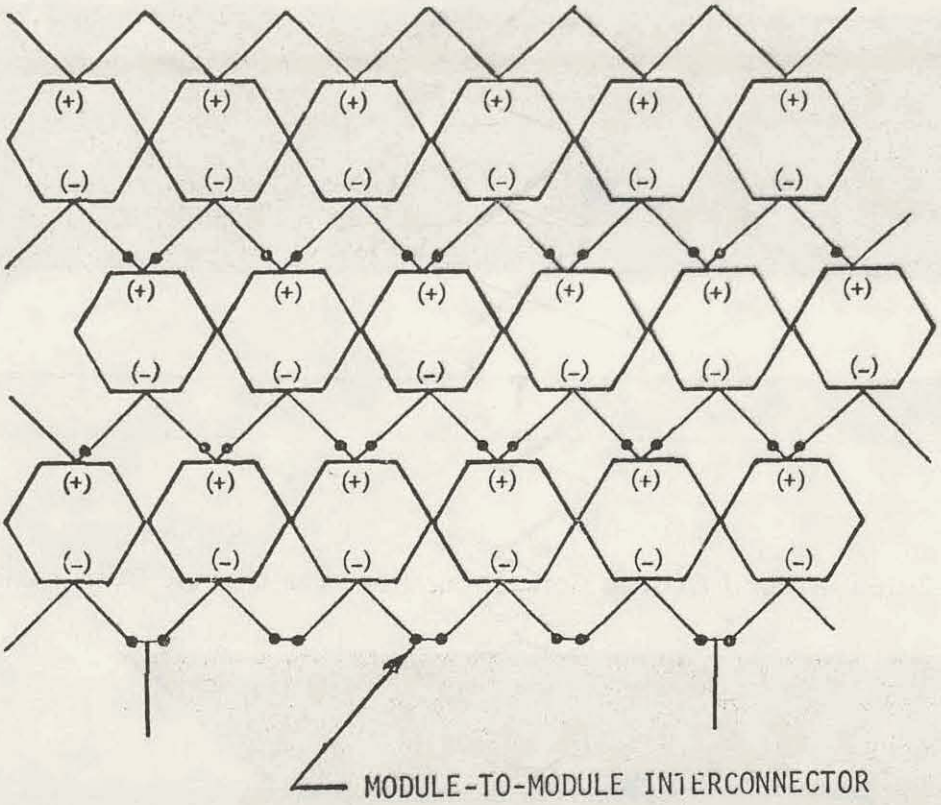

Figure 3-15. Electrical Schematic of Module-to-Module Interconnection

to the central collection point which is at the ridge of the roof. A negative circuit termination which is typical of that required at the eave of the roof is shown in Figure 3-16. The connection between the negative terminals of adjacent modules in the first active course of the roof is made by underlaying a special shingle which contains a built-in printed circuit board to make this jumper connection. At every fifth parallel-connected module a tap is made from this common negative bus by soldering a flat-conductor cable to this special shingle and running this cable under the shingles to the ridge of the roof as shown in Figure 3-17. In this way it is possible to limit the current density in the common negative bus which is the negative conductor within the shingle modules, and control the series resistance losses for the overall installation. Similar terminations are required at the ridge of the roof and at electrically common bus connections which may be required at intermediate points along the slant height because of requirements to provide a specified voltage within the physical constraints imposed by roof dimensions. In this latter case modules with opposite polarity for the output terminals are used to built-up voltage in the opposite sense as the roof is advanced toward the ridge.

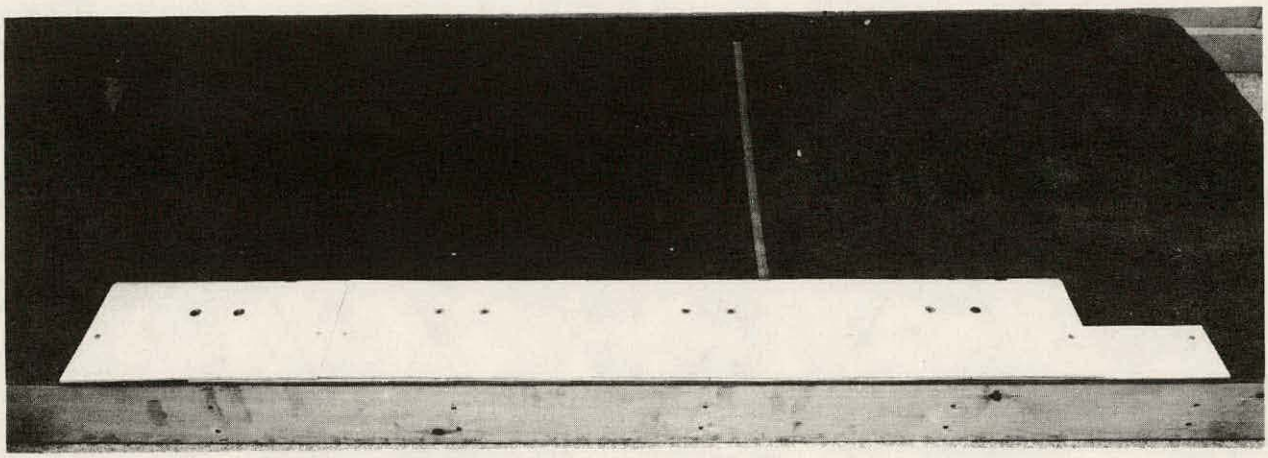

Figure 3-16. Second Course Containing Negative Circuit Termination

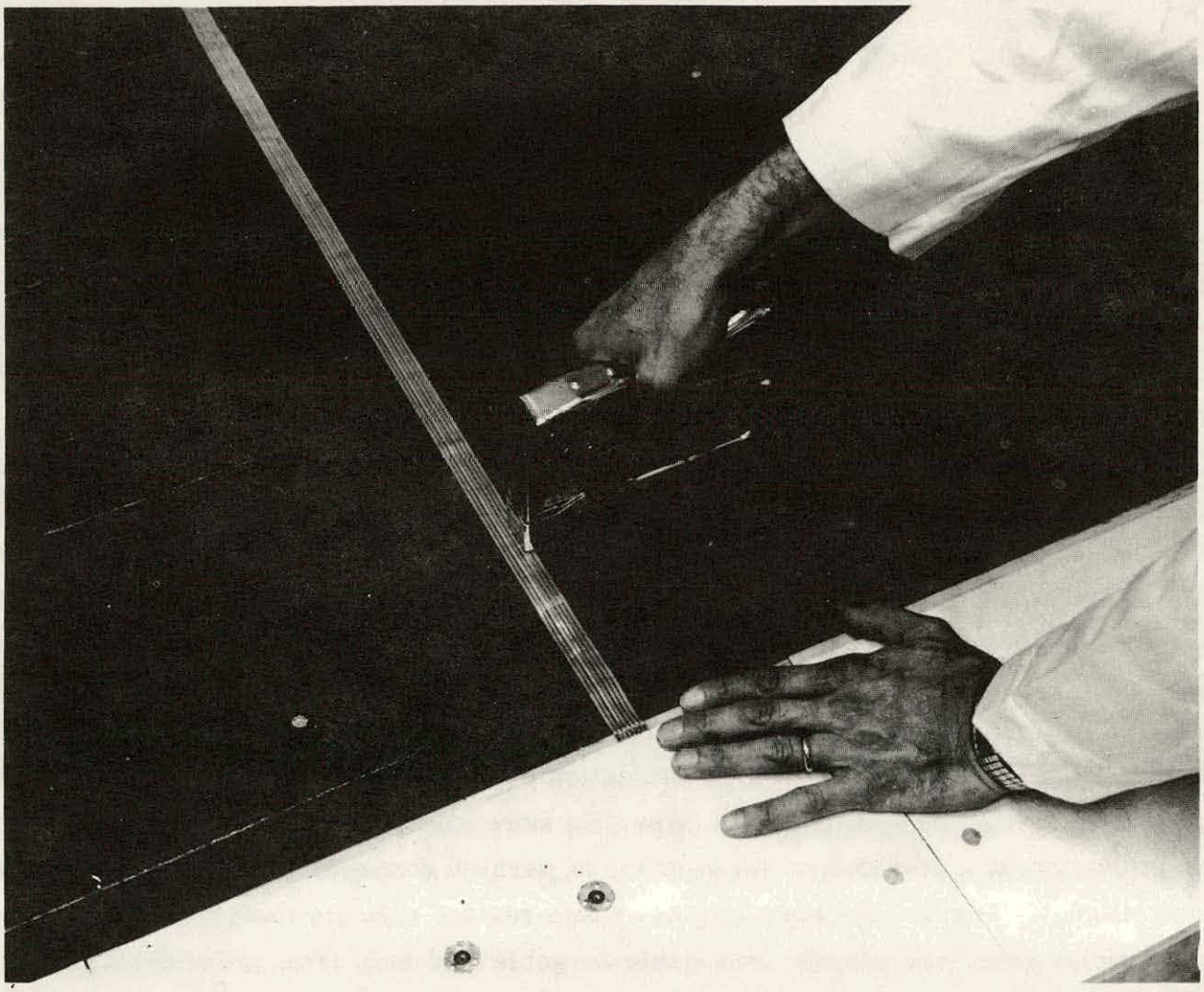

Figure 3-17. Installation of Flat Conductor Cable

The determination of the size for the rectangular roof surface area required for an installation of these shingle modules is based on the general arrangement given in Figure 3-18. Using this nomenclature, W is the required length of the roof measured from gable-to-gable and S is the slant height measured from eave-to-ridge. The values of these dimensions are given by:

$$W = E\ (3\ Np + 1/2)$$

and

$$S = E\ (N_S + 1)\ \cos 30^\circ + T,$$

where:

E = edge dimension of hexagon (mm)

= 139.7 mm

Np = number of parallel-connected modules across the length of the roof

N_S = number of series-connected modules along the slant height at the roof

T = space at ridge required to bus together top terminals (mm)

= 63.5 mm

The cross hatched area on Figure 3-18 represents wasted space which detracts from the overall packing efficiency of the installation. For a typical installation of 1872 modules which are arranged as three circuits, each with 26 series connected modules and 24 parallel-connected modules, the dimension W is 10.128 m. The slant height of the roof (S) is 9.621 m since there are three circuits in this direction which yields a value of N_S = 78 for the installation. Thus, the required roof area of 97.44 m^2 for this typical installation results in an overall area utilization of 0.805, which is defined as the ratio of solar cell area to rectangular roof area. In more general terms Figure 3-19 gives this area utilization as a function of the number of parallel connected modules and the total solar cell area. For smaller installations, these results indicate the importance of using roof sections which are narrow from gable-to-gable and long from eave-to-ridge.

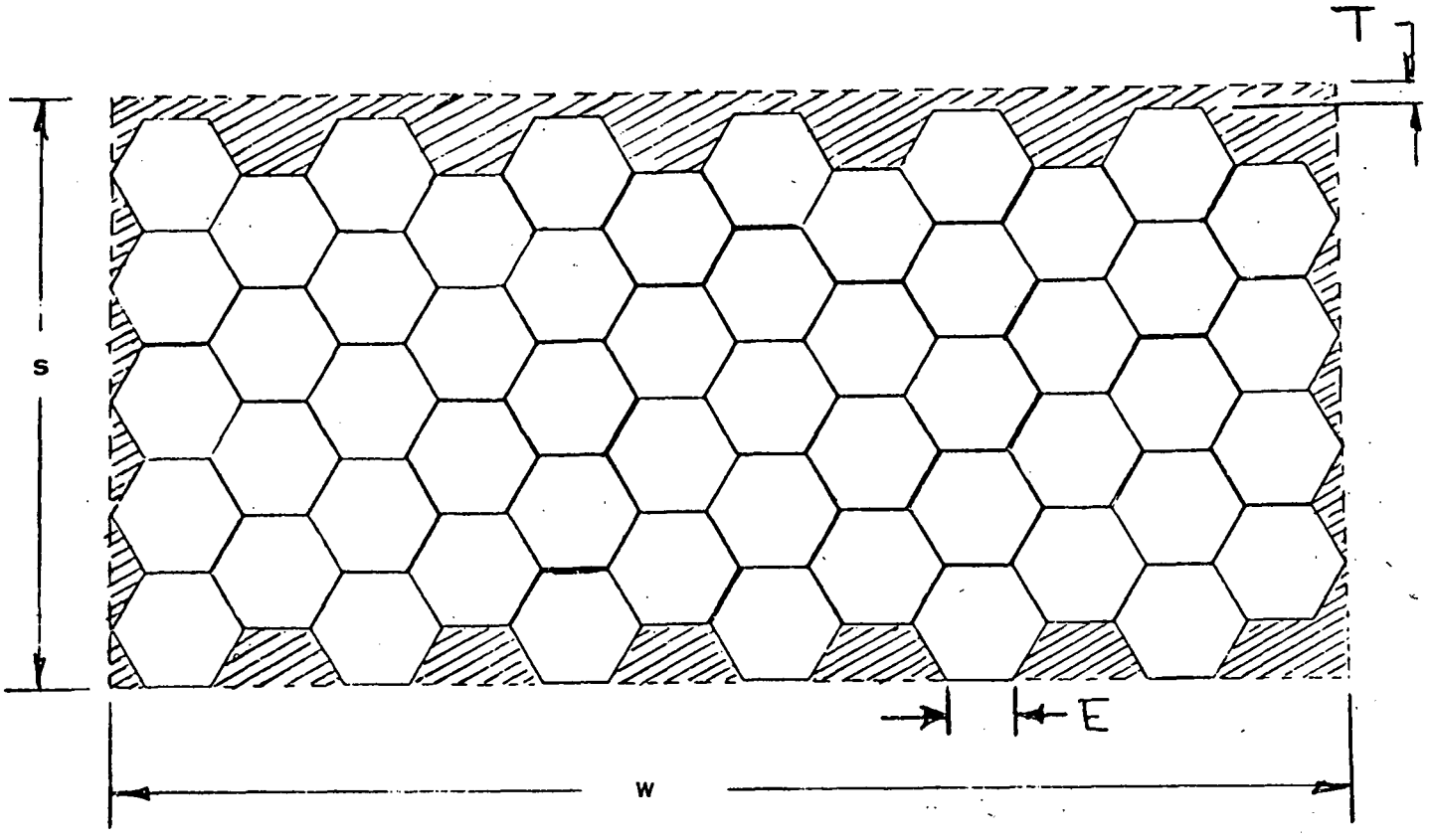

Figure 3-18. Arrangement of Shingle Modules on a Rectangular Roof

3.3 MODULE FABRICATION

3.3.1 INTRODUCTION

The module assembly was begun on February 28, 1978 with the bonding of the 19 cells for module Serial No. SM-1 and completed by May 5, 1978 with the encapsulation of Serial No. SM-59. During this time several changes in design and process control had been instituted to improve the performance and producibility of the shingle modules. Table 3-4 summarizes, by serial number, the significant differences of this type which are latent within each module. The serial numbers which contain an "A" have been subjected to an autoclave processing step as described in Section 3.3.3. As a consequence these modules, which have an unstable solution of air within the PVB, are subject to the appearance of bubbles as a result of slight elevations in temperature. Such a condition did occur on a few of these modules, notably on serial number SM-10AQ when subjected to the thermal cycling test. As reported in Section 3.5.1, a change in maximum power output of only 2 percent resulted from the appearance of these bubbles. The serial numbers which contain a "Q" have been subjected to the qualification testing program as reported in Section 3.5.

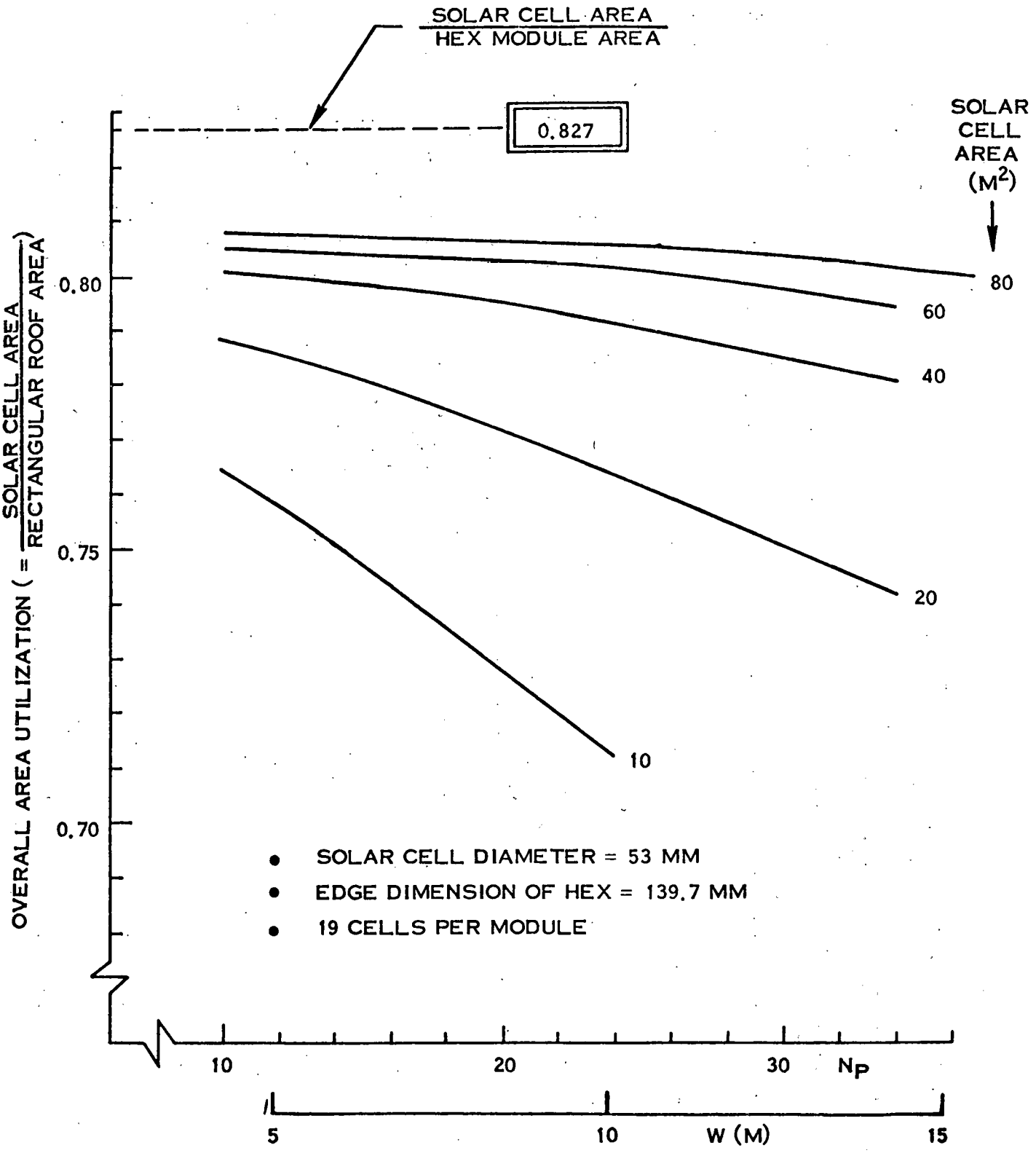

Figure 3-19. Area Utilization for Shingle Modules Mounted on a Rectangular Roof

Table 3-4. Summary of Module Fabrication Differences

Module Serial Number	SAFLEX Type	Autoclave Cycle	Primer on Rear Surface Of Glass	Rework To Replace Broken Cells
SM-1Q	PT-10	No	RTV108	No
-2Q		No	RTV108	No
-3		No	RTV108	Yes (1)
-4Q		No	RTV108	No
-5A		Yes	SS4044 + RTV108	Yes (3)
-6Q		No	RTV108	No
-7Q		No	RTV108	
-10AQ		Yes	RTV108	
-12A		Yes	RTV108	
-13A	PT-10	Yes	SS4044 + RTV108	
-17A	SR-10	Yes	SS4044 + RTV108	
-18		No	RTV108	
-19		No	RTV108	
-20A		Yes	SS4044 + RTV108	
-21		No	RTV108	
-22Q			SS4044 + RTV108	
-23				No
-24				Yes (1)
-26				Yes (3)
-27				No
-28				
-29				
-30				
-31				
-32				No
-34				No
-35				No
-36				Yes (1)
-37				No
-38				No
-39				No
-41				Yes (1)
-42				Yes (1)
-43				No
-44				
-45				
-46				
-47				
-48				No
-49				Yes (1)
-50				No
-51				
-52				
-53				
-54				
-55				
-56				
-57				
-58				
-59	SR-10	No	SS4044 + RTV108	No

A change in SAFLEX type from PT-10 to SR-10 was made with serial number SM-17A. The reasons for this change are discussed in Section 3.3.3. The use of a two step priming system on the rear side of the glass coverplate was instituted as indicated in the table to enhance the adhesion of the RTV11 pottant. A rework procedure to replace cracked solar cells which resulted from the PVB bonding operation was performed on ten of the modules as indicated in parentheses. With the exception of serial number SM-3 all of these replacement cells were bonded to the glass coverplate with RTV655. In the former case the replacement cell was laminated to the glass coverplate with SAFLEX SR-10 using a vacuum bag to apply pressure while locally heating the cell by passing a forward current of approximately 25 amperes through the cell. This rework method proved to be unsatisfactory due to the nonuniform temperature distribution over the surface of the cell with hot spots at the "N" contact solder joints.

3.3.2 SOLAR CELL SOLDERING

Soldering of the interconnector to the solar cell "N" contacts is the first step in the assembly sequence. The solder-plated copper interconnector is performed with the strain relief loop prior to this step. Figure 3-20 shows the "N" contact soldering operation with the solar cell and interconnector held in the correct relative position in a soldering fixture. During process development, joints were made at several soldering iron temperatures in order to determine the effect of this parameter on the resulting contact pull strength. Table 3-5 summarizes the results of these measurements for a 45 degree pull angle between the cell and the interconnector strip. A soldering iron temperature of 310°C (590°F) was found to give satisfactory results. In all cases joint failure occurred by a separation of the cell metalization from the silicon wafer.

Following "N" contact soldering the cells are cleaned untrasonically to remove traces of flux.

Soldering of the "P" contact at three places per cell occurs following bonding of the 19-cell array to the glass coverplate. No positioning fixture is required for this operation since the cells are securely bonded to the glass with the PVB film.

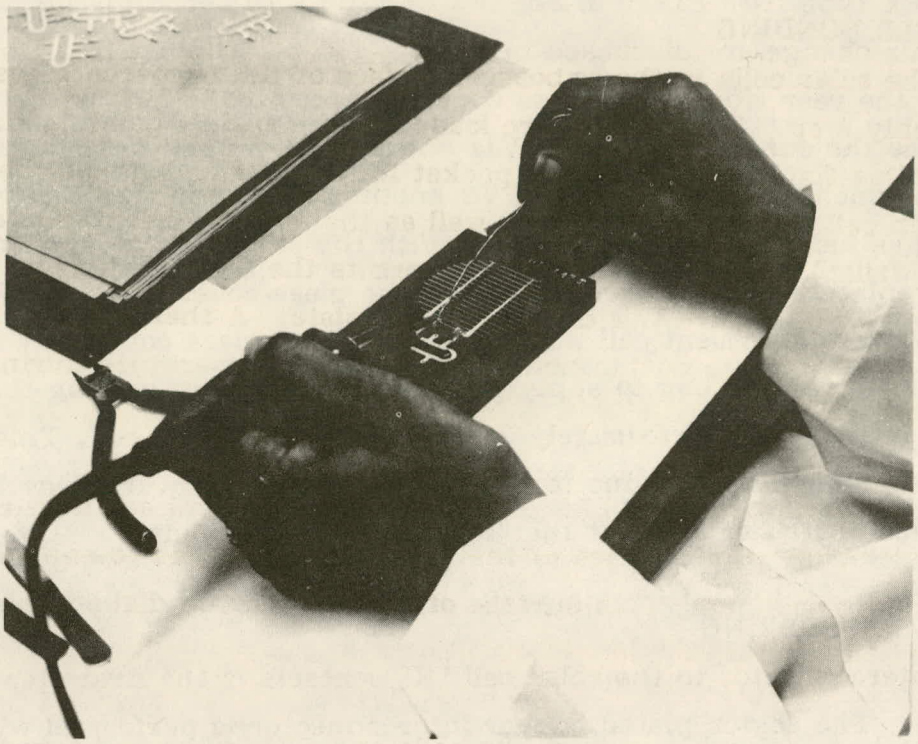

Figure 3-20. Soldering of Solar Cell "N" Contacts

Table 3-5. 45° Contact Pull Test Results on Spectrolab Cells

Solder Type	Soldering Iron Temperature (°F)	"N" Contact Pull Strength (grams)	Remarks
Sn 60	700	397	20% Ag/Si separation
Sn 60	700	397	80% Ag/Si separation
Sn 62	640	1049	30% Ag/Si separation
Sn 62	640	368	100% Ag/Si separation
Sn 62	590	1049	Cell broke
Sn 62	590	822	Interconnect broke at hole
Sn 62	590	709	80% Ag/Si separation
Sn 62	590	737	100% Ag/Si separation
Sn 62	590	567	100% Ag/Si separation

3.3.3 SOLAR CELL BONDING

The bonding of the solar cells to the embossed surface of the tempered glass coverplate is the next assembly step. The 19 cells are loaded in the module bonding fixture shown in Figure 3-21. This fixture, which has a pocket for each cell, controls the linear positioning of each cell within the module as well as the angular orientation of each cell. A series of holes drilled into an internal cavity permits the later application of vacuum to the space between the fixture and the glass coverplate. A thermocouple has been embedded within the fixture to enable monitoring of plate temperature during the subsequent bonding operation.

Two disks of 1.75-inch diameter SAFLEX SR-10 polyvinyl butyral are next centered on the top of each solar cell. One surface of this product is grooved to enhance the escape of air during vacuum lamination. This surface of each of the two disks is placed in contact with the glass or solar cell.

A glass coverplate is positioned on top of the cells and PVB disks and taped to the bonding fixture around the perimeter with high temperature Teflon tape. This fixture is then placed on a preheated hot plate as shown in Figure 3-22(a). An insulation blanket is placed on top of the glass to reduce heat loss from the coverplate surface as shown in Figure 3-22(b). A thermocouple is placed at the center of the module between the glass coverplate and insulation blanket. The insulation blanket reduces the temperature difference between the fixture and glass coverplate and produces a more uniform flow-out of the PVB from cell-to-cell across the module.

Table 3-6 gives the temperature-vacuum profile which has been developed to give satisfactory bonds with two disks of SAFLEX SR-10 as described above. Figure 2-23 shows front and rear views of the glass coverplate for Module Serial No. SM-2 following cell bonding and soldering of the interconnectors to the "P" contacts.

Initial attempts to bond cells to the glass coverplate with a single disk of 2.00-inch diameter SAFLEX PT-10 proved to be unsuccessful in terms of the repeatability of obtaining a void-free lamination. The thickness of the PVB was doubled by adding another 2.00-inch disk of PT-10 to each cell. This approach was successful in eliminating the large area voids in the lamination, but bubbles continued to be a problem. Attempts were made to dissolve these bubbles by subjecting the coverplate assemblies to an autoclave cycle which

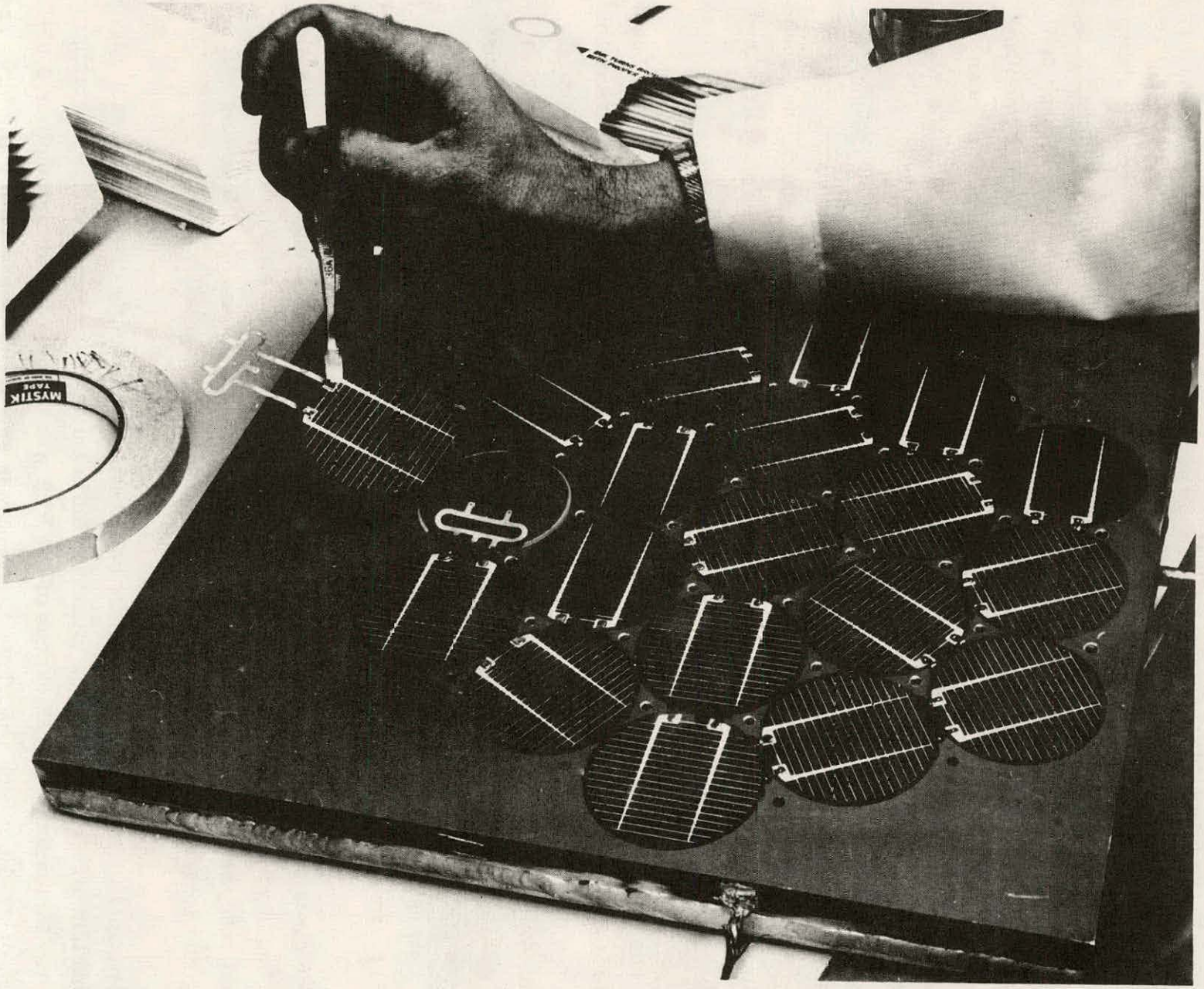

Figure 3-21. Loading of Bonding Fixture

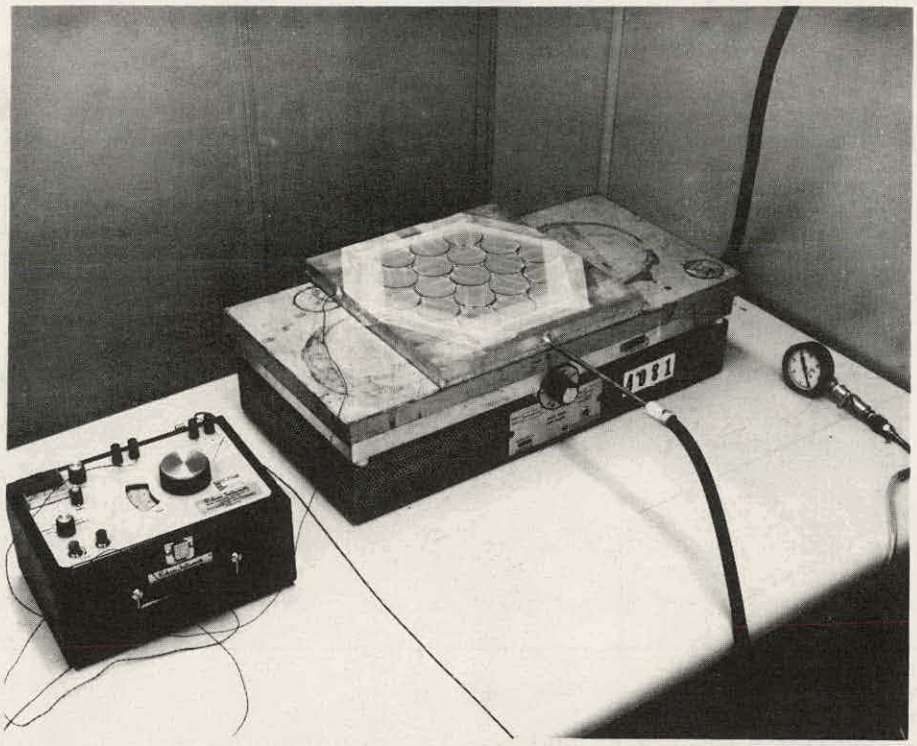

(a) Without Insulation Blanket

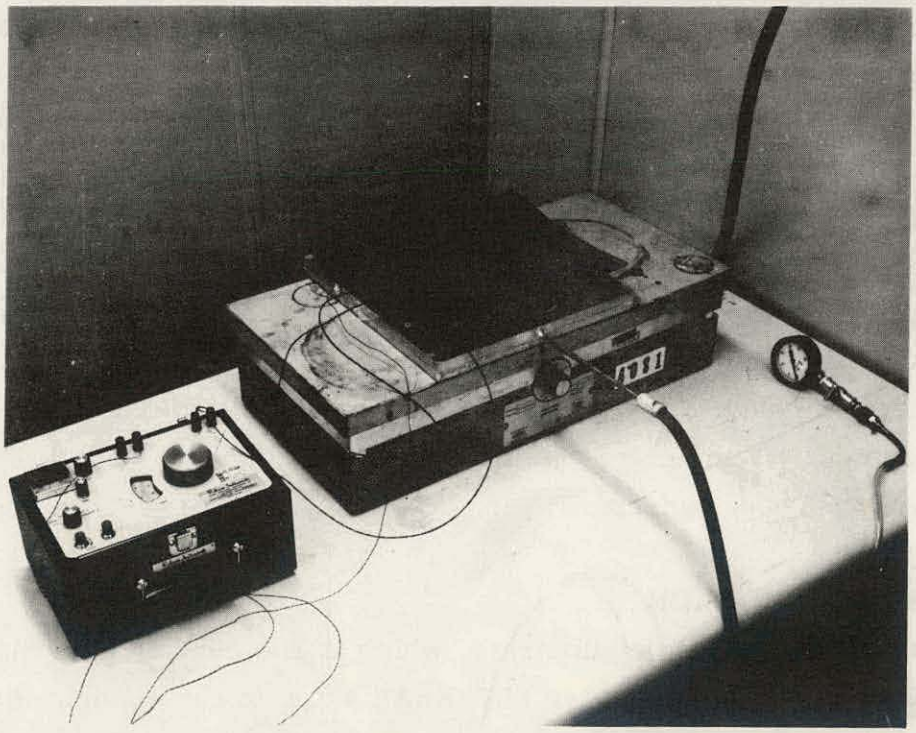

(b) With Insulation Blanket

Figure 3-22. Solar Cell Bonding Operation

Table 3-6. Typical Cell Bonding Cycle

Elapsed Time (minutes)	Fixture Temp. (°F)	Coverplate Temp. (°F)	Vacuum (in. Hg Gauge)	Remarks
0	75	75	0	Place on hot plate
6	150	110	5	
14	200	170	10	
16	220	190	20	
22	250	225	27	
38	285	266	0	Vent for 2 minutes
40	285	268	27	
84			0	Remove from hot plate and cool

consisted of a pressure of 180 psi at 300°F. The coverplates were maintained at this temperature and pressure for at least 30 minutes before the temperature was allowed to decrease. The pressure was maintained until the coverplate temperature was below 120°F. This cycle was successful in eliminating entrapped bubles, but in some cases these bubbles reappeared following overnight soak at ambient conditions. Some yellowing of the PVB where it runs out around the circumference of the cells was also a result of the autoclave cycle. Since this autoclave step is an expensive addition to the processing sequence, efforts were made to obtain bubble-free bonds directly. To this end, the change to SAFLEX SR-10, which has more plasticizer and better flow characteristics at a lower temperature, has resulted in satisfactory bonds without the need for an autoclave processing step. Experiments with the diameter of the SR-10 disks, which included 2.00, 1.87, and 1.75 inch diameters, has led to the selection of two 1.75-inch diameter disks. This selection provides nearly bubble-free bonds with limited run-out around the cell circumference and virtually no underrun.

3.3.4 SUBSTRATE LAMINATION

The lamination of the semi-flexible substrate, which is the next step in the processing sequences, involving bonding the outer FLEXSEAL skins to the epichlorohydrin foam core and to the two-sided flexible printed circuit board. The B.F. Goodrich FLEXSEAL contact adhesive system, which was selected for this application, has been found to give

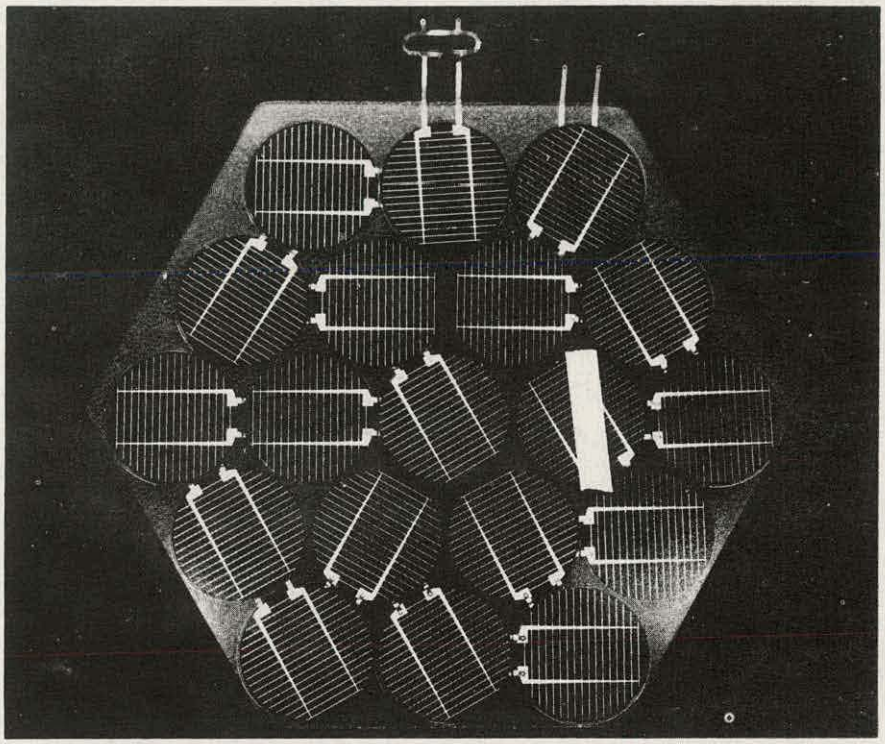

(a) Front

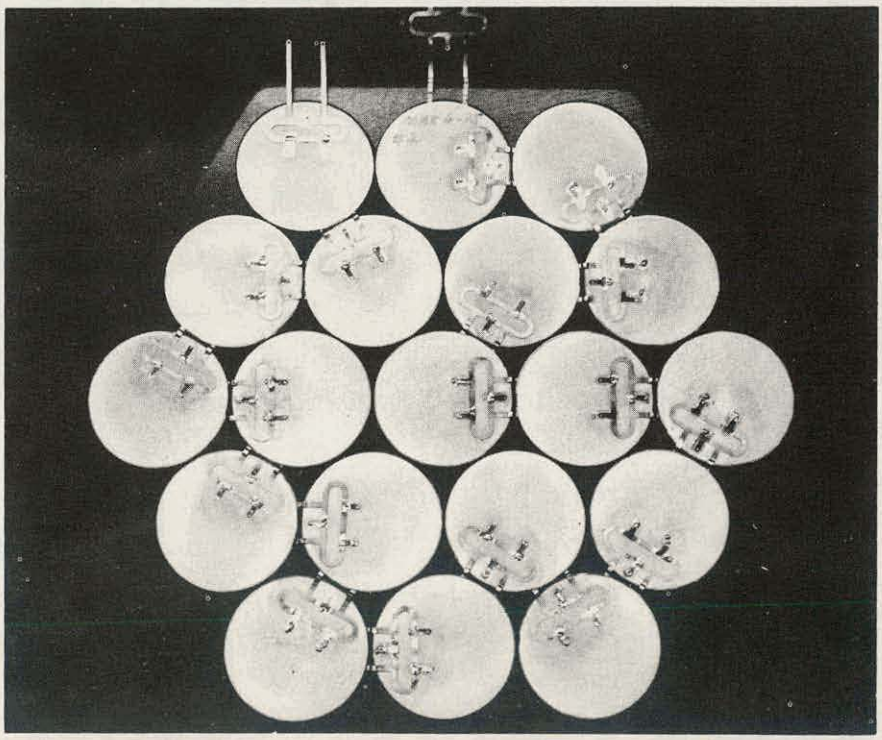

(b) Back

Figure 3-23. Coverplate/Solar Cell Assembly for Module Serial No. SM-2

satisfactory results if care is exercised when the initial contact is made between the adhesive-coated surfaces. Waxed paper is slipped between these surfaces so that proper alignment can be achieved before contact is made. This paper interlayer is then gradually pulled out while the surfaces are rolled together along a line to minimize the amount of entrapped air pockets.

The flexible printed circuit board substrate material has been made large enough to cover the entire area of the foam core. This change was found necessary to reduce the formation of bubbles under the FLEXSEAL skins when the module is exposed to elevated temperatures.

3.3.5 MODULE ENCAPSULATION

The encapsulation of the module and the bonding of the rear TEXTOLITE cover are both accomplished using RTV11. The rear side of the glass coverplate and solar cells are primed with SS-4044 followed by a spray coating of RTV108 (10 to 20% by weight mixed with heptane). The RTV11 is mixed, deaerated and poured over the rear surface of the glass coverplate assembly. The material is spread over the entire glass surface until the height of the silicone just covers the interconnector strain relief loops. The spread RTV-11 is again deaerated in a large vacuum enclosure to remove entrapped bubbles before the rear TEXTOLITE cover, which has also been previously primed with SS-4044 and RTV108, is attached.

3.4 MODULE ELECTRICAL PERFORMANCE

Table 3-7 summarizes the electrical performance measurements made using the Large Area Pulsed Solar Simulator (LAPSS) with JPL-supplied Terrestrial Secondary Standard No. 025 as the reference cell. In the case of the qualification modules which are designated by a "Q" following the serial number, the electrical performance reported in this table represents the final measurement made after all environmental exposures. Figure 3-24 is an example of a typical I-V characteristic as obtained using the LAPSS. The mean performance of these modules is 5.79 watts at the maximum power point with a standard deviation of 0.169 watts. Module Serial Number SM-7Q was eliminated from the average since a cracked cell within this module results in a significant degradation in performance.

This average module performance reflects a net enhancement of 7.8 percent compared to the measured average bare cell performance which is 282.6 mW per cell or 5.37 watts per module. As a further verification of this result, module Serial Number SM-12 was

Table 3-7. Summary of Module Electrical Performance Measurements

Module Serial Number	I_{SC} (mA)	V_{OC} (Volts)	V_{MP} (Volts)	P_{MAX} (Watts)
SM- 1Q	704	11.4	9.35	5.71
- 2Q	714	11.5	9.50	6.16
- 3	702	11.7	9.30	5.90
- 4Q	712	11.6	9.50	6.14
- 5A	710	11.5	9.50	6.05
- 6Q	713	11.5	9.50	5.93
- 7Q	651	11.4	10.10	4.39
-10AQ	695	11.6	9.40	5.80
-12A	713	11.7	9.30	5.99
-13A	702	11.5	9.50	5.96
-17A	710	11.5	9.30	5.94
-18	702	11.7	9.40	5.88
-19	697	11.6	9.30	5.83
-20A	697	11.4	9.30	5.90
-21	706	11.6	9.40	6.02
-22Q	706	11.5	9.40	6.03
-23	704	11.6	9.30	5.90
-24	692	11.5	9.40	5.85
-26	710	11.5	9.40	6.04
-27	714	11.5	9.30	6.02
-28	695	11.3	9.20	5.77
-29	708	11.6	9.30	5.97
-30	699	11.4	9.25	5.83
-31	698	11.4	9.30	5.79
-32	685	11.4	9.40	5.79
-34	699	11.3	9.20	5.70
-35	703	11.4	9.30	5.78
-36	700	11.4	9.20	5.72
-37	693	11.4	9.30	5.74
-38	698	11.4	9.40	5.70
-39	687	11.4	9.40	5.71
-41	682	11.3	9.35	5.64
-42	703	11.4	9.40	5.84
-43	705	11.4	9.40	5.87
-44	684	11.4	9.50	5.86
-45	700	11.4	9.30	5.65
-46	704	11.4	9.20	5.72
-47	700	11.4	9.40	5.67
-48	691	11.3	9.20	5.58
-49	687	11.1	9.20	5.63
-50	699	11.3	9.25	5.70
-51	698	11.3	9.30	5.67
-52	704	11.3	9.25	5.62
-53	695	11.3	9.20	5.56
-54	680	11.0	9.00	5.49
-55	711	11.3	9.20	5.56
-56	694	11.3	9.20	5.56
-57	697	11.3	9.35	5.62
-58	686	11.3	9.20	5.49
-59	701	11.3	9.20	5.55

* At 100 mW/cm^2 using Terrestrial Secondary Standard No. 025 as the reference cell. Cell temperature corrected to 28°C.

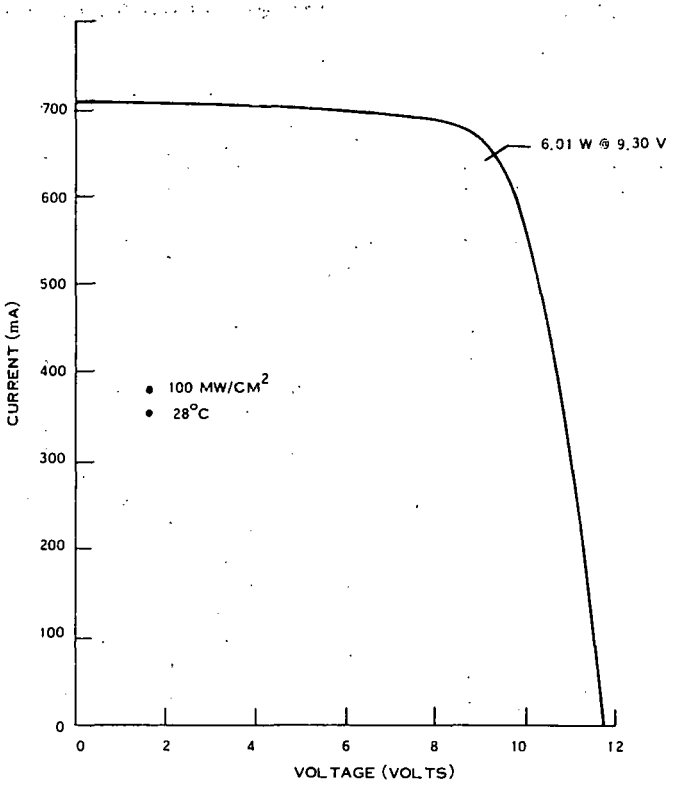

Figure 3-24. I-V Characteristic for Module Serial Number SM-4

built using solar cells which had been previously serialized and illuminated to determine the I-V characteristic for each cell. The use of these cells permits the accurate determination of the absolute gain due to covering and encapsulation.

Table 3-8 gives the voltage reading for each cell at four current values which bracket the maximum power point of the cells. The sum of the values for all 19 cells at each of these four currents yields the composite module characteristic with no coverplate. The overall module performance with bare cells is 5.56 Watts at a maximum power point voltage of 9.25 Volts. This equates to an average bare cell efficiency of 13.3 percent based on a nominal total solar cell area of 419.2 cm^2.

Following the bonding of these cells to the embossed surface of an ASG SUNADEX glass coverplate with PVB film, the I-V characteristic of the entire module was measured before encapsulation with RTV11. Figure 3-25 shows this characteristic both before and after encapsulation with the white silicone pottant. Prior to encapsulation the enhancement in maximum power output is calculated to be 2.3 percent based on the composite

Table 3-8. Performance of Individual Solar Cells in Module Serial No. SM-12*

Cell Position	Cell Identification Number	Voltage at Specified Current (Volts)			
		575 mA	600 mA	625 mA	650 mA
1	580-1	0.497	0.485	0.466	0.432
2	590-1	0.504	0.488	0.460	0.350
3	590-2	0.497	0.485	0.467	0.440
4	590-3	0.504	0.490	0.468	0.420
5	600-1	0.508	0.493	0.470	0.410
6	600-1	0.512	0.500	0.485	0.452
7	590-8	0.503	0.487	0.460	0.400
8	570-13	0.495	0.480	0.456	0.400
9	600-2	0.508	0.495	0.473	0.420
10	610-1	0.502	0.492	0.474	0.442
11	610-2	0.507	0.495	0.476	0.437
12	580-2	0.495	0.480	0.454	0.390
13	580-5	0.500	0.487	0.460	0.385
14	620-1	0.499	0.486	0.469	0.435
15	580-3	0.500	0.488	0.470	0.423
16	580-7	0.499	0.482	0.452	0.350
17	580-9	0.499	0.485	0.456	0.375
18	580-12	0.498	0.484	0.465	0.407
19	590-10	0.500	0.483	0.455	0.375
Total Voltage		9.52	9.27	8.84	7.74
Measured on SM-12 Before Encapsulation		9.72	9.50	9.00	8.00
Measured on SM-12 After Encapsulation		10.00	9.80	9.30	9.22

* At 100 mW/cm^2 insolation and at $28^{\circ}C$

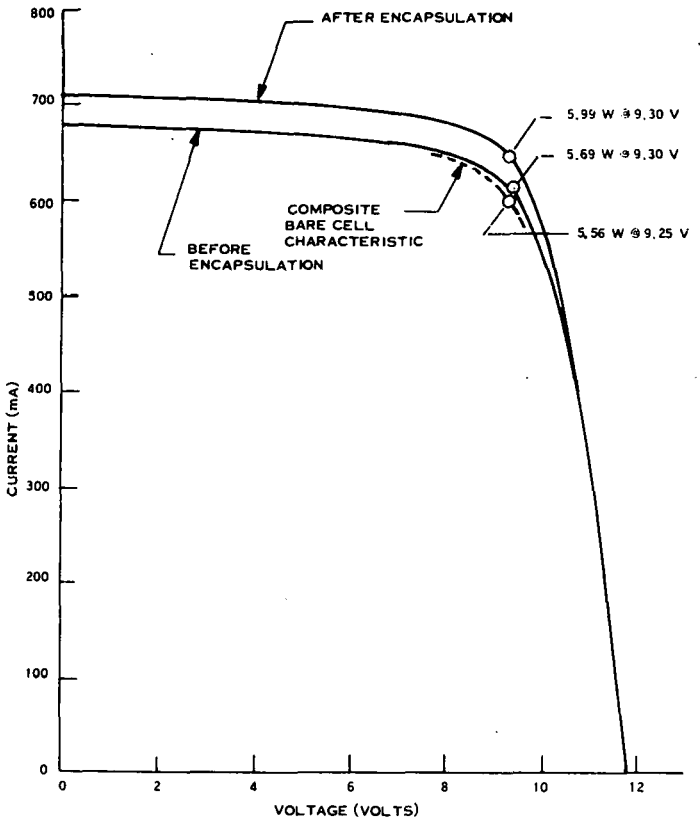

Figure 3-25. I-V Characteristics of Module Serial No. SM-12 Before and After Encapsulation

characteristic of the 19 bare solar cells. Following encapsulation, this enhancement is increased to 7.7 percent compared to the same composite bare cell characteristic. This agrees closely with the result sighted above based on the average performance of all modules.

It should be noted that this is the net enhancement, which includes the transmission and reflection losses associated with the glass and PVB. The exposed surface of the glass coverplate was untreated. The addition of a suitable anti-reflective coating to this outside surface could further augment the module output by an additional 1.5 to 2.0 percent.

This enhancement in module electrical output can be attributed to the internal reflection of light incident on the embossed surface of the SUNADEX glass in the white interstices. This light, which would be otherwise wasted, is internally reflected within the glass coverplate until some portion is absorbed by the solar cell active surface or converted into electrical output. This phenomenon which has been called the "zero depth concentrator", was reported

under the New Technology provision of this contract (See Section 6). Figure 3-26 shows the enhancement in short-circuit current as a function of packing factor. These results were obtained using the test specimen shown in Figure 3-27 and varying the size on the circular aperture which was placed over the glass coverplate to achieve differing exposed annulus areas around the solar cell. Appendix A describes an analytical model for the zero depth concentrator enhancement phenomenon.

3.5 MODULE QUALIFICATION TESTING

3.5.1 ELECTRICAL PERFORMANCE RESULTS

The electrical performance of each qualification module was measured initially and again after each of the environmental exposures. Table 3-9 summarizes the results of these illumination tests which were performed using the LAPSS with JPL-supplied Terrestrial Secondary Standard No. 025 used as the reference.

With the exception of module serial number SM-10AQ, the change in maximum power output due to the thermal cycling exposure was positive with an average improvement of 2 percent. This improvement was due to an increase in the curve fill factor (CFF) in all cases, which would tend to indicate a decrease in contact series resistance or an increase in shunt resistance. In the case of module serial number SM-10AQ the appearance of a relatively large number of bubbles within the PVB caused a 2.5 percent decrease in the short-circuit current. However, even in this case the module experienced an increase in the CFF as a result of the thermal cycling exposure.

The humidity-temperature exposure was found to cause no significant change in the module electrical performance. Similarly the mechanical integrity test did not cause a change in module electrical performance beyond the expected accuracy of the measurement. However, in the case of module serial number SM-7Q the 22 percent decrease in maximum power output can be attributed to a single cracked cell which resulted from a highly localized bearing load imposed by standing on the glass coverplate as discussed in Section 3.5.4.

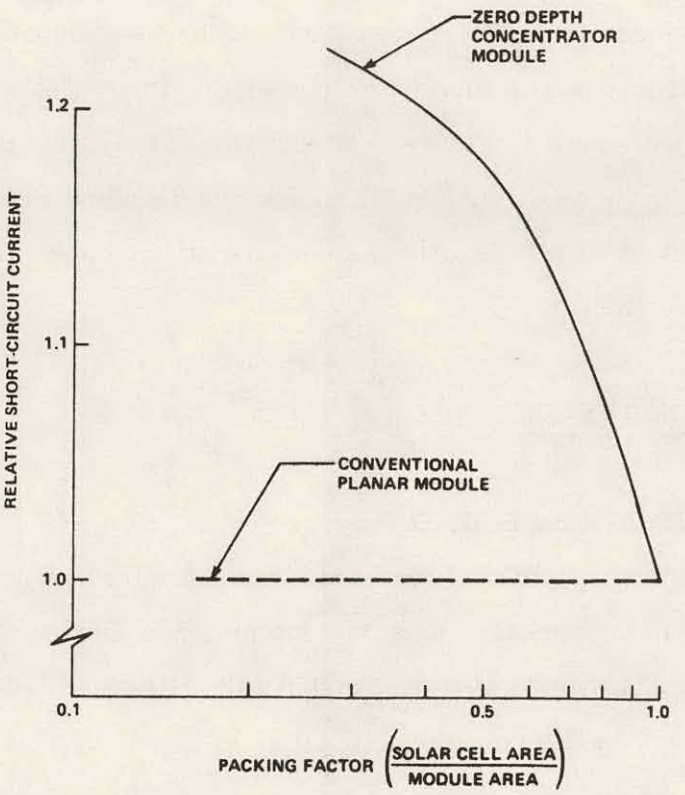

Figure 3-26. Enhance Module Output with an Embossed Glass Coverplate and White Interstices

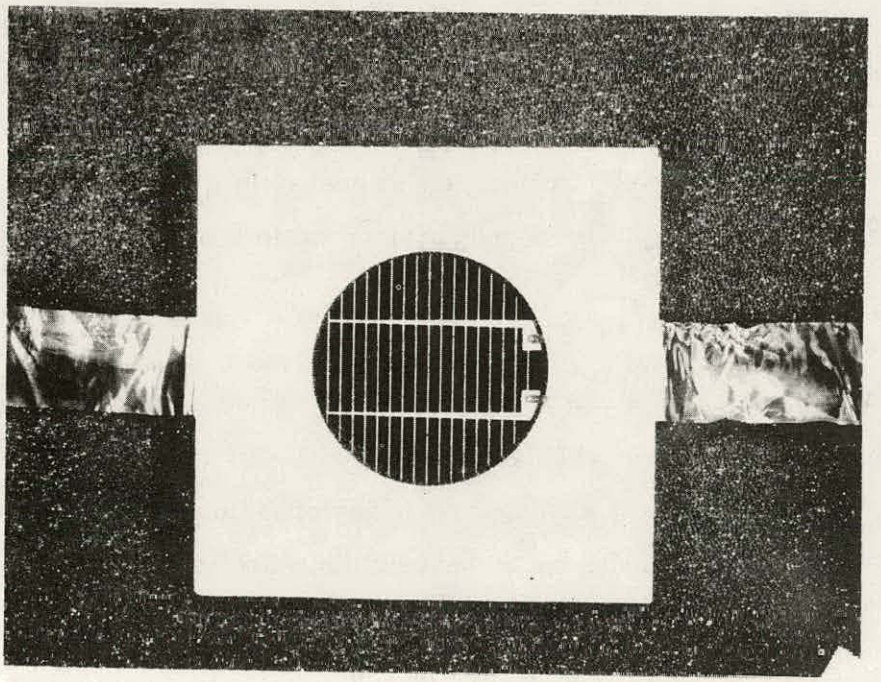

Figure 3-27. SUNADEX Glass-Covered Test Specim

Table 3-9. Summary of Qualification Module Electrical Performance

Module Serial Number	Initial Measurement				After Thermal Cycle Test				After Humidity-Temperature Test				After Mechanical Integrity Test			
	I_{SC} (mA)	V_{OC} (Volts)	V_{mP} (Volts)	P_{MAX} (Watts)	I_{SC} (mA)	V_{OC} (Volts)	V_{mP} (Volts)	P_{MAX} (Watts)	I_{SC} (mA)	V_{OC} (Volts)	V_{mP} (Volts)	P_{MAX} (Watts)	I_{SC} (mA)	V_{OC} (Volts)	V_{mP} (Volts)	P_{MAX} (Watts)
SM-1Q	705	11.3	9.10	5.32	705	11.5	9.30	5.67	705	11.5	9.30	5.69	704	11.4	9.35	5.71
SM-2Q	720	11.7	9.30	6.05	714	11.6	9.40	6.10	715	11.65	9.40	6.11	714	11.5	9.50	6.16
SM-4Q	713	11.8	9.30	6.01	713	11.7	9.40	6.08	713	11.65	9.35	6.09	712	11.6	9.50	6.14
SM-6Q	719	11.7	9.25	5.79	715	11.5	9.40	5.86	716	11.6	9.40	5.90	713	11.5	9.50	5.93
SM-7Q	707	11.5	9.25	5.68	706	11.5	9.30	5.76	707	11.6	9.20	5.66	651	11.4	10.10	4.39
SM-10AQ	713	11.7	9.30	5.92	695	11.7	9.40	5.79	695	11.6	9.40	5.80	—	—	—	—
SM-22Q	706	11.6	9.30	5.91	712	11.6	9.30	6.03	712	11.6	9.35	6.02	706	11.5	9.40	6.03

Notes: (1) Module SM-22Q subjected to 17 thermal cycles.

(2) Module SM-7Q performance indicates broken cell resulting from bearing load due to 68 kg man standing on one leg near center of glass coverplate. This is only module which was subjected to this loading.

(3) Module SM-10AQ was not subjected to the mechanical integrity test.

Module serial number SM-10AQ was not subjected to the mechanical integrity test since there were only six positions for qualification modules within the simulated roof test matrix.

3.5.2 THERMAL CYCLE TESTING

The qualification modules were arranged within the thermal cycling chamber as shown in Figure 3-28. An aluminum foil tent was constructed over the modules to reduce the rate of change of temperature and provide a uniform temperature distribution in the gas surrounding the modules. Thermocouples within this tent were monitored during the test and were indicative of the chamber temperature as the cycling was performed in accordance with the profile shown in Figure 3-29.

A visual examination of the modules, which was performed after the completion of a few thermal cycles, revealed that delamination was occurring between the RTV11 encapsulant and the glass coverplate. This was generally localized around the perimeter of the glass coverplate. These modules had a thin coating of diluted RTV108 applied to the rear side of the glass coverplate to act as a primer for the RTV11. In view of this development an effort was made to improve this adhesion by applying SS-4044 primer to the glass coverplate prior to coating with diluted RTV108. A module (Serial Number SM-22Q) was fabricated with this two step priming system and introduced into the thermal cycling chamber at the conclusion of cycle number 33.

Post-test examination of this module revealed no evidence of delamination resulting from the 17 cycle exposure while the other six initial modules had shown delaminations after a few thermal cycles with no observable increase in area affected after the completion of the 50 cycles. Based on these observations it can be concluded that the two-step priming system provided the necessary adhesion between the glass and the RTV11.

The formation of bubbles between the top FLEXSEAL skin and the foam core was also observed at the conclusion of this exposure. The occurrence of these bubbles, which is not considered to be a functional problem, appears to be related to the initial uniformity of the layer of CA1056 contact adhesive which bonds this interface. A thin, uniform application of

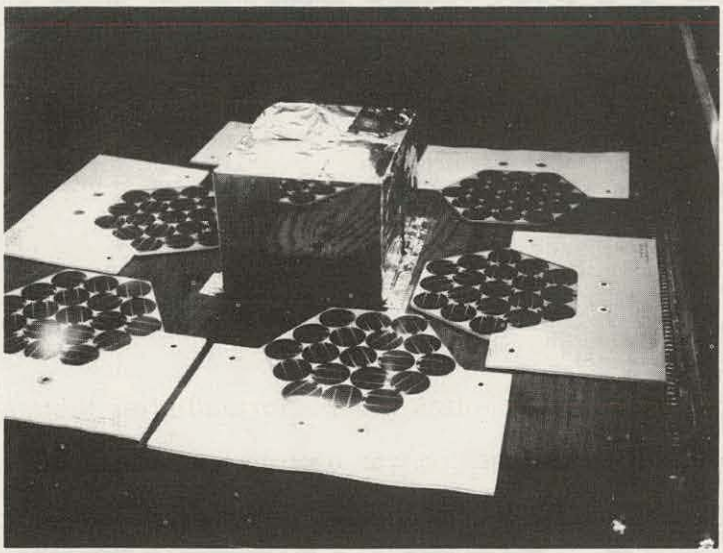

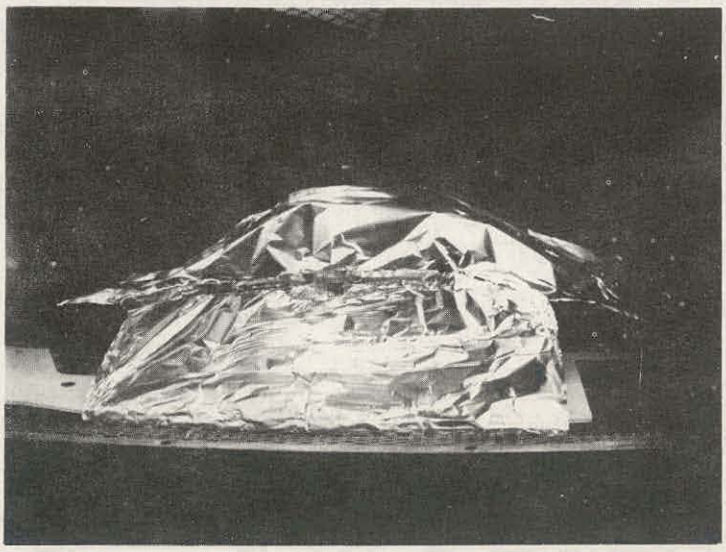

Figure 3-28. Test Set-up for Thermal Cycling Exposure

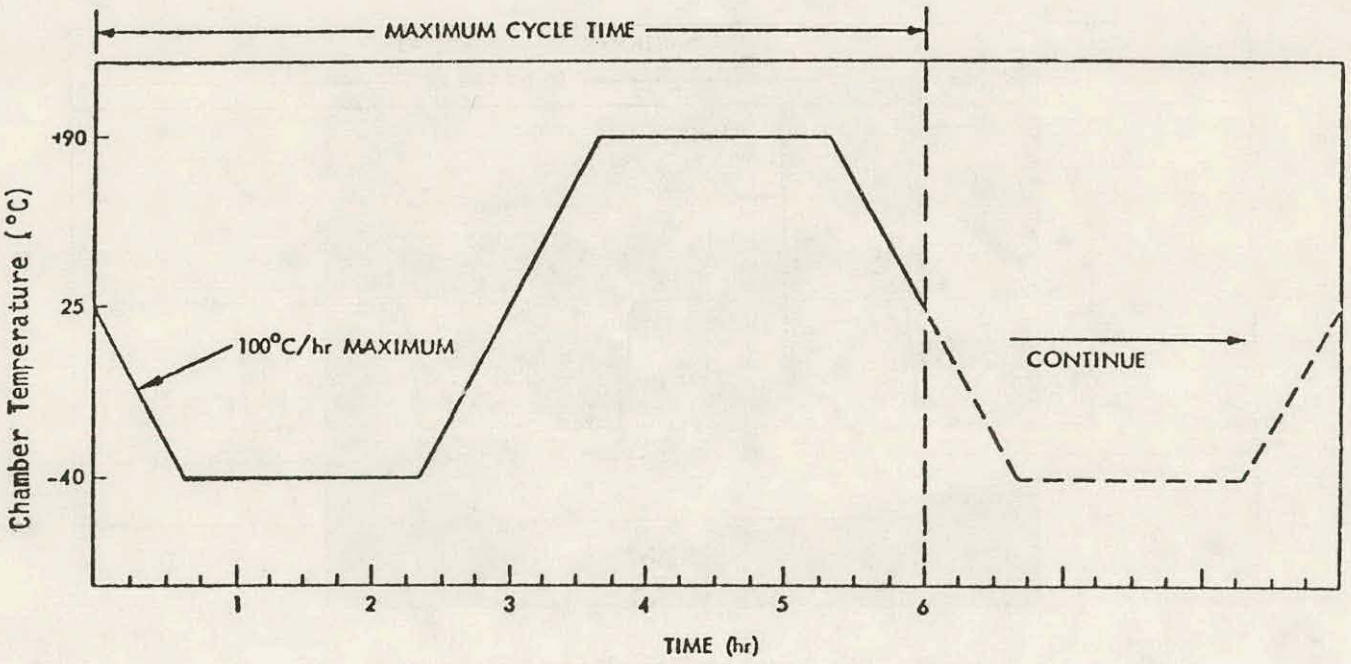

Figure 3-29. Thermal Cycle Test Profile

this adhesive is necessary to prevent bond failure during thermal cycling. Efforts have been made on subsequent modules to achieve the necessary uniformity of this adhesive and to prevent the initial entrapment of air during lamination.

3.5.3 TEMPERATURE-HUMIDITY TESTING

The qualification modules were subjected to the temperature-humidity profile shown in Figure 3-30. A post-test visual examination of these modules revealed a failure of the bonded joint between the glass coverplate and the top FLEXSEAL skin. This failure was a lack of adhesion between the CA 1056 contact adhesive and the glass surface. These joints were reworked by bonding with RTV102 on all modules and using RTV102 as the bonding adhesive for all new modules.

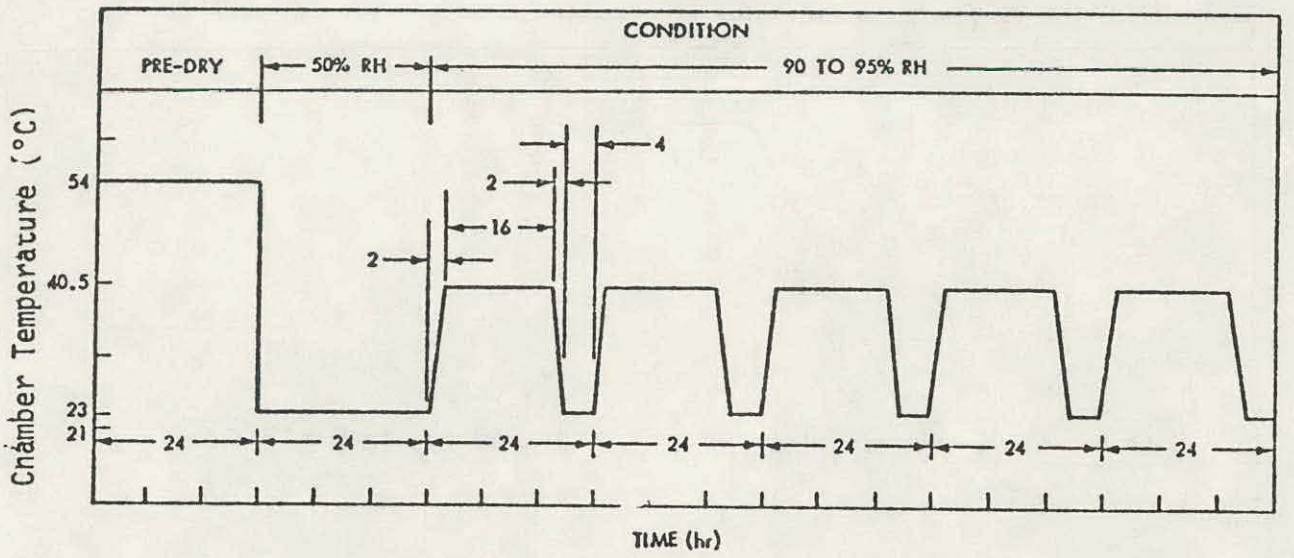

Figure 3-30. Temperature-Humidity Test Profile

3.5.4 MECHANICAL INTEGRITY TESTING

The mechanical integrity testing consisted of 100 cycles of bidirectional loading at 2394 Pa (50 lb/ft^2) applied as a uniformly distributed load over the exposed coverplate surface of each individual qualification shingle. This loading was accomplished as shown in Figure 3-31. A vacuum fixture was designed to fit over the top of the glass coverplate. This fixture was weighted to obtain a total mass of 12.38 kg (27.3 lb). With an exposed module area of 0.0507 m^2 this amounts to the required 2394 Pa in the downward direction. The upward loading was then obtained by pulling up on the loaded vacuum fixture until the force gauge read approximately 243N (54.6 lb). This loading cycle was repeated 100 times for each of the six qualification shingles.

The maximum upward deflection measured at the bottom edge of the coverplate ranged from 25 to 13 mm (1.0 to 0.5 inches) depending on the location of the module within the matrix.

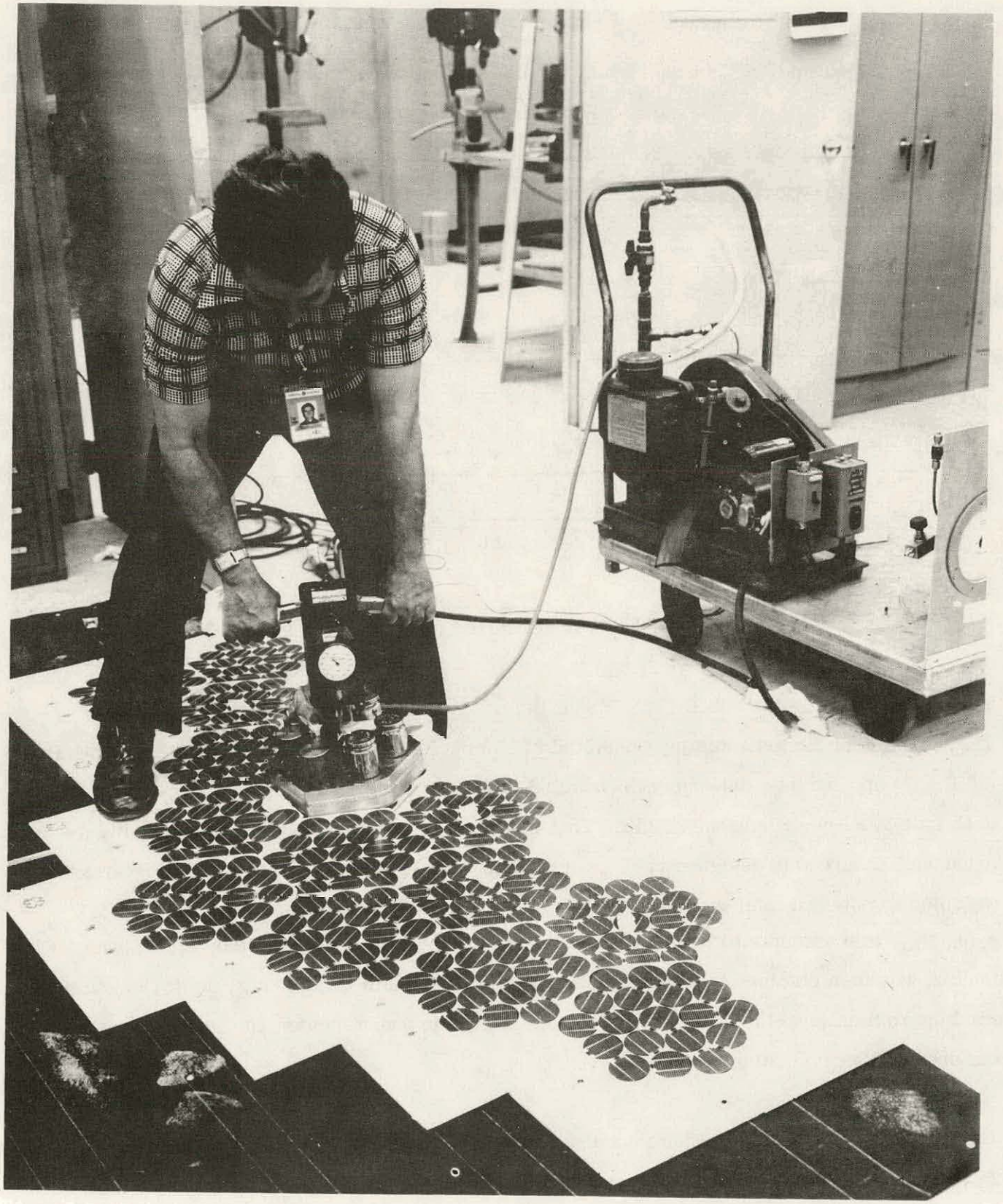

Figure 3-31. Test Set-up for Mechanical Integrity Testing
(Photo No. VF 78-249)

There was no visual damage as a result of this loading test. However, a post-test examination of module no. SM-7Q revealed the presence of one cracked solar cell. Since this was the module which was previously loaded by standing on the glass coverplate as shown in Figure 3-32, it is probable that this crack was caused by this highly localized bearing load which was at one time 667 N (150 lb) distributed over the area of the ball of one foot.

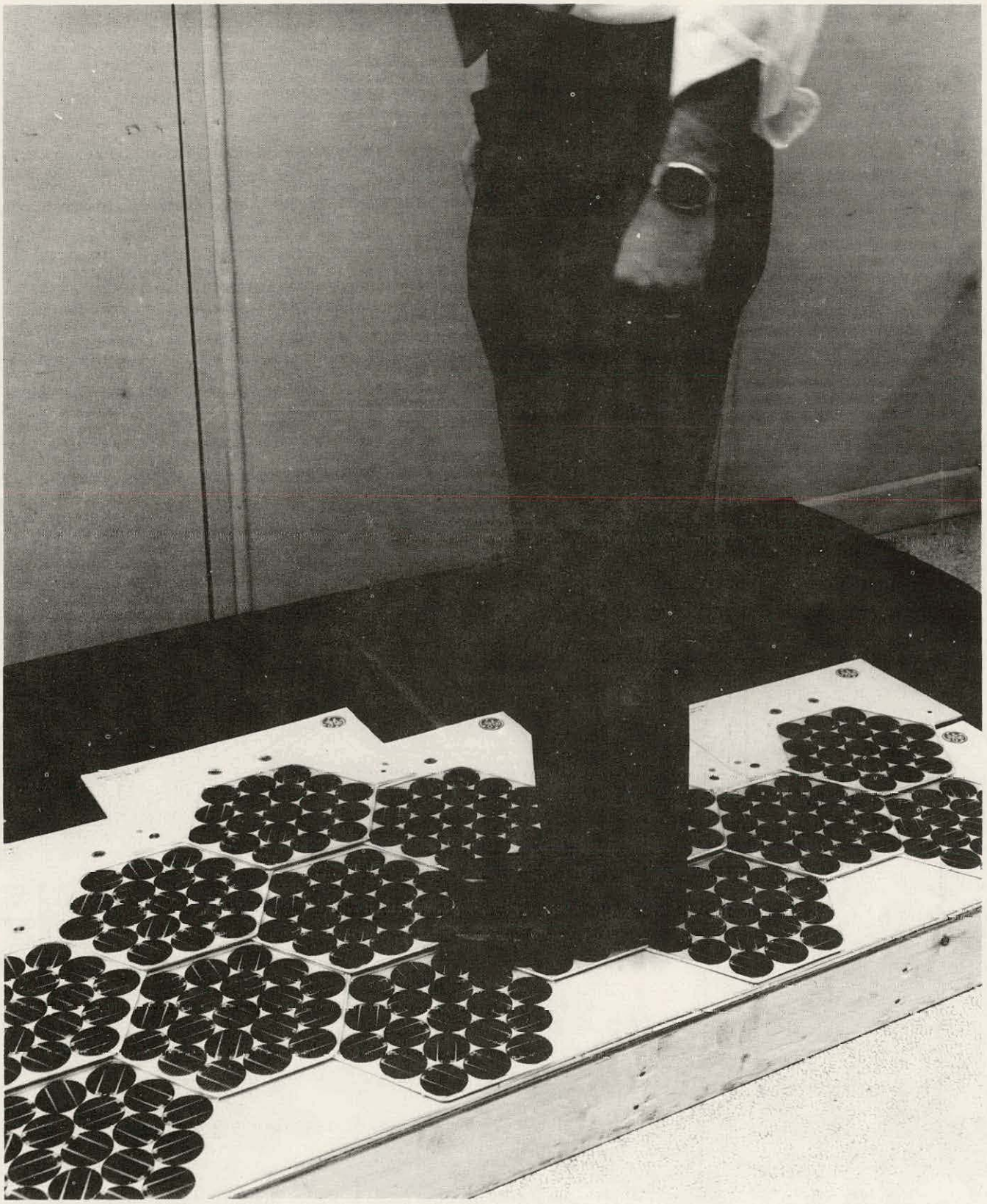

Figure 3-32. Standing on Installed Shingle Modules
(Photo No. VF 78-237A)

SECTION 4
CONCLUSIONS

The shingle module design described herein offers many advantages for applications which require the mounting of photovoltaic modules on the sloping roofs of new or existing residential or commercial buildings since no changes in conventional roof construction are imposed by the photovoltaic installation. The ancillary function of this module, viz., that of a weathertight roof covering; affects additional economy by eliminating the need for a conventional roof surface under the photovoltaic module installation. The relatively high areal specific output of this shingle module makes its use particularly attractive for installation on area limited roof surfaces. An average module maximum power output of 98 watts/m^2 of exposed module area at the Standard Operating Conditions has been calculated based on the measured performance of the 50 modules delivered under this contract. This high specific power output can be attributed to the efficient packing of the circular cells within the hexagon shape and to the enhancement of the output due to the reflected light from the embossed glass pattern in the white interstices. An enhancement of 7.7 percent, compared to bare cell performance, has been measured on a shingle module of this design. Another way of looking at this enhancement is that the white interstices, which amount to 87 cm^2 per module, perform as solar cells with an efficiency of about 5 percent.

A typical installation of 1872 modules which are arranged as three circuits, each with 26 series-connected modules and 24 parallel-connected modules, would require a roof length of 10.128 m. A slant height of 9.621 m is required to accommodate three circuits in this direction. Thus, the required roof area of 97.44 m^2 for this typical installation results in an overall area utilization of 0.805, which is defined as the ratio of solar cell area to rectangular roof area. This installation will produce a rated output of 9.2 kW at 205 vdc at the Standard Operating Conditions which include a calculated NOCT of 61°C.

The installation of a shingle solar cell module roof will require special precautions and procedures to protect against electrical shock hazards and mechanical damage to the modules. Each module could be covered with an opaque pressure-sensitive layer over the exposed

glass coverplate that would remain in place until after the electrical installation is completed, or, as an alternative, the module installation could be performed at night. The localized bearing loads associated with standing or kneeling on the installed module coverplate must be distributed over a large coverplate surface area to prevent breakage of solar cells due to excessive deflection near the center of the coverplate. Specially constructed platforms which distribute the load uniformly over the area of four coverplates should be employed during installation to prevent breakage of solar cells.

SECTION 5

RECOMMENDATIONS

An outdoor exposure test of an assembly of shingle modules would seem appropriate as the next step in the application of this development. This exposure is currently underway at the JPL Field Test Site.

The matching of individual solar cells to fully utilize the electrical output of each cell within a module is an important consideration which is often overlooked and could have a significant impact on the overall cost per watt of delivered module output. This matching requires more than just knowledge of the individual solar cell current output at a specified test voltage. Of equal importance is the short-circuit current (I_{SC}) output of each cell since a cell with low I_{SC}, when connected as a series element with cells of higher I_{SC} will limit the total module output I_{SC} to its value. Therefore, it is recommended that both the I_{SC} and the current at a specified test voltage, which is slightly lower than the anticipated maximum power voltage, be measured for each individual solar cell. Matching of cells within a module should be based primarily on the I_{SC} readings with secondary emphasis given to the difference between the two current readings which is measure of the slope of the "constant" current portion of the I-V characteristics.

Design optimization studies using the analytical model for the zero depth concentrator should be performed to determine if further enhancements in module output are possible.

SECTION 6

NEW TECHNOLOGY

The following New Technology disclosures have been reported to JPL:

1. Descriptive Title: A Zero Depth Solar Photovoltaic Concentrator
   Date Submitted: November 14, 1977
   Name of Innovator: N. F. Shepard, Jr.
   References: Quarterly Report No. 2-DOE/JPL 954607-78/2, pages 3-14, 3-15, 6-1

2. Descriptive Title: Interconnector for Overlapping Solar Cell Modules
   Date Submitted: March 23, 1978
   Name of Innovator: N. F. Shepard, Jr.
   References: Quarterly Report No. 2-DOE/JPL 954607-78/2, pages 3-11, 3-13, 3-29, 3-32, 3-33, 3-34

3. Descriptive Title: Embossed Glass-Covered Shingle Solar Cell Module
   Date Submitted: March 23, 1978
   Name of Innovator: N. F. Shepard, Jr.
   References: Quarterly Report No. 2-DOE/JPL 954607-78/2, pages 1-1, 1-2, 3-1 through 3-16

APPENDIX A

ANALYTICAL MODEL OF A ZERO DEPTH SOLAR PHOTOVOLTAIC CONCENTRATOR

A.1 INTRODUCTION

Light incident on the white interstices of an embossed glass covered module results in an enhancement of the electrical output. The additional task activity described herein concerns the development of an analytical model to calculate the improvement possible for a variety of module design parameters. This model is capable of assessing the impact on optical performance of the following variables acting independently:

1. indices of refraction of each of the encapsulant layers
2. cover plate thickness
3. cell diameter
4. cell spacing
5. surface roughness of outer coverplate surface
6. surface roughness of inner coverplate surface
7. reflection properties of the interstices
8. optical transmission of each of the layers through which solar energy passes
9. varying angles of light incidence upon the outer coverplate surface

This model will permit the optical performance of a glass-covered, hexagon-shaped shingle solar cell module, in terms of the enhancement in the annual energy incident on the active solar cell surfaces, to be evaluated for various combinations of the above mentioned variables.

In combination with algorithms which define the shingle module cost as a function of cell diameter and spacing, it will be possible to evaluate the shingle module cost per unit of annual energy output as a function of shingle geometry.

A.2 GENERAL DESCRIPTION OF OPTICAL MODEL

The factors to be considered in the optical model can be visualized with the aid of Figure A-1 which shows a section through the glass coverplate with the underlying solar cells. Related to the letter designations on the figure, the factors to be considered include the following:

A. orientation of the earth-sun line relative to the normal to the coverplate of the shingle module

B. surface coating at the air-to-glass interface

C. structure of the outside or exposed surface of the glass coverplate. In the case of SUNDADEX glass, this surface has a slightly matte finish.

D. the glass material

E. structure of the inside surface of the glass coverplate. In the case of SUNADEX glass, this surface has a deeply embossed regular pattern of indentations.

F. the material in contact with the inside surface of the glass coverplate in the interstices between the solar cell pattern

G. the transparent solar cell bonding material

H. the solar cell spacing and configuration

As described above, the optical portion of this model entails the consideration of many factors which influence the ultimate conversion of incident solar energy into electrical energy at the solar cell array. For maximum annual electrical energy output from a shingle, the goal is to maximize the useful solar energy which crosses the glass coverplate outside surface and to maximize the containment and absorption, by the solar cells, of the admitted energy.

The analytical approach to the optical portion of this problem will first consider the incident solar energy particularly as it relates to the angle of incidence effects. Light incident on the shingle module and traversing the glass is definable in terms of two angles as shown in Figure A-2: an angle of incidence (I), measured with respect to the shingle normal; and an azimuth angle (A), measured with respect to a due south axis in the plane of the module surface.

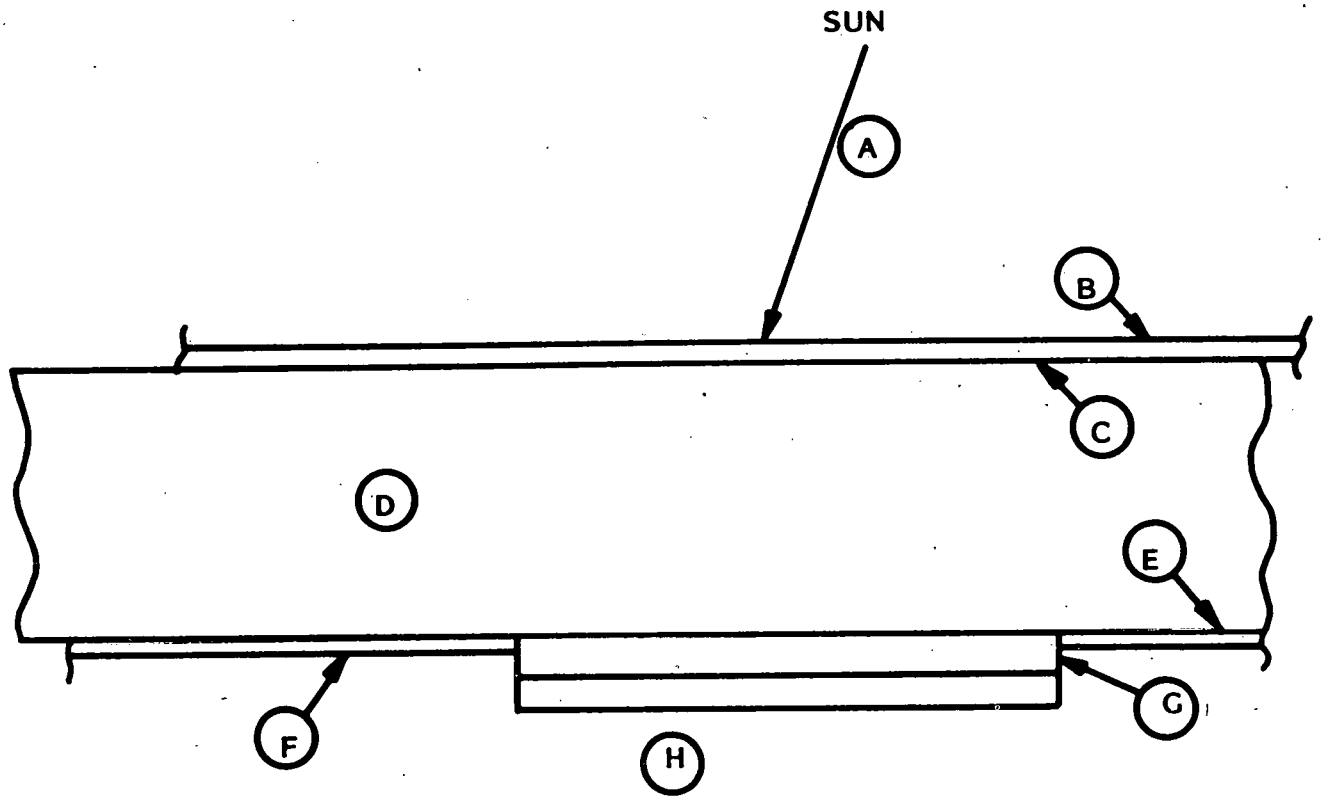

Figure A-1. Section Through Glass Coverplate Showing Factors Influencing Enhancement of Output Due to Zero Depth Concentrator Phenomena

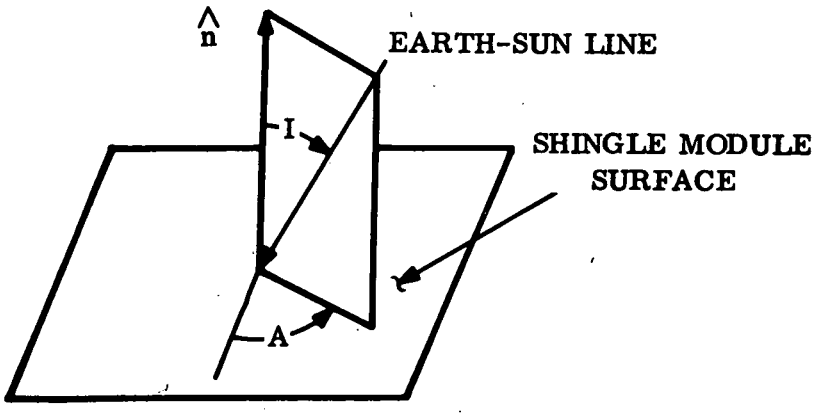

Figure A-2. Earth-Sun Line Orientation on Shingle Module Surface

Since the solar cell pattern is not point-symmetrical, performance will, in general, depend on azimuth, which will vary with time. Over a period of a year, however, the dependence on azimuth will be at least suppressed, if not washed out completely. Therefore, since the ultimate concern is with energy collected over a one year period, the problem will be defined only in terms of incidence angle, with all dependencies on azimuth being averaged out in the computation.

The basic form of the input data will be a histogram representing the annual energy incident on the glass coverplate surface over 2 degree intervals of the angle of incidence. As shown in Figure A-3, this histogram can be represented in the data structure as an array W (I) of 45 elements.

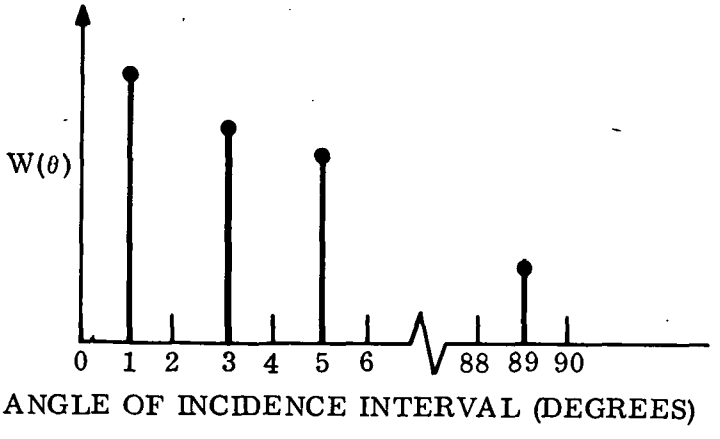

Figure A-3. Histogram of Annual Input Direct Beam Solar Energy

The various refraction and reflection processes within the transparent coverplate are shown in Figure A-4. Process (1) represents the entrance of incident solar energy into the coverplate. A portion of this energy is lost by a Fresnel reflection process at the rare to dense outer surface interface. Figure A-5 represents a typical Fresnel reflection process function.

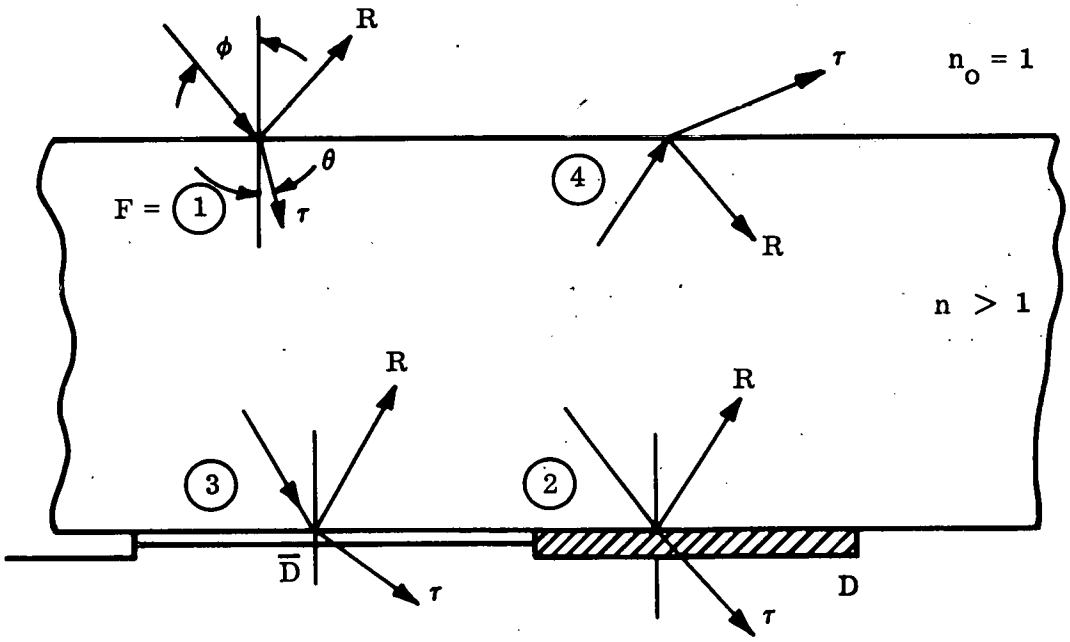

Figure A-4. Refraction and Reflection Processes Within Transparent Coverplate

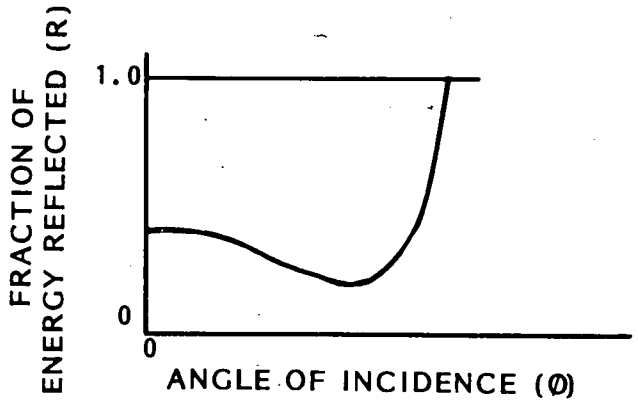

Figure A-5. Typical Function for Fresnel Reflection

This function can be modified by appropriate anti-reflective surface coatings. The specular beam of energy which passes into the coverplate is refracted by a Snell's Law refraction process where the ray is deflected toward the surface normal when passing from the rare-to-dense medium. The exit angle, θ is given by:

$$\theta = \sin^{-1}\left(\frac{\sin\phi}{n}\right)$$

Similar reflection and refraction processes occur at the internal coverplate-to-solar cell interface, represented by Process (2) ; at the internal coverplate-to-interstices interface, represented by Process (3) ; and at the internal coverplate-to-air interface, represented by Process (4) .

At each of these interfaces the specular beam is modifed by a scattering function which is shown diagramically in Figure A-6.

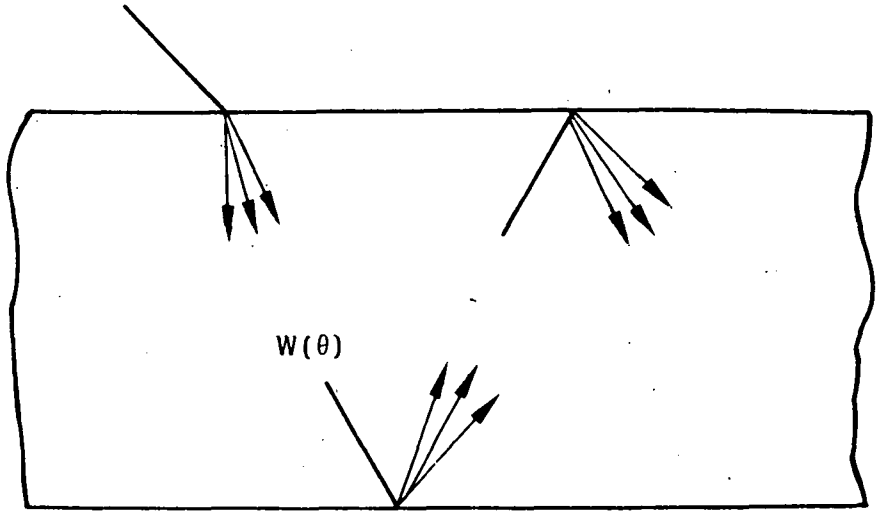

Figure A-6. Scattering at Outer and Inner Coverplate Surfaces

A scattering function, which operates on W (θ) by convolution, can be identified for each of these surfaces to account for this angular spread of the incident beam.

The passage of light through the coverplate material is also influenced by a bulk absorption process which is shown in Figure A-7. The absorption coefficient k is defined as an average over the sunlight spectrum.

Beam division processes also play an important role in the analytical definition of optical performance of the zero depth concentrator. Figure A-8 shows an array of circular beams representing reflected light from a solar cell pattern at an inclination angle ϕ. In making two passes through the coverplate (bottom to top and back to bottom) this pattern is sheared with respect to the original by an amount, S, given by:

$$S = 2t. \tan \phi$$

The overlap of the sheared pattern and original pattern is defined as the beam division function AA(s). Compound beam division functions are definable as a consequence of sequential passes through the coverplate as shown in Figure A-9.

A diagram of the various processes involved in the optical model is given in Figure A-10. Starting at the top of the page, this diagram shows the sequential process steps which operate on the incident energy distribution array W (I) to produce consecutive definitions of W as the energy passes through the coverplate for the first time and is incident on a solar cell, in the case of the "A" branch of the flow diagram, or on the interstices, is the case of the "A" branch. The various processes described above and enumerated on Figure A-10 operate on each "2-pass" branch after the initial reflection and beam division at the bottom surface of the coverplate. The "2-pass" sequence of operations relates to energy which passes from the bottom surface through the glass, is reflected and scattered from the top surface, and passes through the glass again before being incident on the bottom surface. At each occurence of reflection at the bottom surface an areal beam division takes place, accompanied by an associated translation or shear of the geometric pattern of circles within a hexagon. The program continues until the light energy has reached the bottom surface for the third time, or until two "2-pass" sequences have been completed. At appropriate places within the sequence the amount of energy incident on the solar cells is accumulated. The amount of energy available for collection is successively reduced as the chain of processes continues until after two "2-pass" sequences it is felt that the residual energy will be quite small.

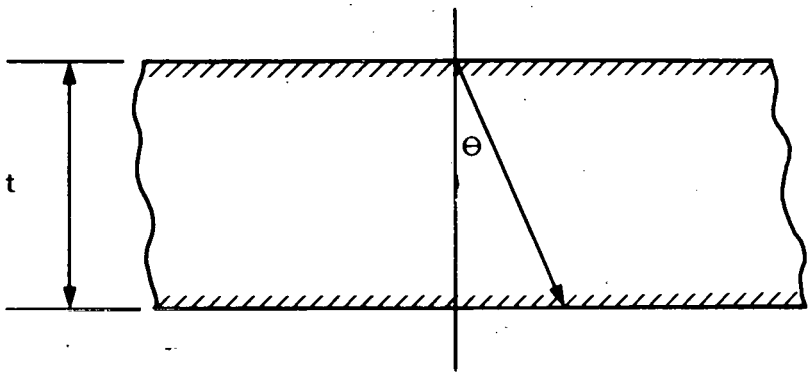

$$\tau(\Theta) = e^{-kt \sec \Theta}$$

Figure A-7. Bulk Absorption Process

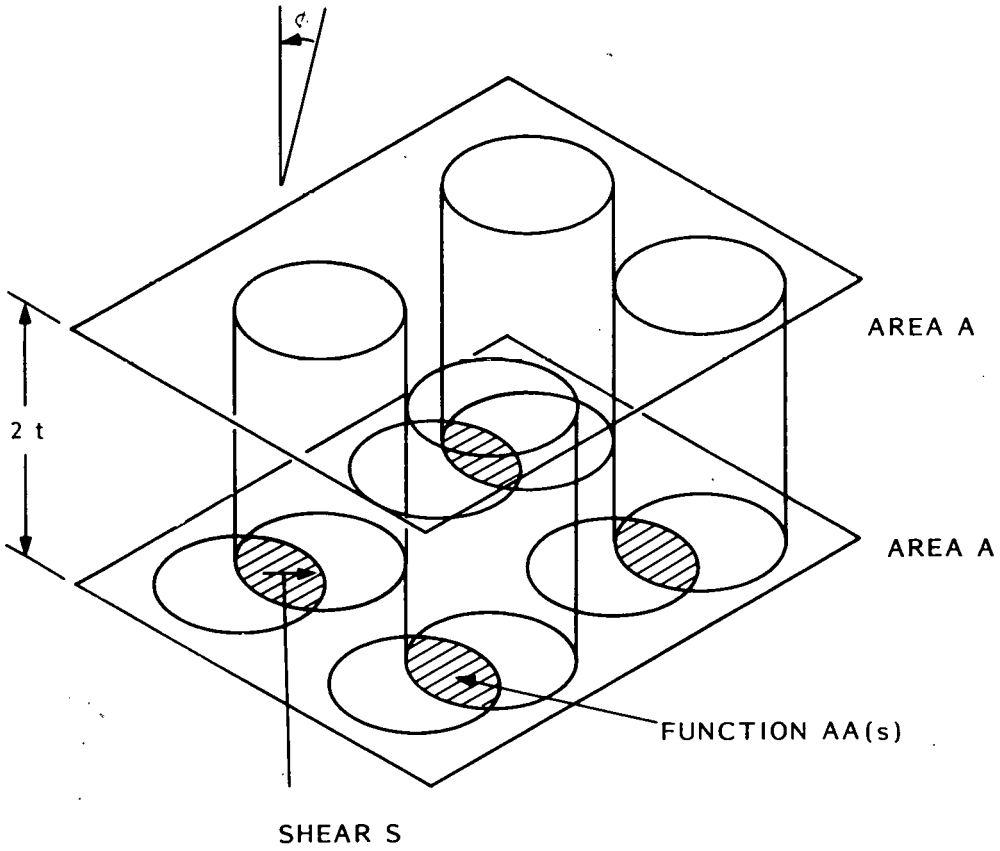

Figure A-8. Beam Division Processes

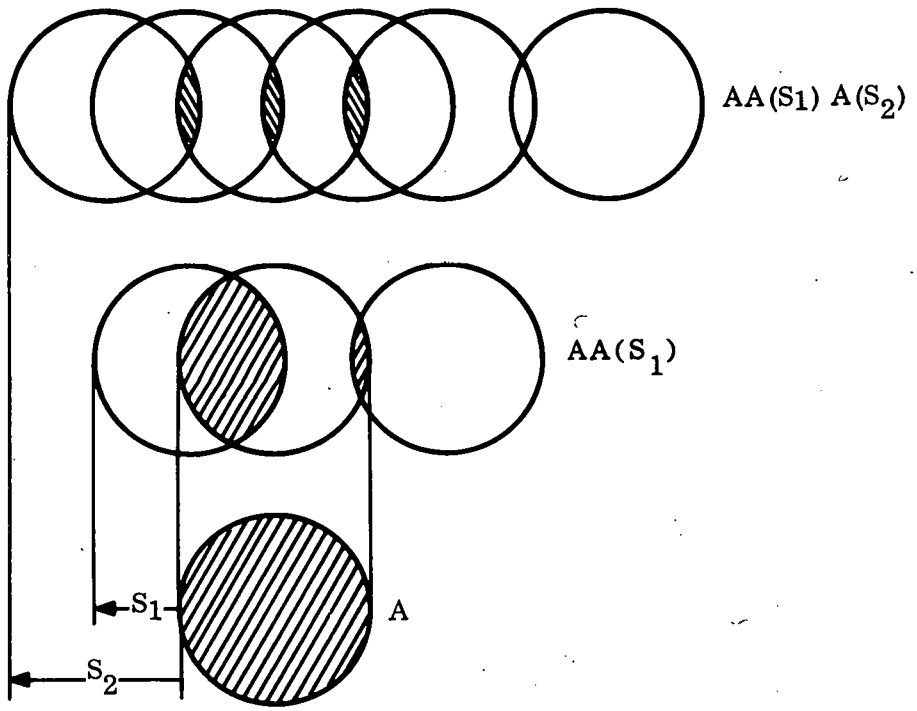

Figure A-9. Definition of Beam Division Functions

A.3 ASSUMPTIONS

The development of the analytical model will be based on the existing shingle solar cell module concept which consists of an array of circular solar cells arranged in a hexagon configuration under a common glass coverplate, as shown in Figure A-11. The cell diameter (d), spacing (S) and the number of solar cells (7 or 19) will be varied in the model but the basic hexagon geometry will be retained. For this module geometry the edge dimension of the hexagon (E) can be expressed in terms of the aforementioned variables by the following relationships.

$$E = 2.57735d + 3.1547S \text{ (for 19 cell module)}$$

$$E = 1.57735d + 2.1547S \text{ (for 7 cell module)}$$

Using the shingle module geometry shown in Figure A-12, the areas of the coverplate (A_{cp}) and substrate (A_s) can be expressed as a function of E by the following expressions:

$$A_{cp} = 2.598E^2$$

$$A_s = 3.8971E^2$$

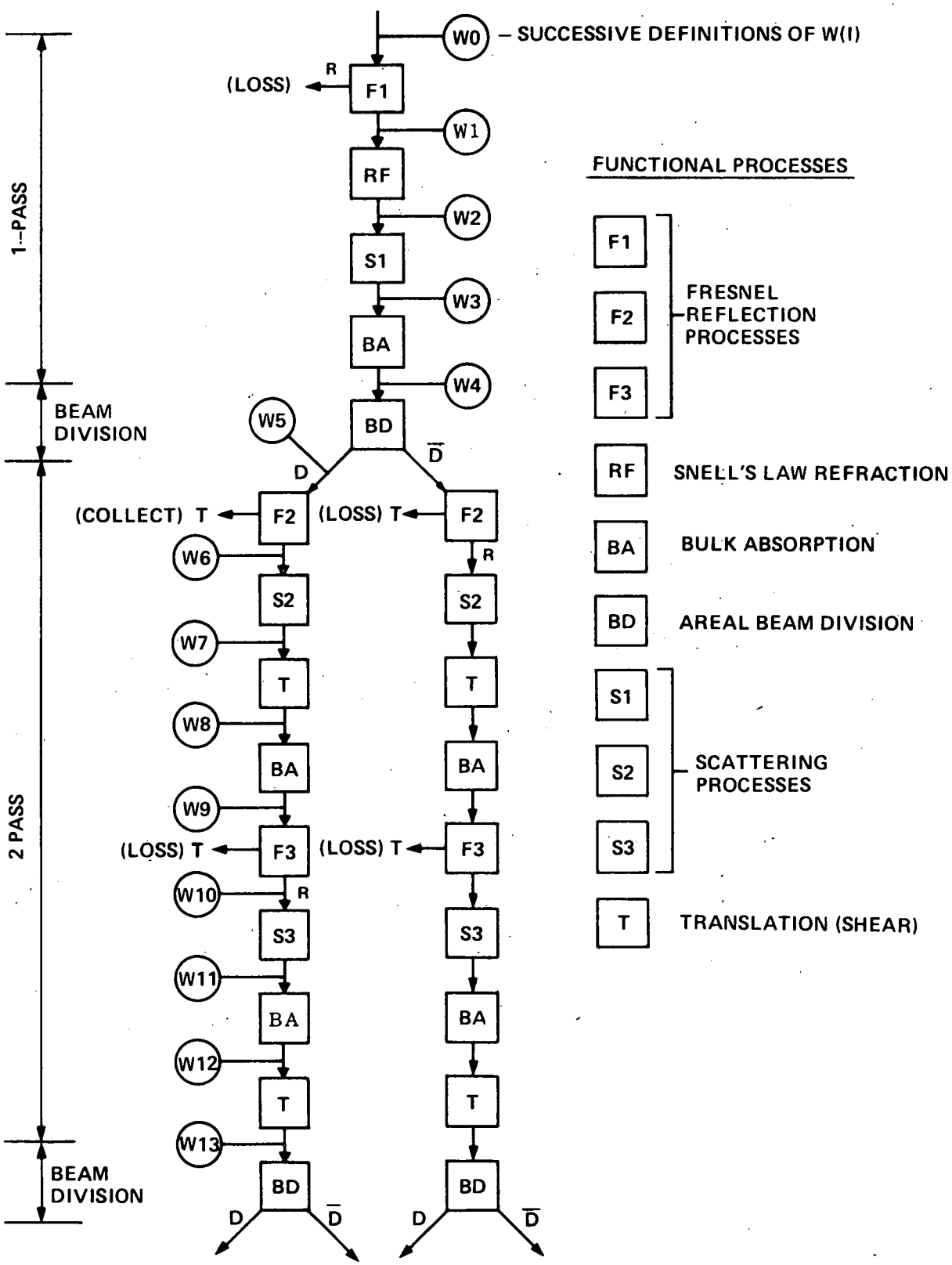

Figure A-10. Diagram of Processes Involved in the Optical Model

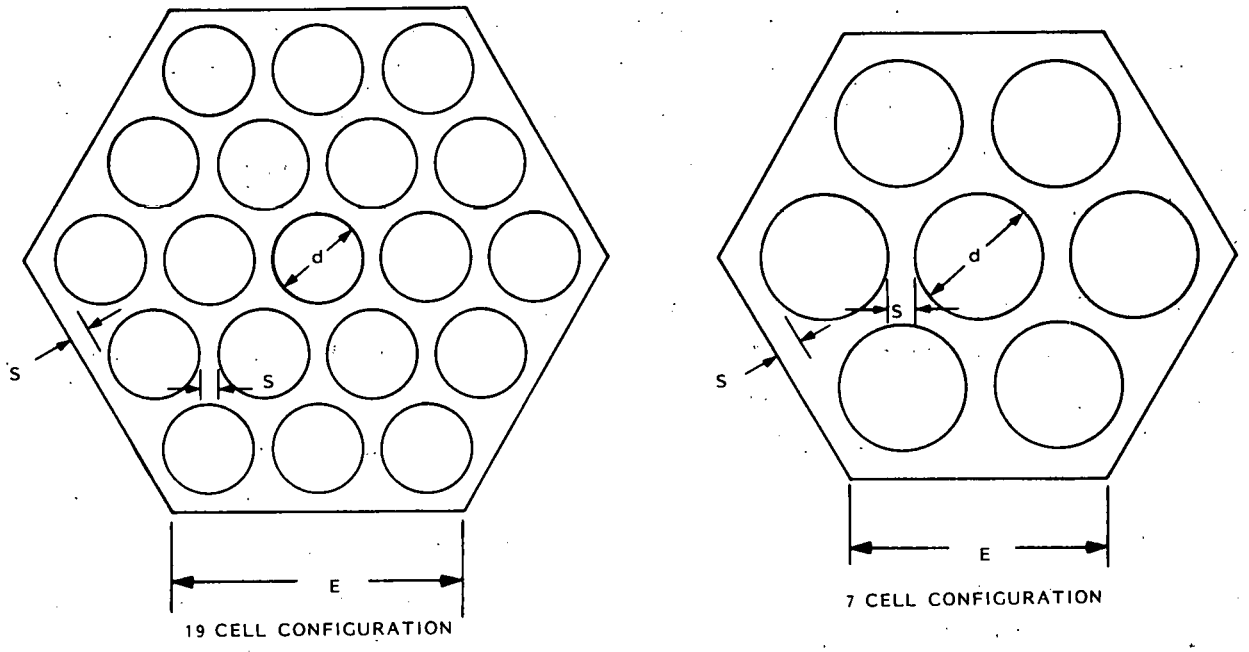

Figure A-11. Basic Hexagon Shingle Configurations

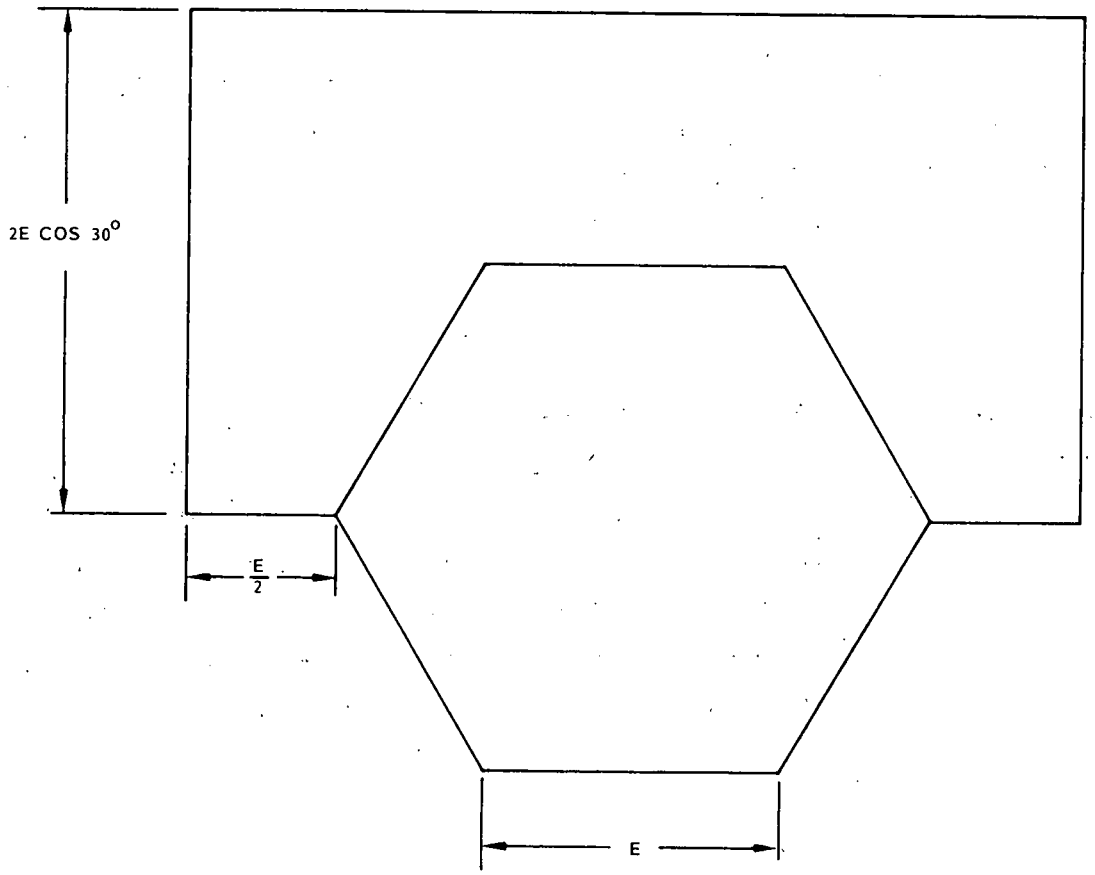

Figure A-12. Shingle Module Geometry

The minimum required glass coverplate thickness is given in Figure A-13 as a function of the hexagon edge dimension. A constant deflection at the center of a simply supported plate subjected to a central point load was used as the criterion for establishing this curve. It was assumed that the existing shingle design, which uses 3.2mm thick glass with a 139.7 mm edge dimension, gives a marginally acceptable deflection under these loading conditions.

Only direct beam radiation will be considered in the model. The assumption is made that the combination of factors which optimize the enhancement due to the direct component of insolation will also act in a similar manner to enhance the contribution due to the diffuse component. Since the angle of incidence on the outer coverplate surface has a major influence on the enhancement due to this phenomenon, the evaluation of the system performance will be made based on calculated hourly values for the angle of incidence and corresponding direct beam insolation component on the module surface. SOLMET data tapes for Boston, MA and Phoenix, AZ will be used to represent two diverse sites for this analysis. Figures A-14 and A-15 give the accumulative distribution of the annual direct beam energy density on the module surface as a function of angle of incidence for Bostom, MA and Phoenix, AZ, respectively. Hourly SOLMET data were used in both cases with a roof slope angle of 10 degrees less than the site latitude. These data show that a fixed E-W tilted solar array collects more than 50 percent of its annual direct energy at incidence angles of greater than 30 degrees. Table A-1 tabulates these data in 2 degree angular intervals for use as an input to the model.

A.4 EXPERIMENTAL RESULTS

A.4.1 SCATTERING FUNCTIONS FOR SUNADEX GLASS

The determination of the scattering functions for each surface of SUNADEX glass involved the measurement of the reflected energy which passes through an aperture of known size. Two different experimental test set-ups were required as shown in Figures A-16 and A-17. The first of these was used to determine the scattering function for the matte surface of the coverplate, but a focusing lens could not be obtained with a small enough f/ number to permit the measurement of the more widely dispersed pattern from the embossed surface. Consequently the test set-up shown in Figure A-18 was used for this case.

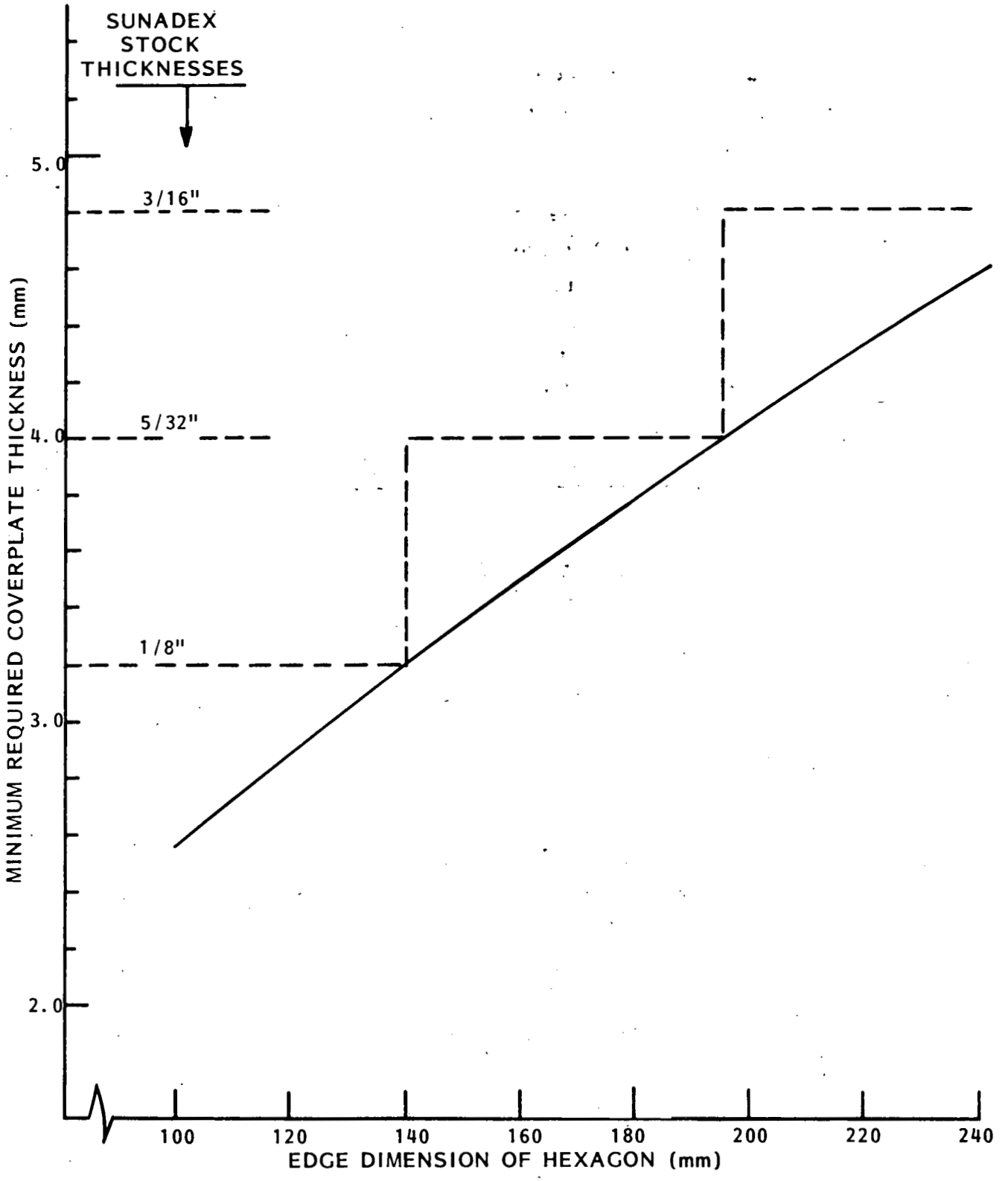

Figure A-13. Minimum Required Glass Coverplate Thickness vs. Hexagon Size

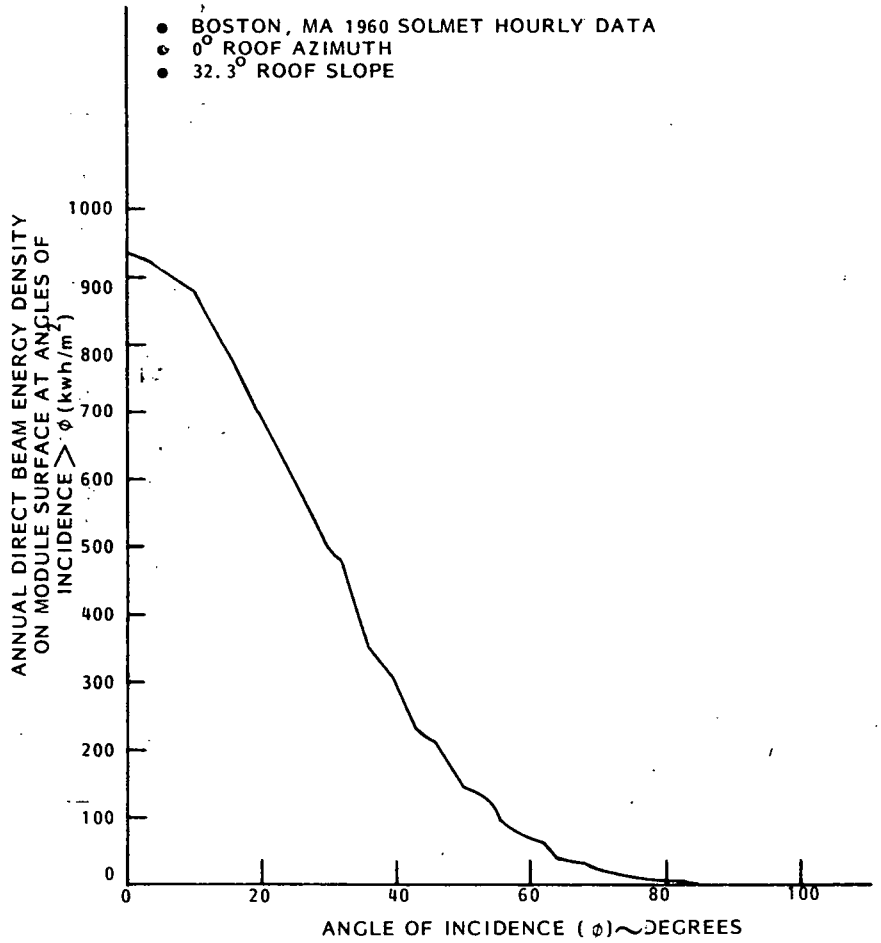

Figure A-14. Accumulative Distribution of Annual Direct Beam Energy Density as a Function of Angle of Incidence for a Boston, MA Site Location

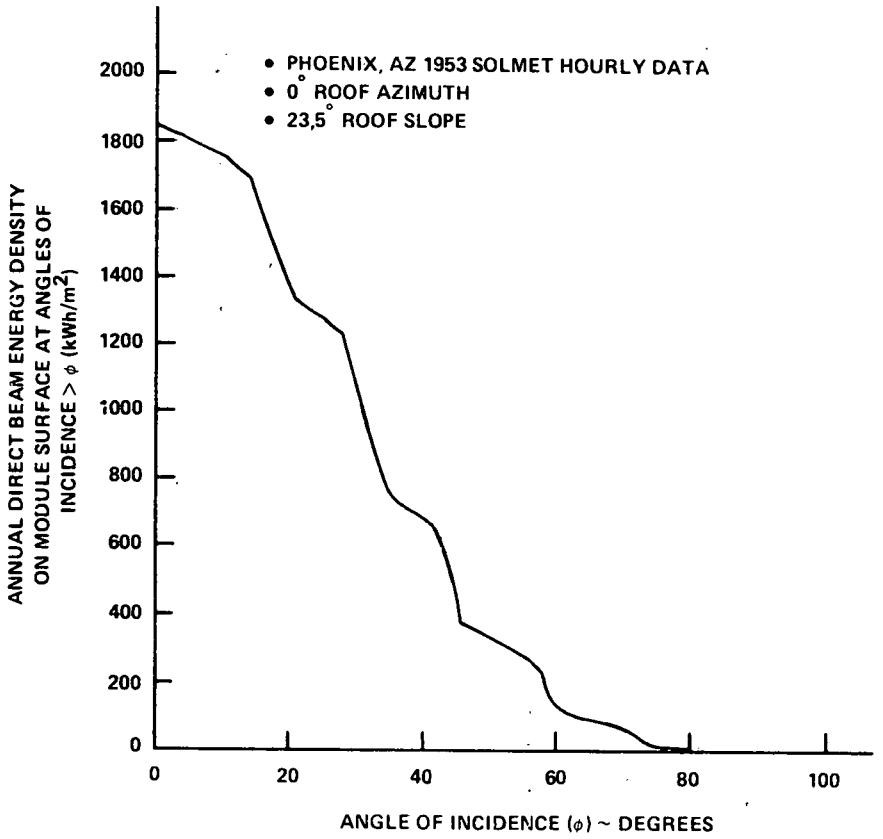

Figure A-15. Accumulative Distribution of Annual Direct Beam Energy Density as a Function of Angle of Incidence for a Phoenix, AZ Site Location

Table A-1. Angular Distribution of Annual Direct Beam Energy Density for Boston, MA and Phoenix, AZ

ANGLE of INCIDENCE		BOSTON, MA 1960 SOLMET DATA TAPE			PHOENIZ, AZ 1953 SOLMET DATA TAPE		
ϕ_1	ϕ_2	ANNUAL DIRECT BEAM ENERGY DENSITY ON MODULE SURFACE AT ANGLES OF INCIDENCE $\geq \phi_1$ (kWh/m^2)	ANNUAL DIRECT BEAM ENERGY DENSITY ON MODULE SURFACE IN INTERVAL ($\phi_1 - \phi_2$) (kWh/m^2)	FRACTION OF ANNUAL DIRECT BEAM ENERGY DENSITY ON MODULE SURFACE IN INTERNAL ($\phi_1 - \phi_2$)	ANNUAL DIRECT BEAM ENERGY DENSITY ON MODULE SURFACE AT ANGLES OF INCIDENCE $\geq \phi_1$ (kWh/m^2)	ANNUAL DIRECT BEAM ENERGY DENSITY ON MODULE SURFACE IN INTERVAL ($\phi_1 - \phi_2$) (kWh/m^2)	FRACTION OF ANNUAL DIRECT BEAM ENERGY DENSITY ON MODULE SURFACE IN INTERVAL ($\phi_1 - \phi_2$)
0	2	932.4	0.	0.	1853.6	16.7	0.00901
2	4	932.4	9.6	0.01030	1836.9	20.1	0.01084
4	6	922.8	15.5	0.01662	1816.8	19.3	0.01041
6	8	907.3	12.1	0.01298	1797.5	19.3	0.01041
8	10	895.2	12.8	0.01373	1778.2	20.5	0.01106
10	12	882.4	33.9	0.03636	1757.7	26.2	0.01413
12	14	848.5	40.8	0.04376	1731.5	43.1	0.02325
14	16	807.7	34.9	0.03743	1688.4	130.2	0.07024
16	18	772.8	37.9	0.04065	1558.2	90.9	0.04904
18	20	734.9	46.1	0.04944	1467.3	101.1	0.05454
20	22	688.8	30.4	0.03260	1366.2	54.1	0.02919
22	24	658.4	40.0	0.04290	1312.1	29.4	0.01586
24	26	618.4	32.1	0.03443	1282.7	27.4	0.01478
26	28	586.3	47.2	0.05062	1255.3	30.0	0.01618
28	30	539.1	40.8	0.04376	1225.4	144.8	0.07812
30	32	498.3	22.0	0.02360	1080.6	173.0	0.09333
32	34	476.3	70.0	0.07508	907.6	101.9	0.05497
34	36	406.3	59.7	0.06403	805.7	68.0	0.03669
36	38	346.6	22.9	0.02456	737.7	35.0	0.01888
38	40	323.7	22.2	0.02381	702.7	21.6	0.01165
40	42	301.5	54.8	0.05877	681.1	24.2	0.01306
42	44	246.7	26.0	0.02789	656.9	106.2	0.05729
44	46	220.7	10.6	0.01137	550.7	176.7	0.09533
46	48	210.1	35.8	0.03840	374.0	24.6	0.01327
48	50	174.3	34.8	0.03732	349.4	21.4	0.01155
50	52	139.5	9.2	0.00987	328.0	17.9	0.00966
52	54	130.3	14.3	0.01534	310.1	20.1	0.01084
54	56	116.0	28.3	0.03035	290.0	26.5	0.01430
56	58	87.7	12.9	0.01384	263.5	38.1	0.02055
58	60	74.8	5.0	0.00536	225.4	103.9	0.05605
60	62	69.8	9.5	0.01019	121.5	19.3	0.01041
62	64	60.3	24.4	0.02617	102.2	11.4	0.00615
64	66	35.9	3.4	0.00365	90.8	9.1	0.00491
66	68	32.5	1.3	0.00139	81.7	11.7	0.00631
68	70	31.2	11.8	0.01266	70.0	4.5	0.00243
70	72	19.4	5.8	0.00622	65.5	12.5	0.00674
72	74	13.6	0.9	0.00097	53.0	33.3	0.01797
74	76	12.7	3.6	0.00386	19.7	12.1	0.00653
76	78	9.1	5.8	0.00622	7.6	2.5	0.00135
78	80	3.3	0.3	0.00032	5.1	0.8	0.00043
80	82	3.0	0.4	0.00043	4.3	0.4	0.00022
82	84	2.6	1.9	0.00204	3.9	0.0	0.
84	86	0.7	0.6	0.00064	3.9	1.7	0.00092
86	88	0.1	0.0	0.	2.2	1.7	0.00092
88	90	0.1	0.1	0.00011	0.5	0.5	0.00027
90		0.			0.		

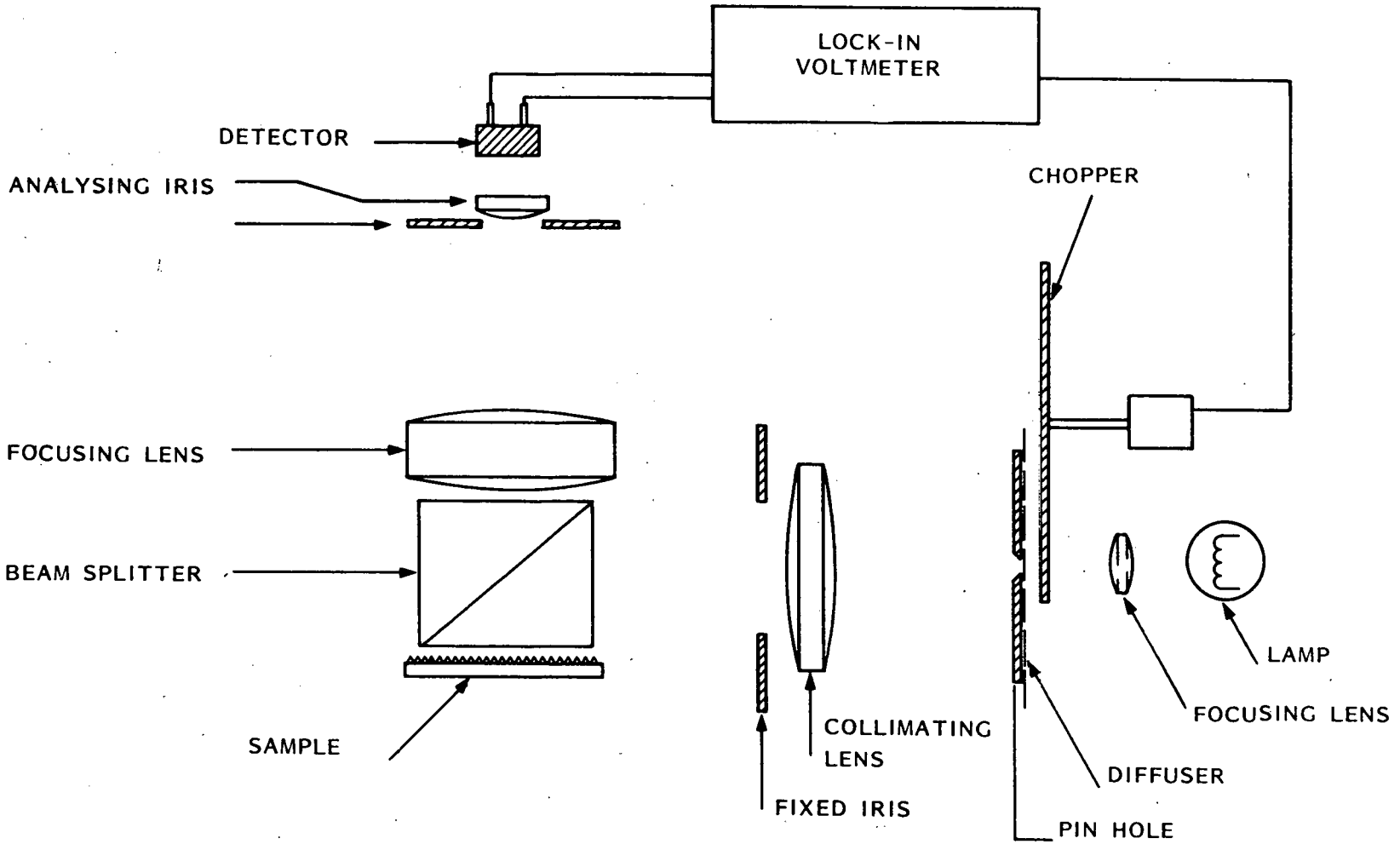

Figure A-16. Schematic of Experimental Apparatus for the Determination of the Scattering Function of the Matte Surface

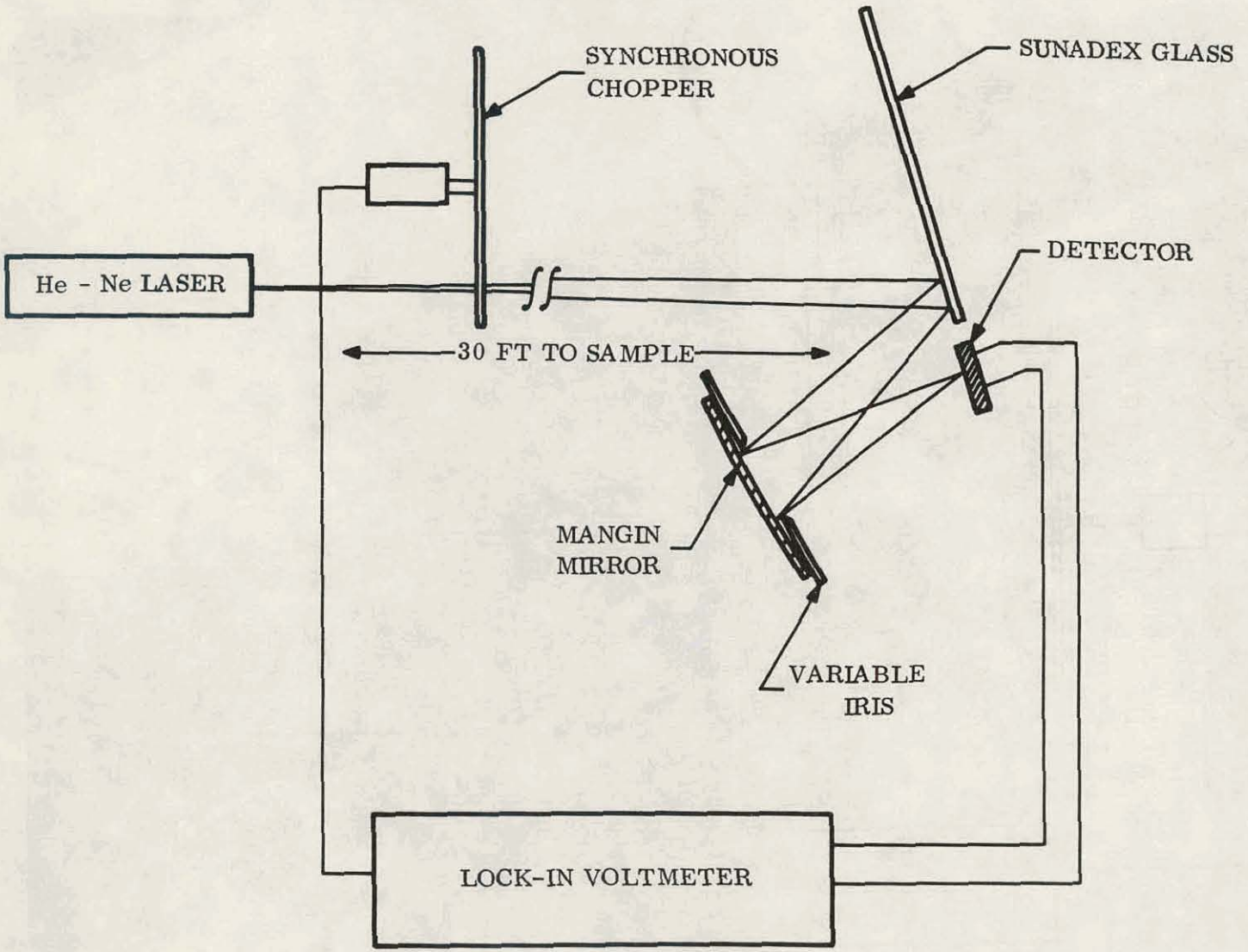

Figure A-17. Schematic of Experimental Apparatus for the Determination of the Scattering Function of the Embossed Surface

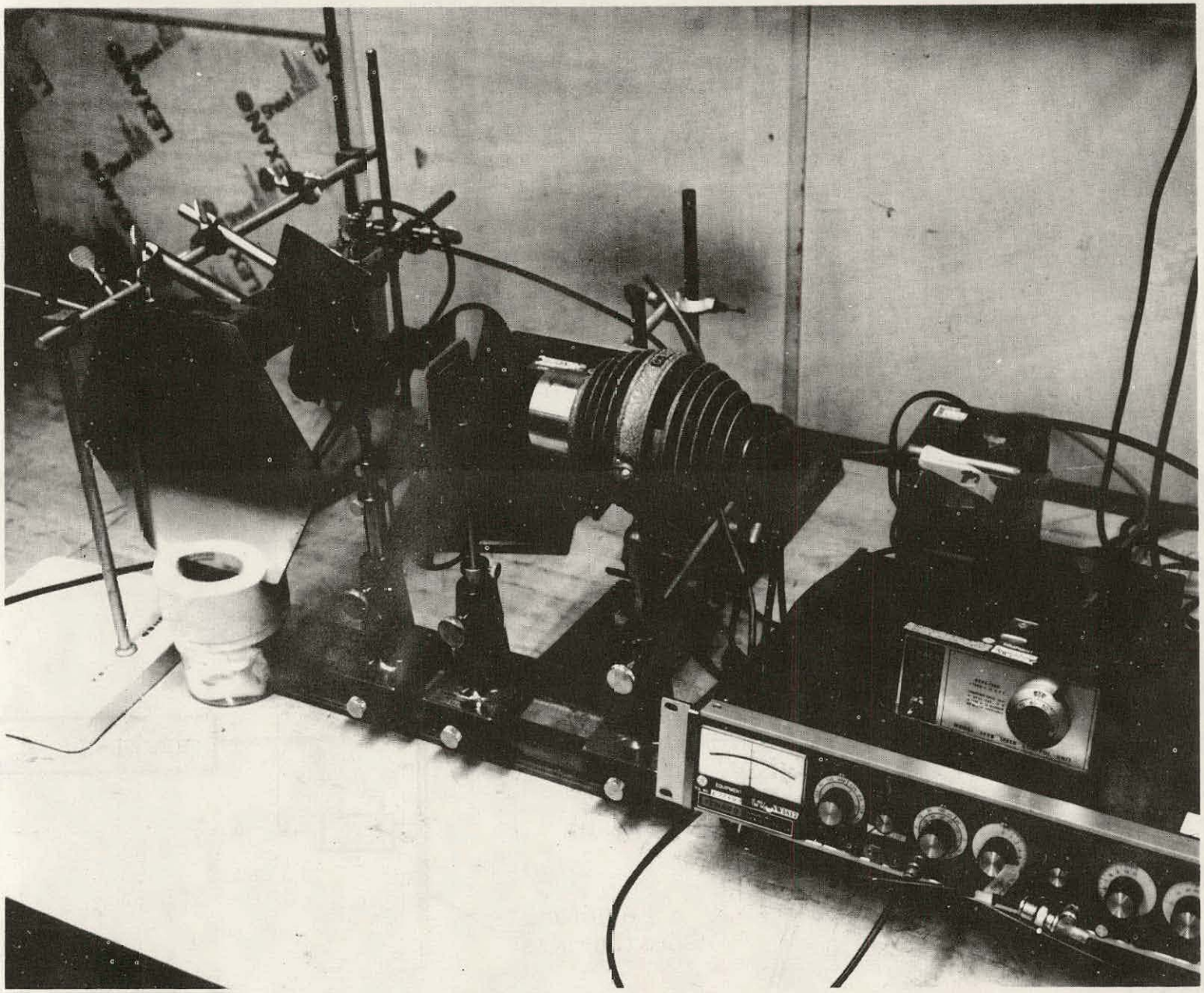

Figure A-18. Experimental Set-up for the Determination of Scattering Function of Matte Surface (VF78-526A)

For the limited scattering from the matte surface the apparatus shown in Figure A-18 proved to give satisfactory results. A lamp, whose brightness is controlled by a Variac, is focused on the pin hole aperture. Energy passing through the pin hole is collimated and passes through an iris whose function is to limit the collimated bundle to a controlled size.

Approximately 50 percent of the illuminating bundle is reflected by the beam splitter face. The SUNADEX glass has previously been aluminized with a thin but opaque coating. The coating was deliberately kept thin in order to retain the print of the rough surface. The reflected beam, which is diverging due to the diffuse reflection, passes through the beam splitter. It is important to keep the bundle as large as possible, but relatively small with respect to the size of the beam splitter, to prevent internal reflection from interfering with the measurements.

An "image" of the diffuse bundle is formed at the focal plane of the focusing lens. This plane coincides with the variable size analyzing iris. The diameter of the iris is related to the slope by:

$$D = 4f \tan\alpha$$

where

D = the image diameter

f = the focal length of the focusing lens

= 3.00 inches for the test set-up in Figure A-16

α = the surface slope error

The signal received is a function of the analyzing iris diameter. If the pin hole were an infinitesimal point source, and the sample perfectly smooth, the output signal would be constant as the analyzing aperture diameter is varied. Since the hole is finite, however, there is a variable signal as a function of the analyzing aperture but only for very small values of diameter. If the scattered "image" is fairly large compared to the pin hole image, the analyzing function is essentially constant representing a delta function input. In such a case the measured signal from the matte surface, as a function

of iris diameter, is a direct function of surface slope error. The function of the field lens is to relay the energy passing through the analyzing iris to the detector. Its focal length is chosen so that the entire diameter of the focusing lens is imaged on the detector surface and its diameter is chosen to match the largest surface slope deviation to be considered. In this way, all energy passing through the focusing lens is imaged on the detector.

A photovoltaic detector coupled to a lock-in voltmeter whose reference signal was derived from a mechanical chopper was employed. A chopping frequency of 200 Hertz was employed to avoid interference from room light which operate on a base frequency of 120 Hertz.

In the case of the embossed surface, shown in the scanning electron micrograph of Figure A-19 the test set-up was changed to accomodate the wider scatter of the reflected light from this surface. As shown schematically in Figure A-17 a laser beam impinges on the embossed glass surface and is reflected onto a Mangin mirror through an analyzing iris. The Mangin mirror then focuses the scattered radiation, which passes through the iris, onto a photovoltaic detector which yields an electrical signal proportional to the intensity of the light on the detector. The formula for the determination of surface slope error is the same as previously presented for the matte surface set-up except that (f) becomes the distance between the plane of the analyzing iris and the point of focus on the embossed surface. In the case of the set-up shown in Figure A-17, the value of (f) is 4.875 inches.

Figure A-20 gives the normalized detector signal as a function of analyzing iris diameter for both surfaces of the SUNADEX glass. These data were fitted with a polynomial of the form:

$$V = a_o + a_1 D \; a_2 D^2 + a_3 D^3 + a_4 D^4 + a_5 D^5 + a_6 D^6 + a_7 D^7$$

where

V = normalized detector signal

D = analyzing iris diameter (inches)

Figure A-19. SEM of the Embossed Surface of SUNADEX Glass

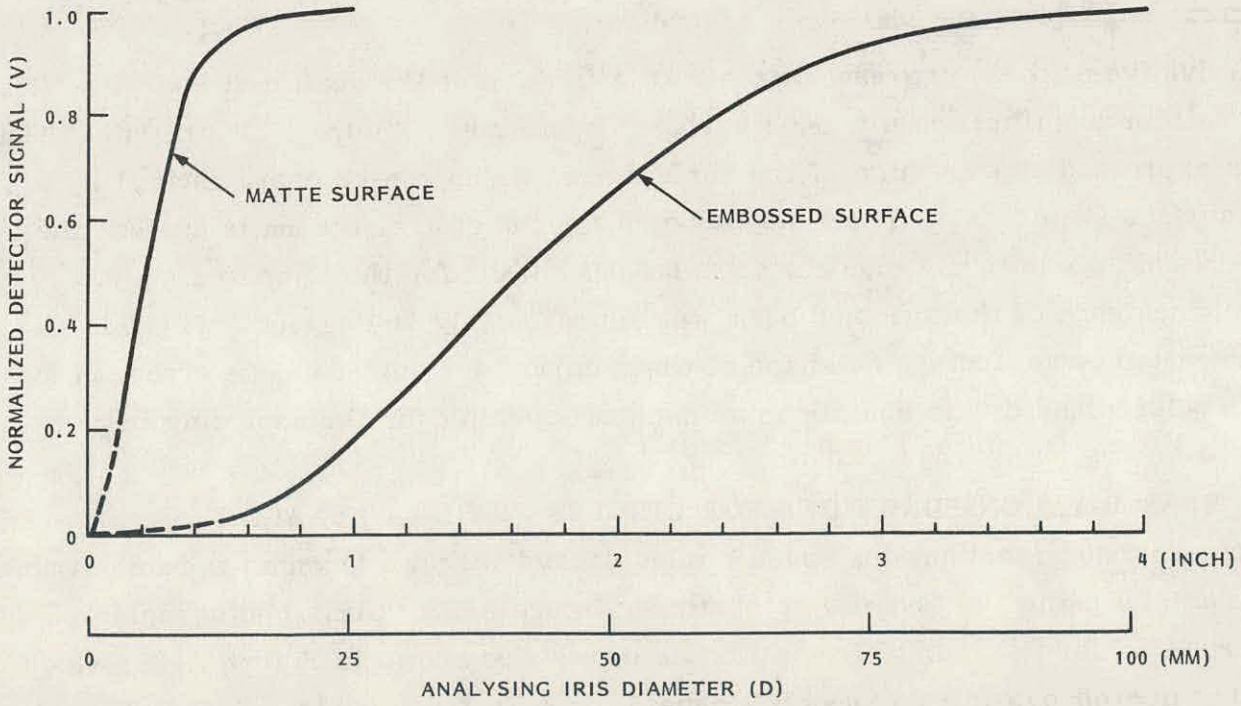

Figure A-20. Normalized Detector Signal vs. Analyzing Iris Diameter

For these two surfaces the values for the polynomial coefficients are as given in Table A-2.

Table A-2. Coefficients of the Polynomial Describing the Detector Signal as a Function of the Analyzing Iris Diameter

	Embossed Surface	Matte Surface
a_0	1.44754E-4	-4.10052E-3
a_1	1.31156E-1	6.65302E-1
a_2	-6.97379E-1	1.51415E1
a_3	1.47873	-4.40255E1
a_4	-1.03139	4.56052E1
a_5	3.44919E-1	-1.63851E1
a_6	-5.70684E-2	0
a_7	3.75892E-3	0

The derivative of these expressions yields the fraction of the scattered energy which occurs within an infinitesimally small surface slope error. Figure A-21 presents these results expressed as a fraction of the surface area which can be characterized by a given surface slope error. It should be noted for the case of the matte surface the data pertains to a normally incident specular beam while for the embossed surface the angle of incidence of the specular beam was approximately 20 degrees. There is also some uncertainty regarding the shape of these curves for surface slope errors of less than 10 milliradians due to limitations on minimum opening for the analyzing iris.

A.4.2 BEAM DIVISION FUNCTIONS FOR CIRCLES WITHIN A HEXAGON

The beam division functions for seven circles packed within a hexagon were determined experimentally using the test set-up shown in Figure A-22. Glass photographic plates were prepared for the four different module geometries shown in Figure A-23, which represent overall packing factors (PF) ranging from 0.814 to 0.514. These glass plates representing the various patterns were shifted in the test setup to obtain the various

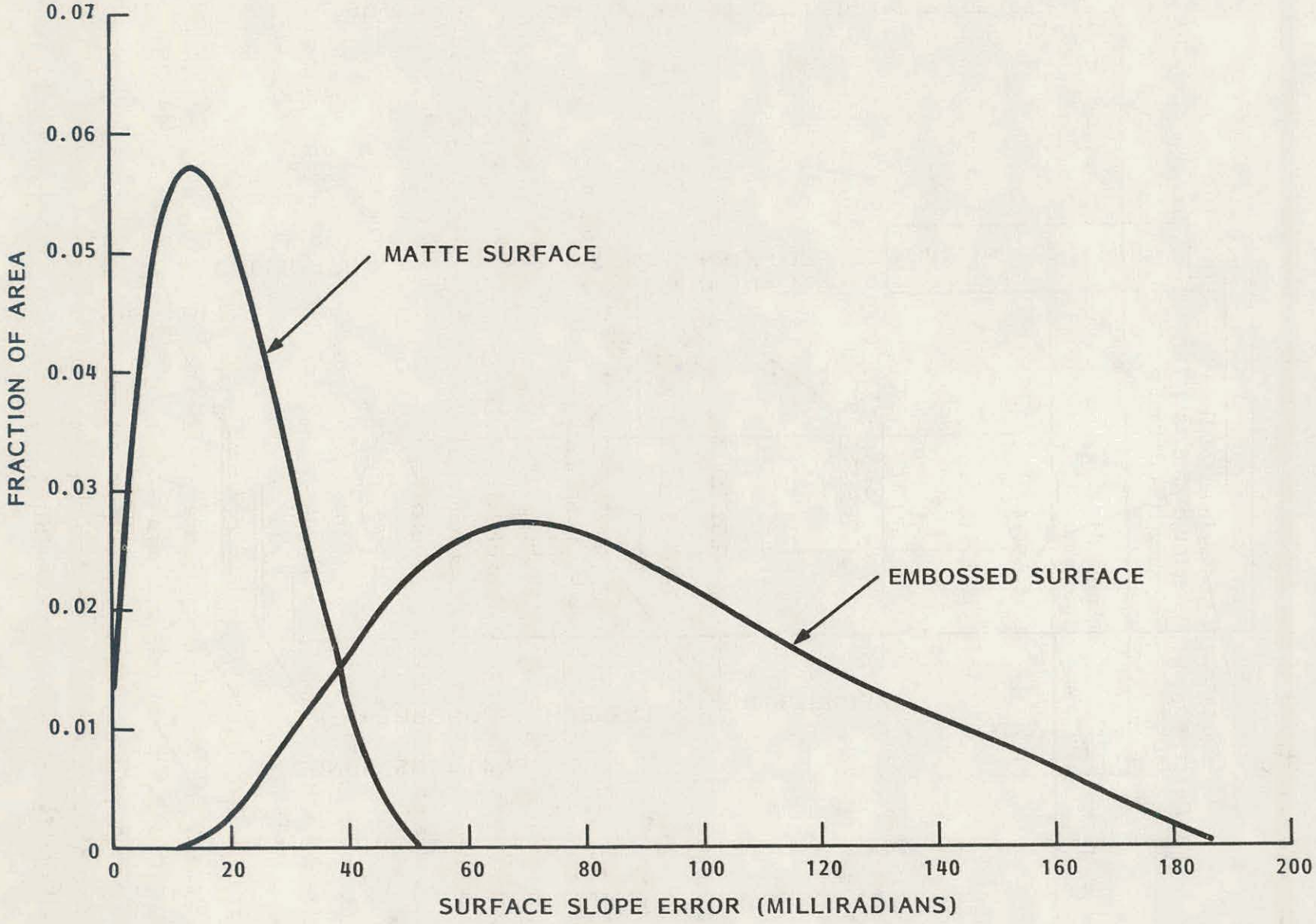

Figure A-21. Characteristic Reflective Scattering Functions for SUNADEX Glass

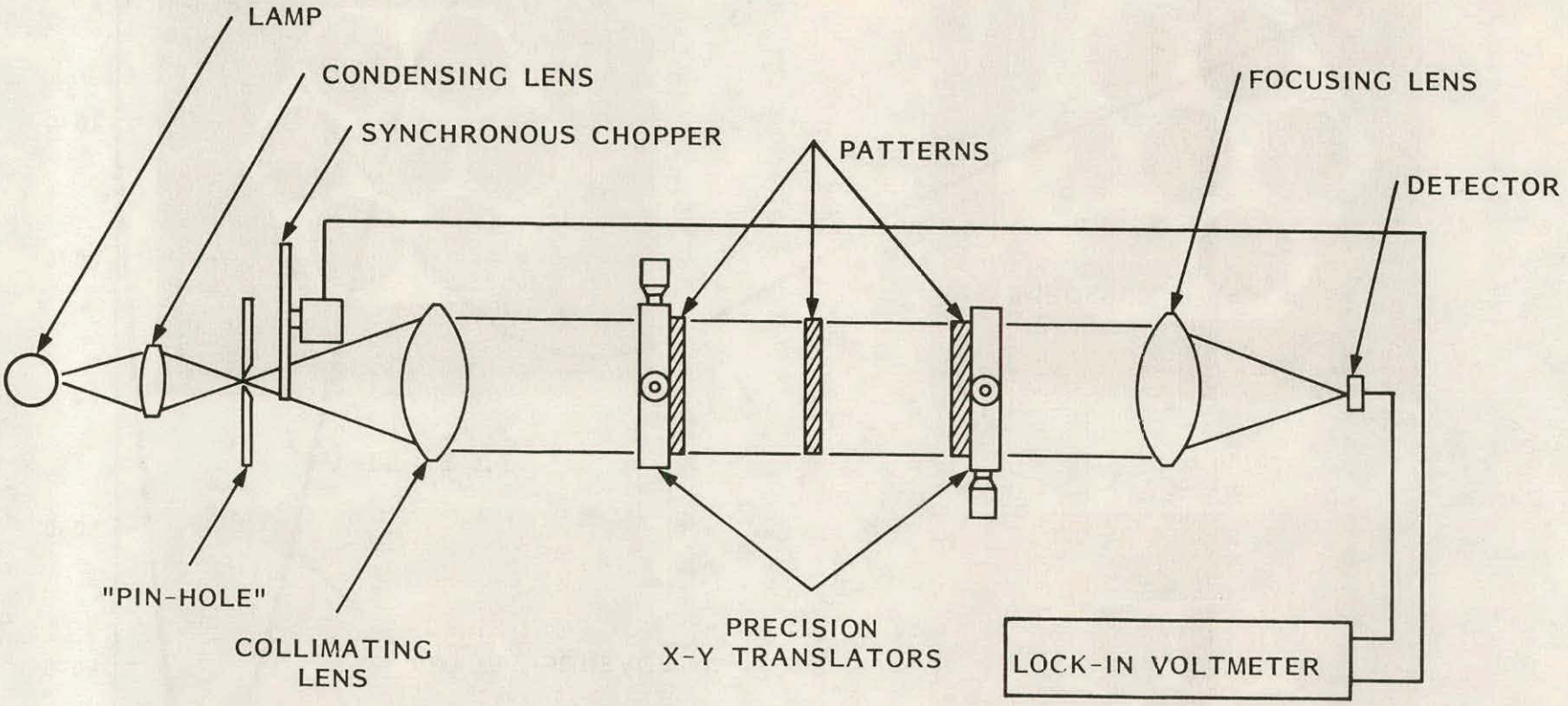

Figure A-22. Schematic of Experimental Apparatus for the Determination of the Beam Division Functions

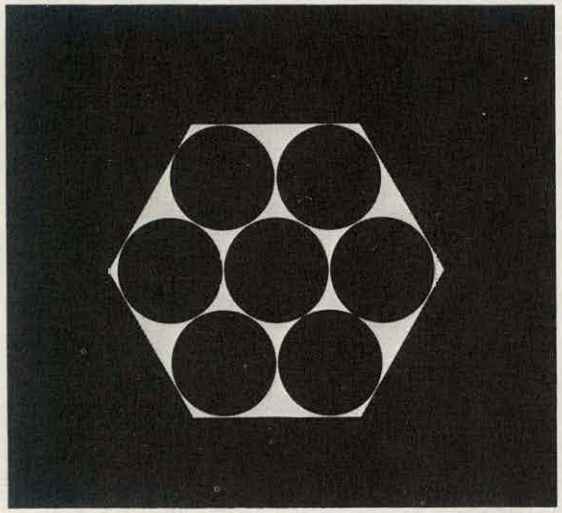

(a) PF = 0.814

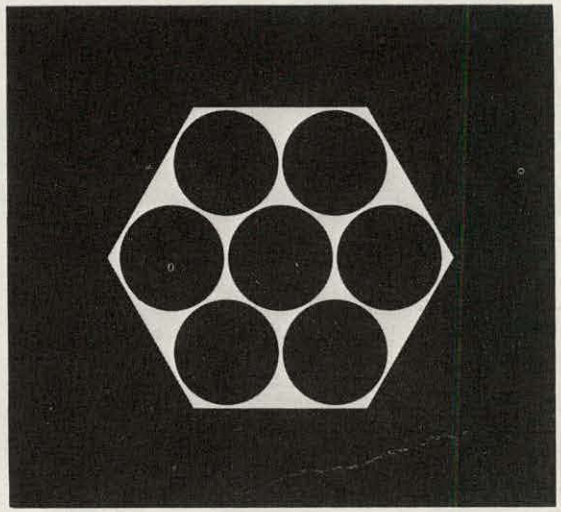

(b) PF = 0.782

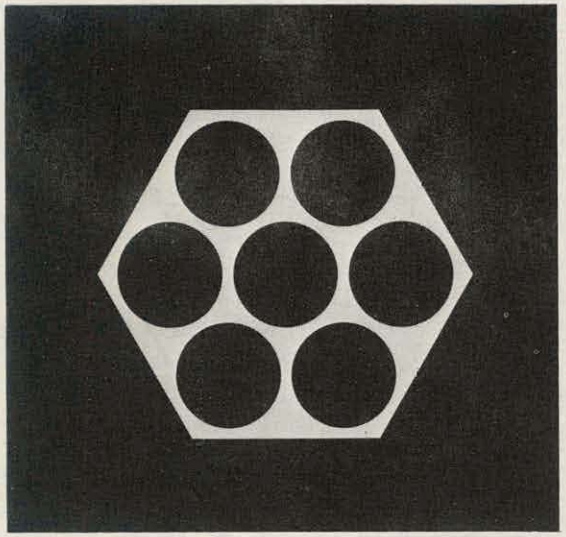

(c) PF = 0.658

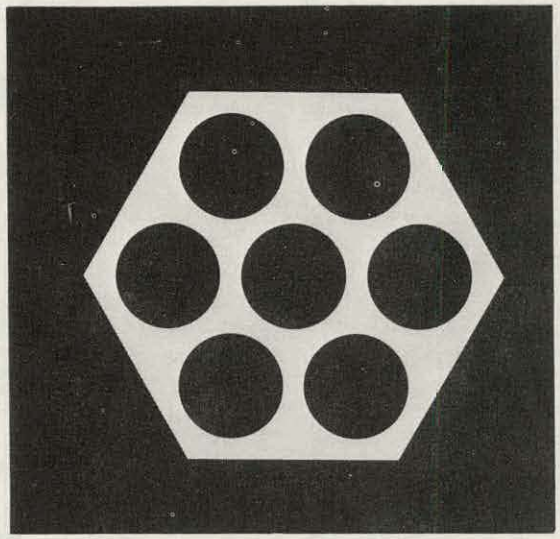

(d) PF = 0.514

Figure A-23. Photographic Masks used for the Determination of Beam Division Functions

beam division functions given in Figure A-24. The nomenclature DD, $\overline{D}$D refers to energy which is reflected from a solar cell (D) or from the interstices ($\overline{D}$) and consequently falls on a solar cell (D) after a single reflection from the top coverplate surface. This nomenclature is further clarified by referring to Figure A-25 which graphically represents the four possible combinations with a single reflection from the top coverplate surface.

For the case where two reflections are involved the nomenclature consist of three characters, e.g., DDD. In this example the beam division function represents that energy which falls on a solar cell after two reflections from the top coverplate surface of energy which falls on a solar cell.

A.5 DESCRIPTION OF OPTICAL ANALYSIS PROGRAM

A.5.1 OVERALL PROGRAM FLOW

The overall organization of the optical analysis program is shown in Figure A-26. The program is written in Honeywell Level 66/6000 FORTRAN and should be compatible, with minor modifications, with any FORTRAN compiler. The program is configured for execution in a time-sharing mode from a remote terminal. An introductory program explanation will be outputted on request after compilation has been completed. Input data will then be requested before the main portion of the program is entered. As shown in Figure A-27 this main program consists of an accounting of various integer identifiers or flags and repeated calls of two principal calculation procedures identified as "1-PASS" and "2-PASS". These two procedures consist of the sequential call of five subroutines as shown in Figures A-28 and A-29, respectively.

The details of the main program logic are given in Figure A-27 along with the status of the five integer identifiers or flags at each stage of the calculation sequence. The notations D, D, (D)D, (D)D, etc. can be explained with the aid of Figure A-30 which shows the successive routes through the glass coverplate for the two 2-PASS sequences considered in the model.

The notation "C" beside some blocks on Figure A-27 indicates that energy is collected by the solar cell as a consequence of that set of processes.

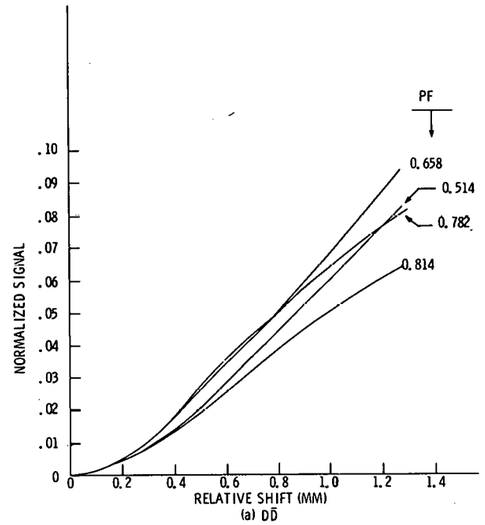

(a) $D\bar{D}$

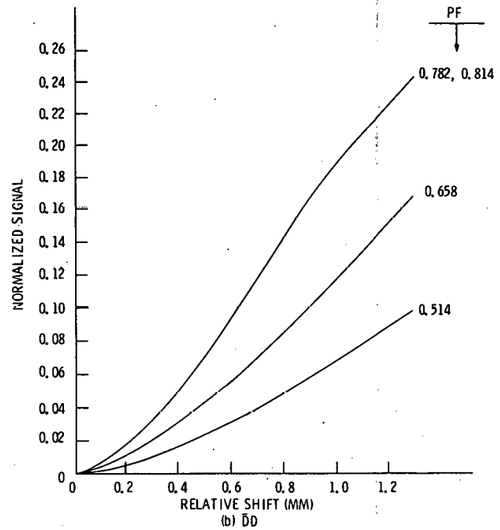

(b) $\bar{D}D$

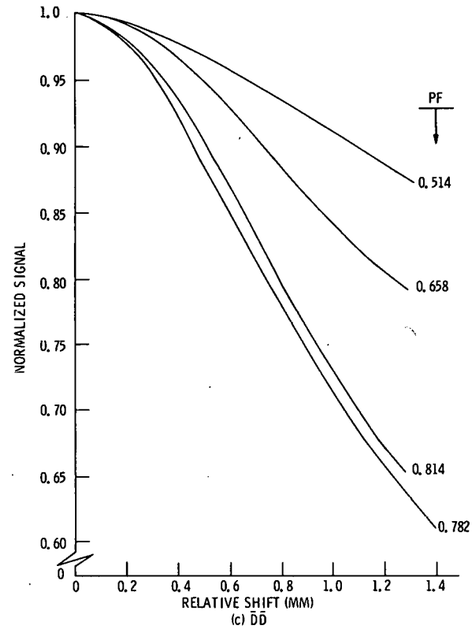

(c) $\bar{D}\bar{D}$

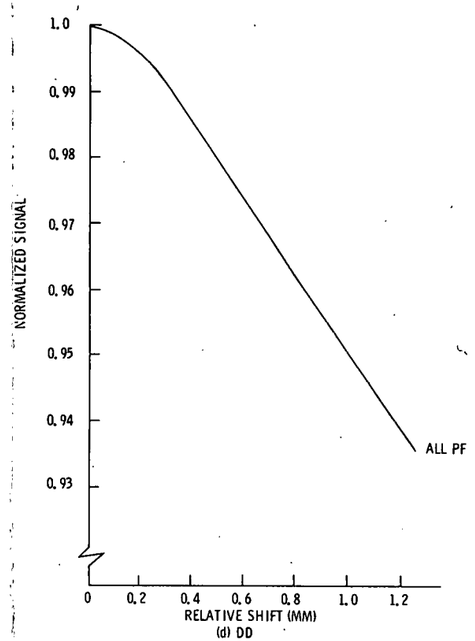

(d) DD

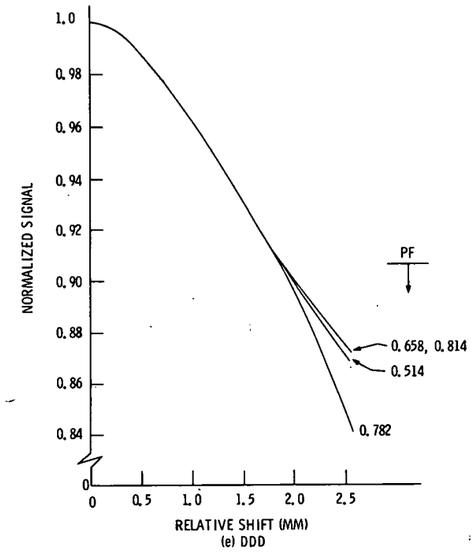

(e) DDD

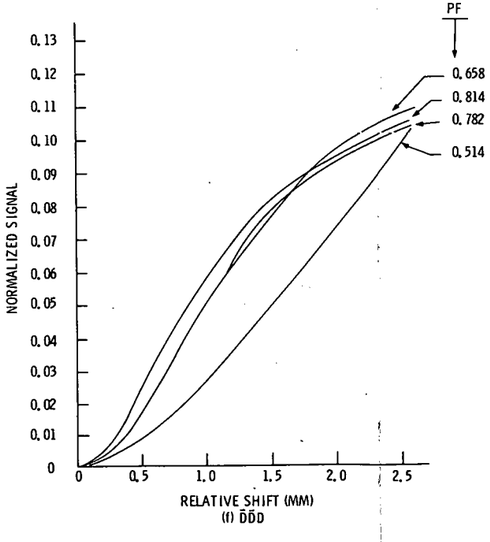

(f) $D\bar{D}D$

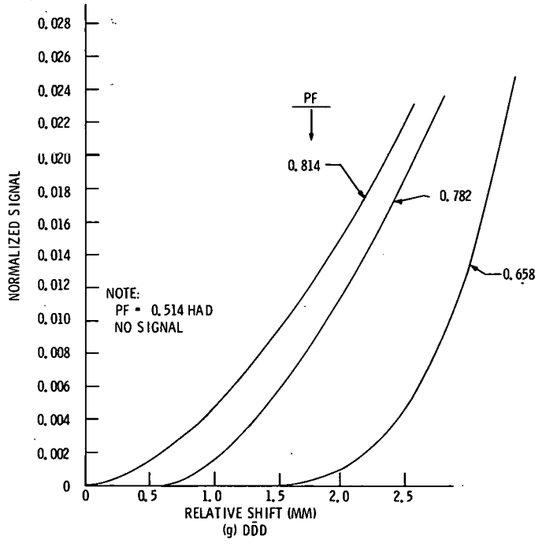

(g) $D\bar{D}D$

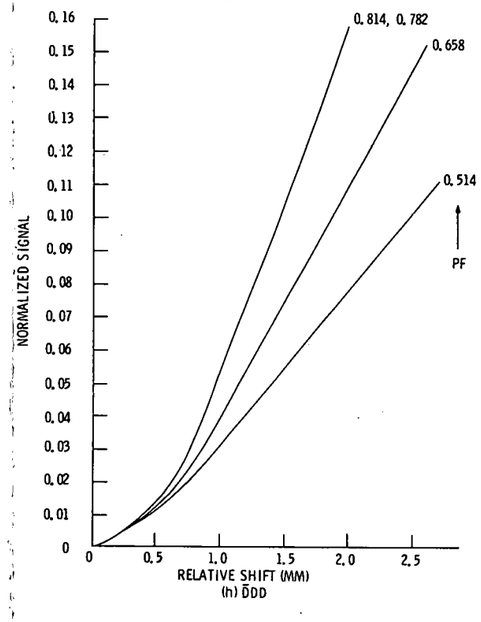

(h) $\bar{D}DD$

Figure A-24. Beam Division Functions

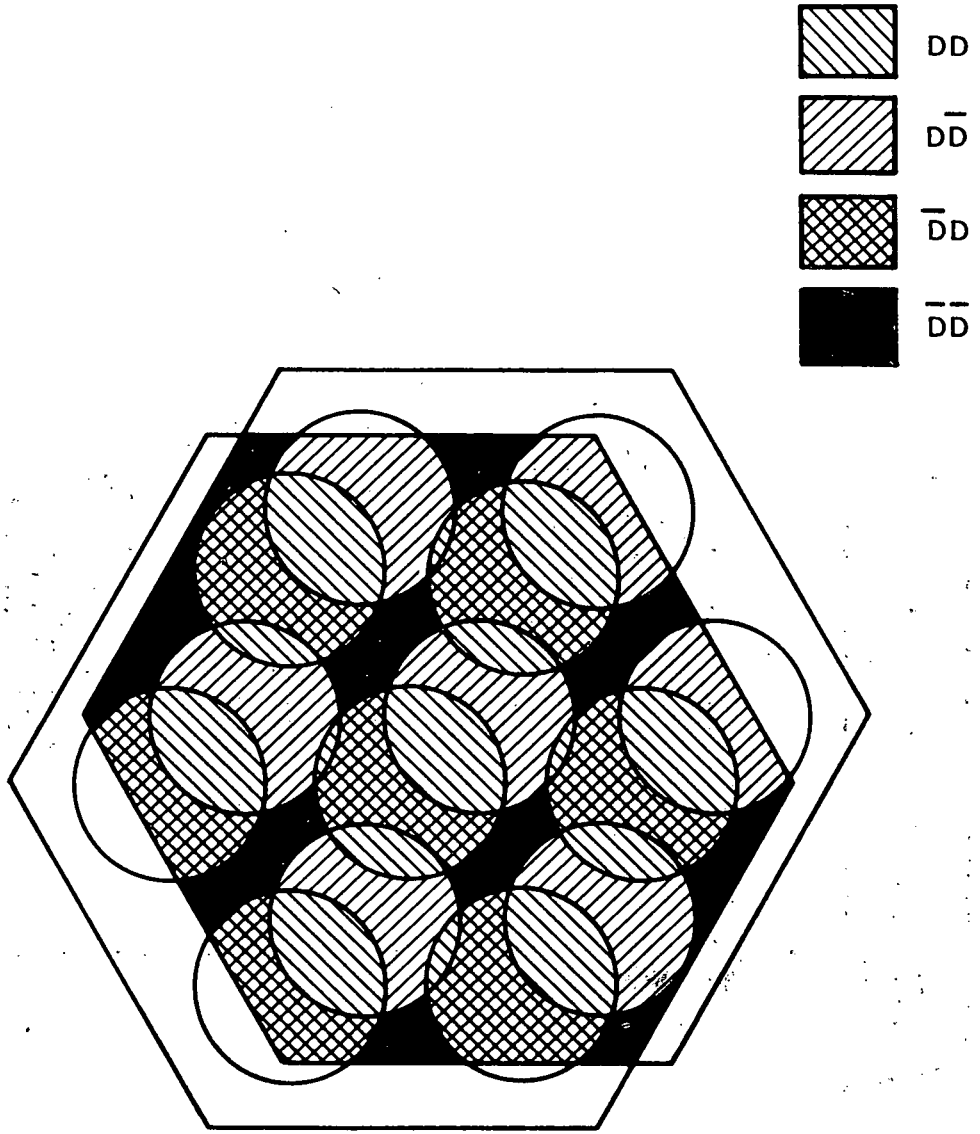

Figure A-25. Graphical Representation of Beam Division Functions

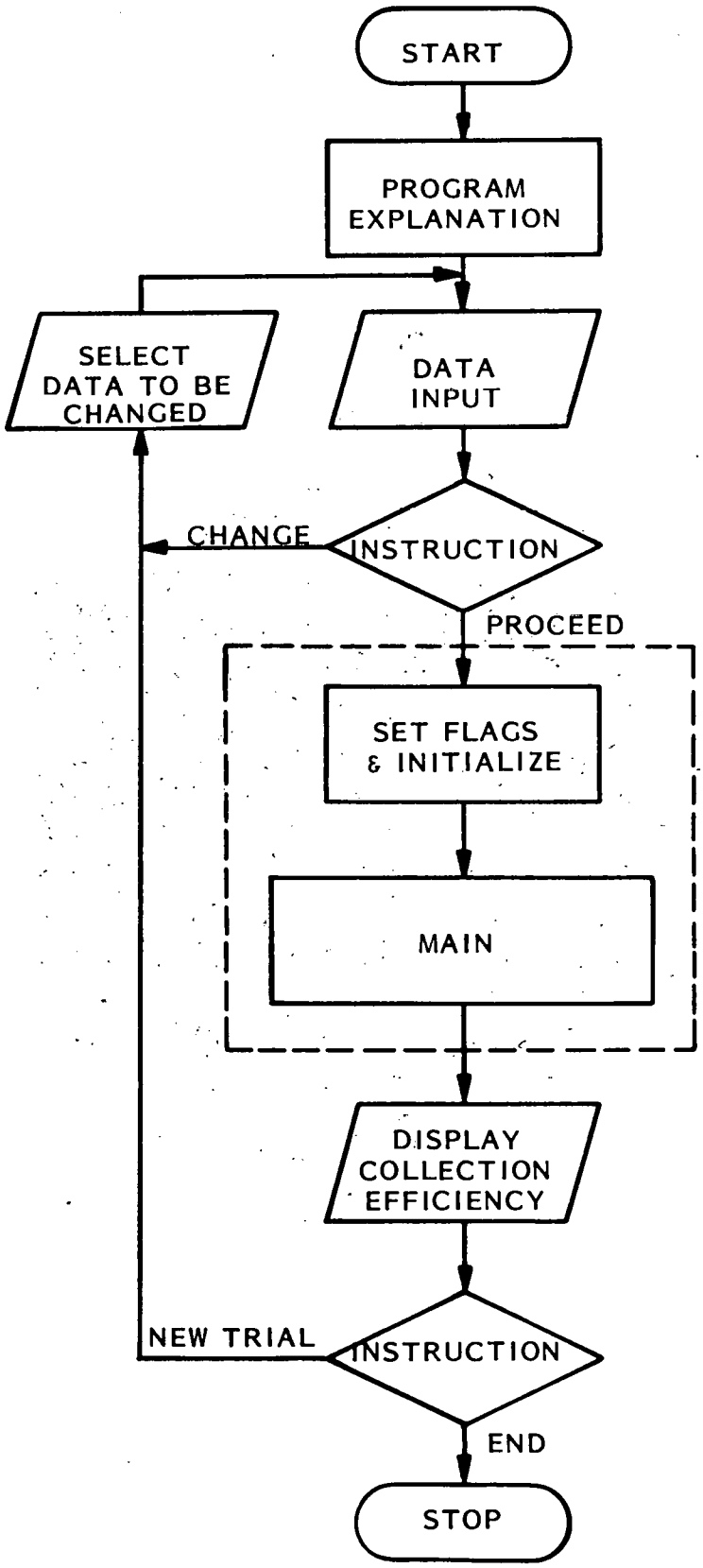

Figure A-26. Overall Program Organization

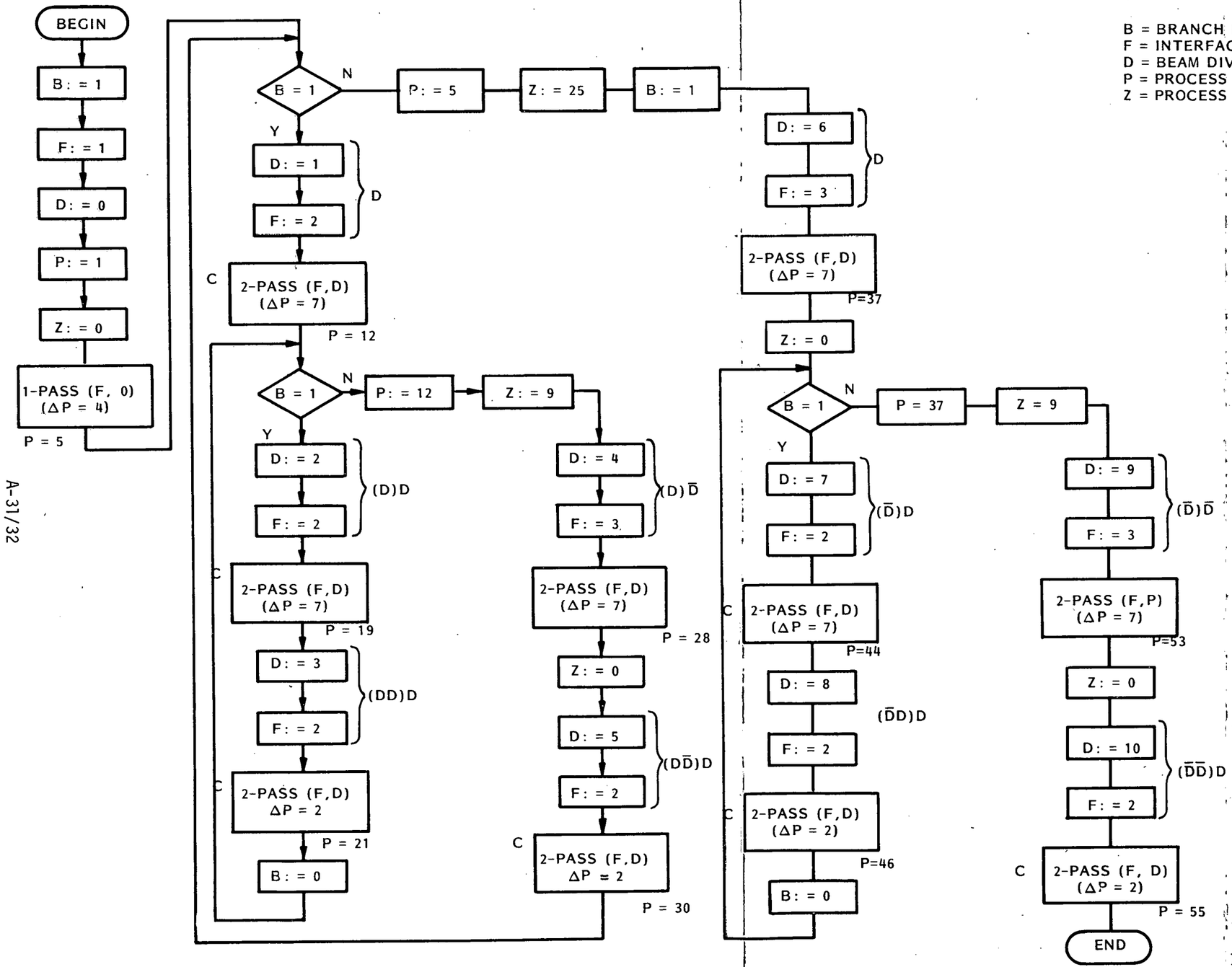

B = BRANCH IDENTIFIER
F = INTERFACE IDENTIFIER
D = BEAM DIVISION CASE
P = PROCESS COMPLETION FLAG
Z = PROCESS COUNT DISPLAY FLAG

Figure A-27. Main Program Logic Flow Diagram

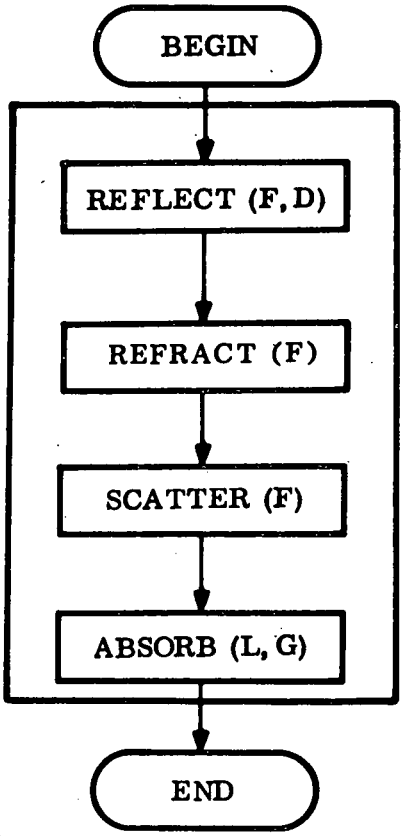

Figure A-28. Logic Flow Diagram for the 1-PASS Procedure

A.5.2 SUBROUTINE REFLECT

Figure A-31 gives a detailed logic flow diagram for the REFLECT subroutine. The function of this subroutine is the account for the Fresnel reflection from both the upper and lower surfaces of the glass coverplate. The logic diagram has been annotated to indicate the nature of the operation being performed in each block. The routine includes the flexibility to consider a single-layer anti-reflective coating on the upper surface of the coverplate. The following definitions are appropriate to the understanding of this routine:

F=1 Upper surface, rare-to-dense interface

F=2 Lower surface, solar cell interface

F=3 Lower surface, interstices interface

F=4 Upper surface, dense-to-rare interface

N(1) = Index of refraction for air (=1)

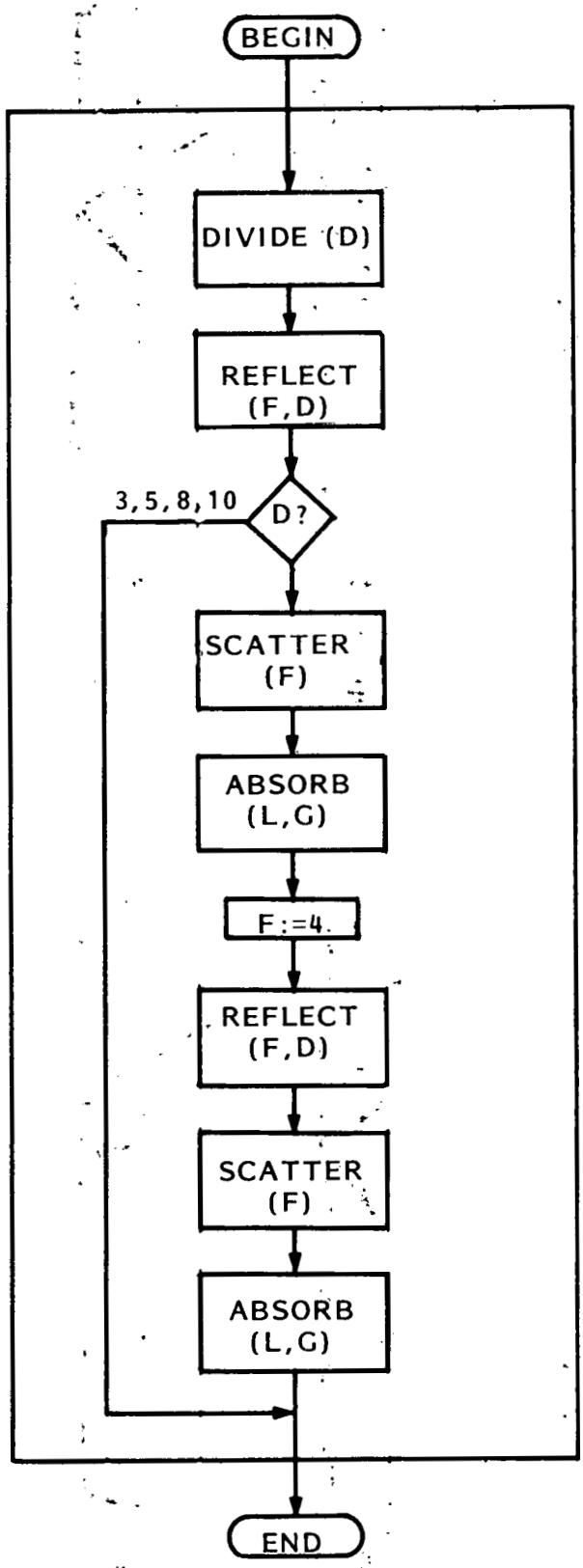

Figure A-29. Logic Flow Diagram for the 2-PASS Procedure

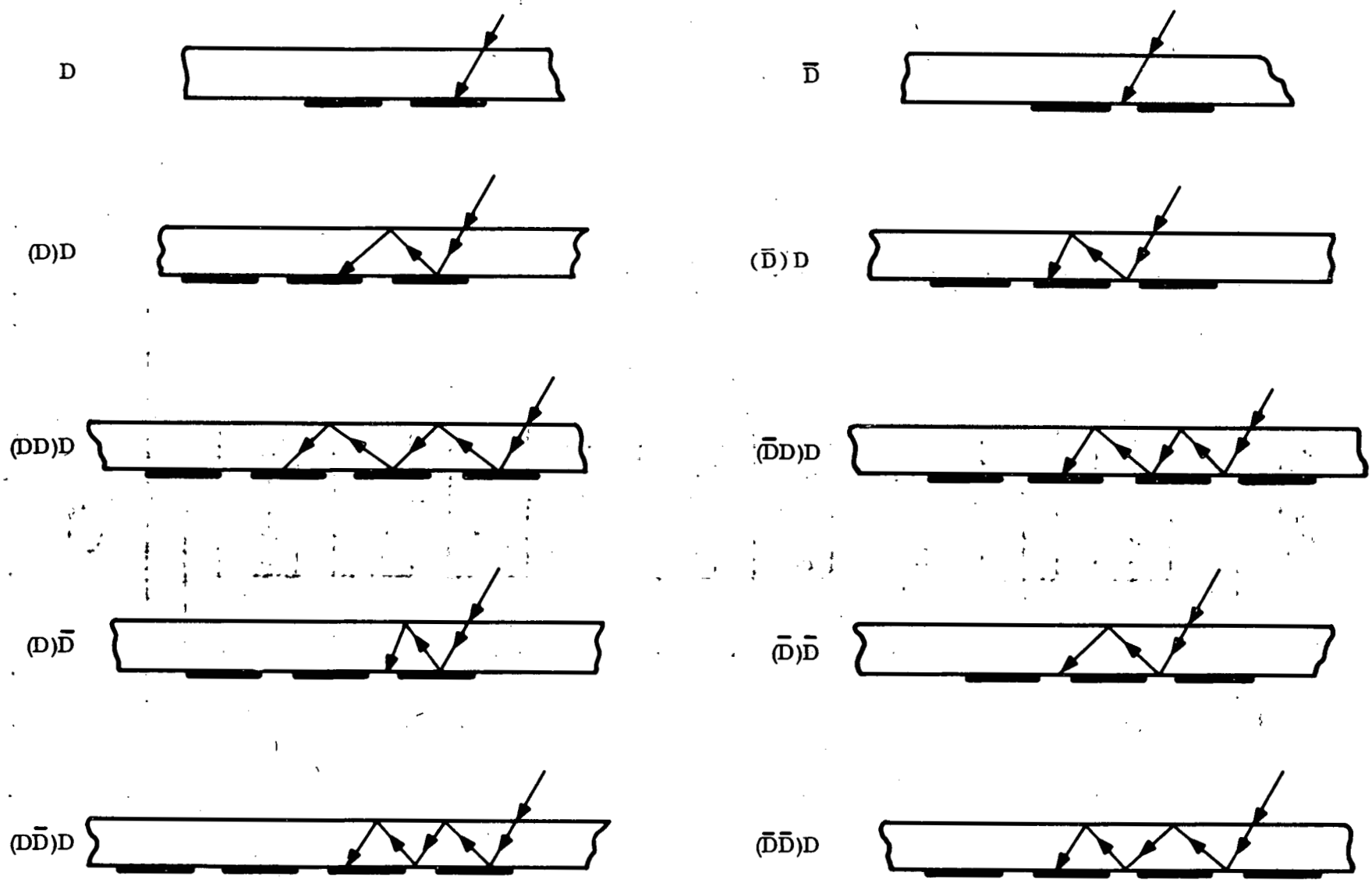

Figure A-30. Description of Beam Division Notation

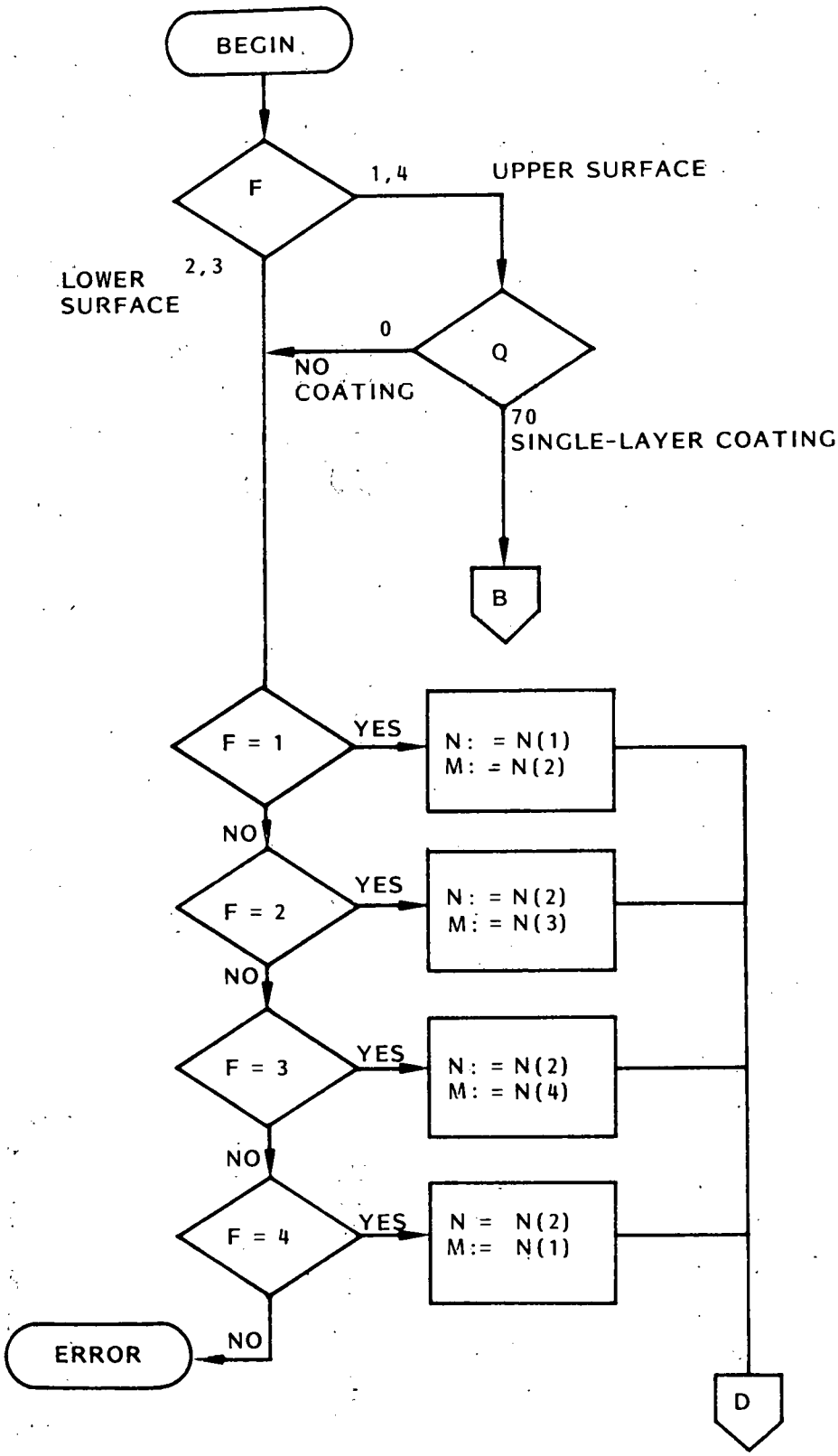

Figure A-31. Logic Flow Diagram for Subroutine REFLECT

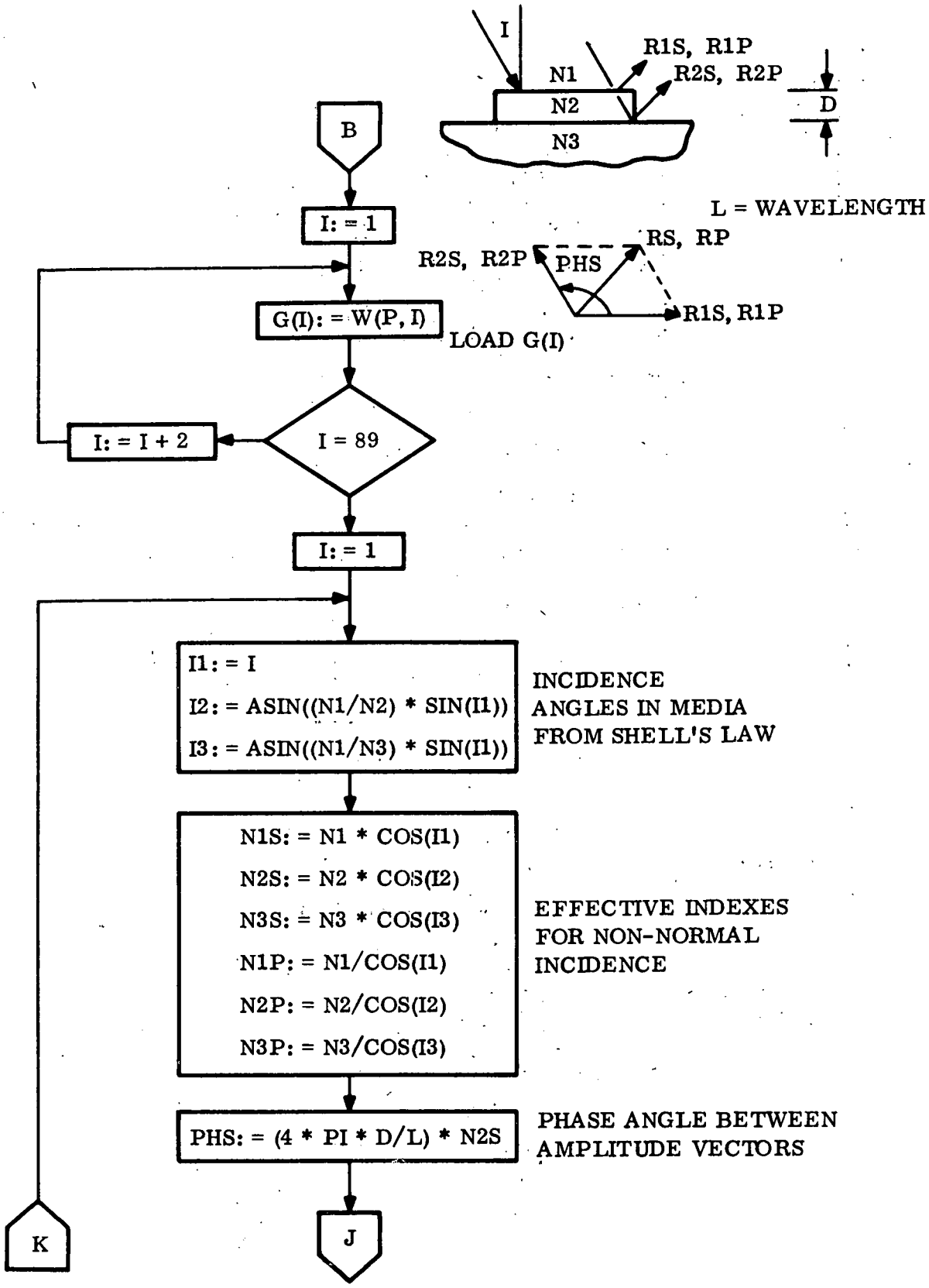

Figure A-31. Logic Flow Diagram for Subroutine REFLECT (Cont'd)

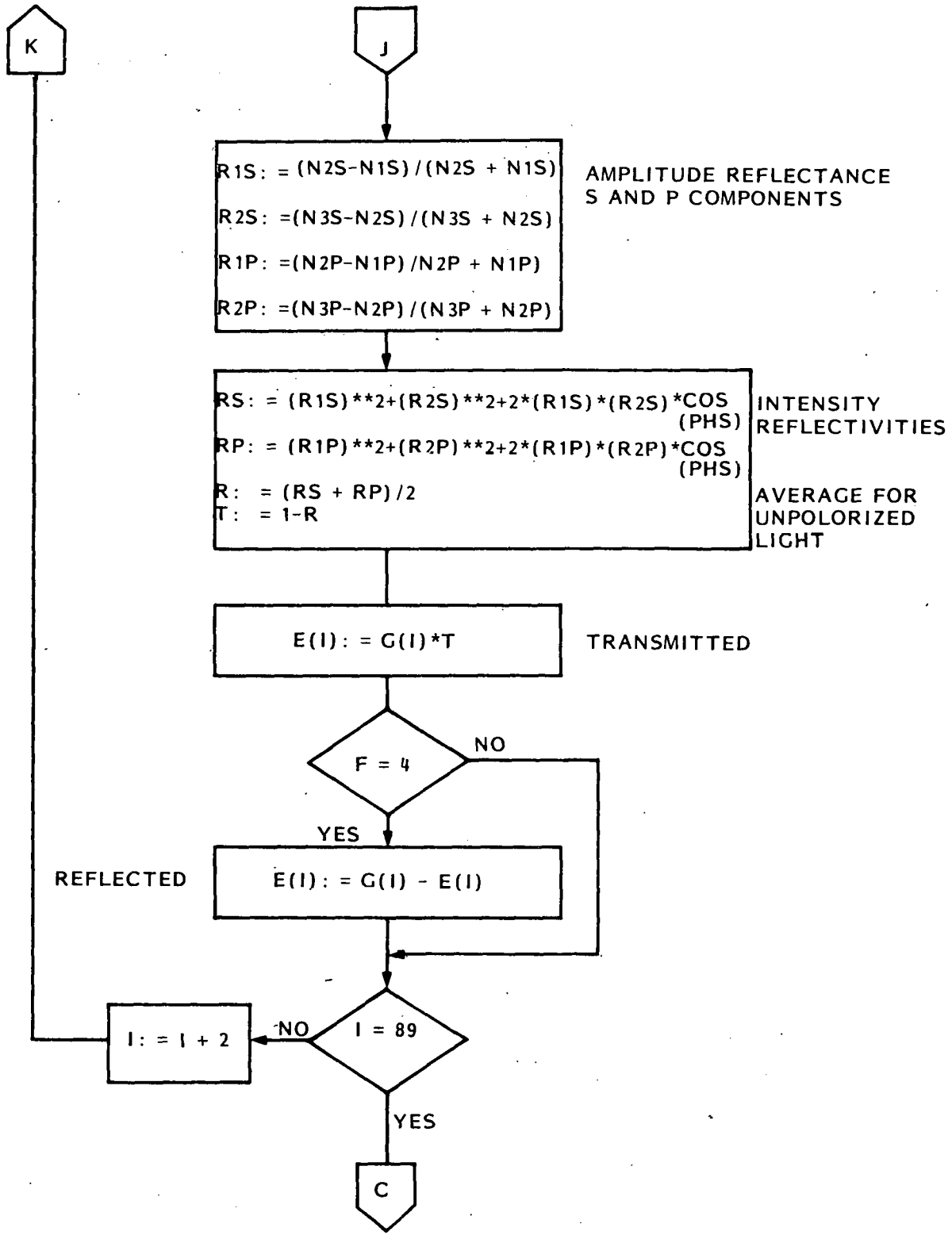

Figure A-31. Logic Flow Diagram for Subroutine REFLECT (Cont'd)

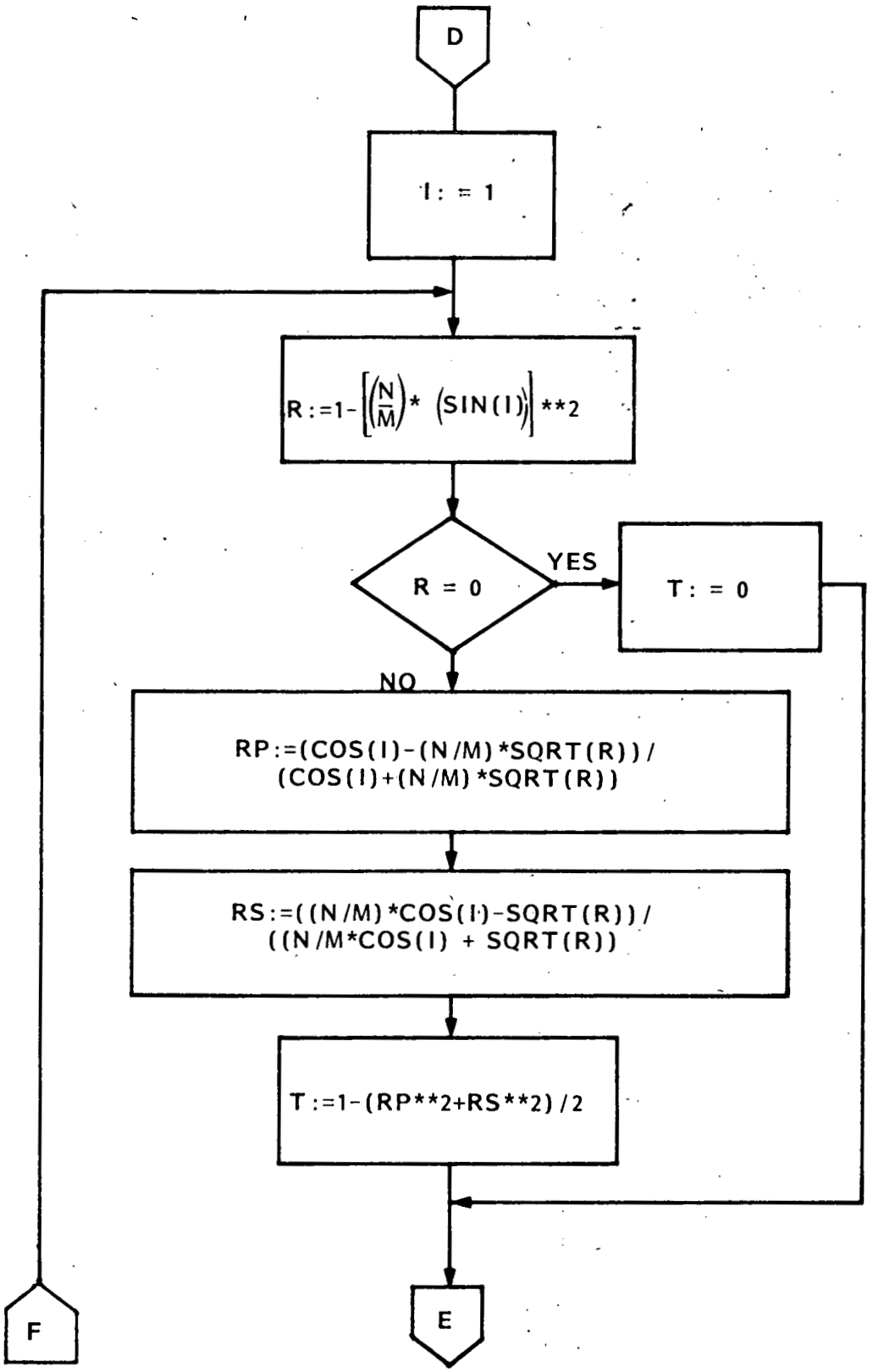

Figure A-31. Logic Flow Diagram for Subroutine REFLECT (Cont'd)

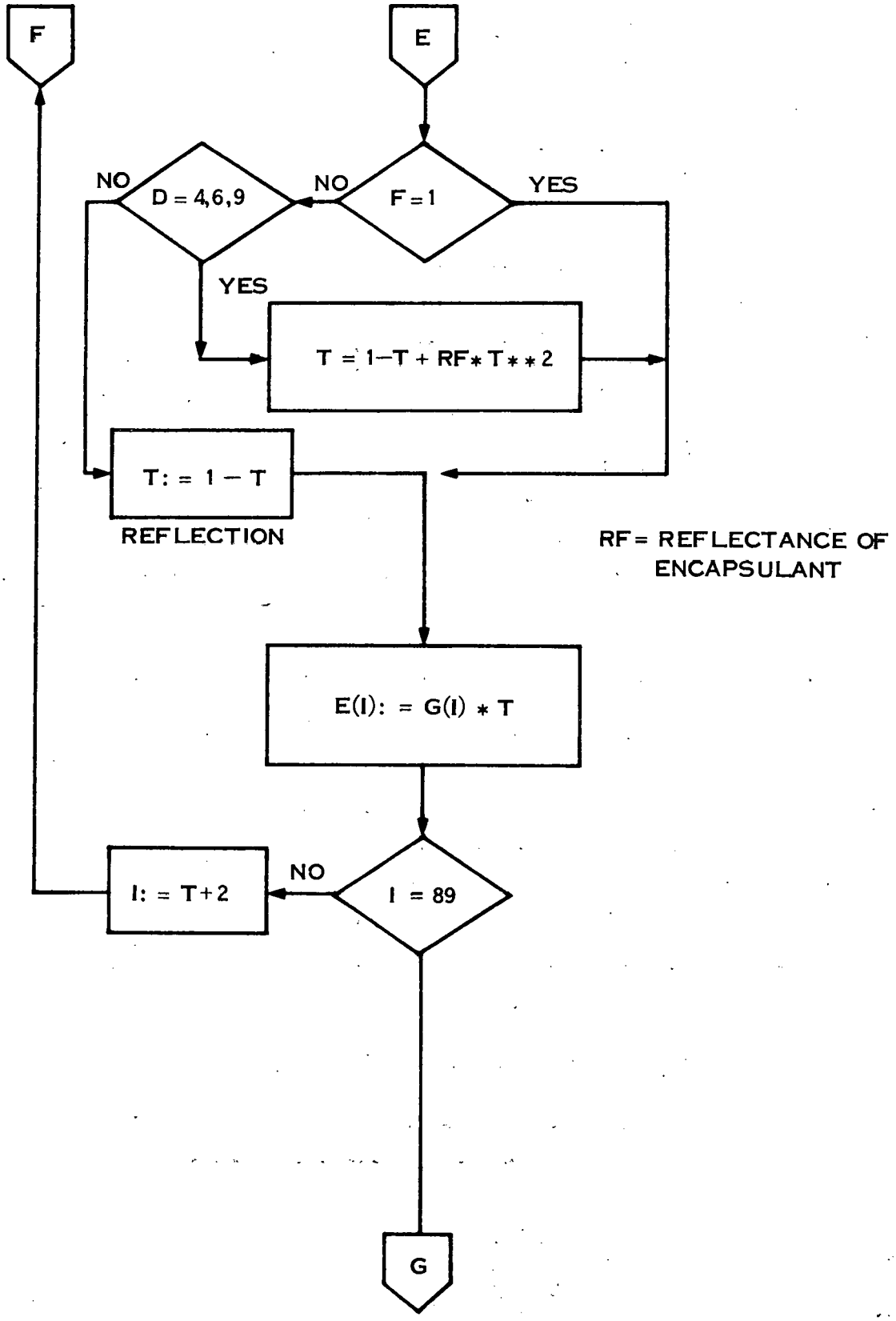

Figure A-31. Logic Flow Diagram for Subroutine REFLECT (Cont'd)

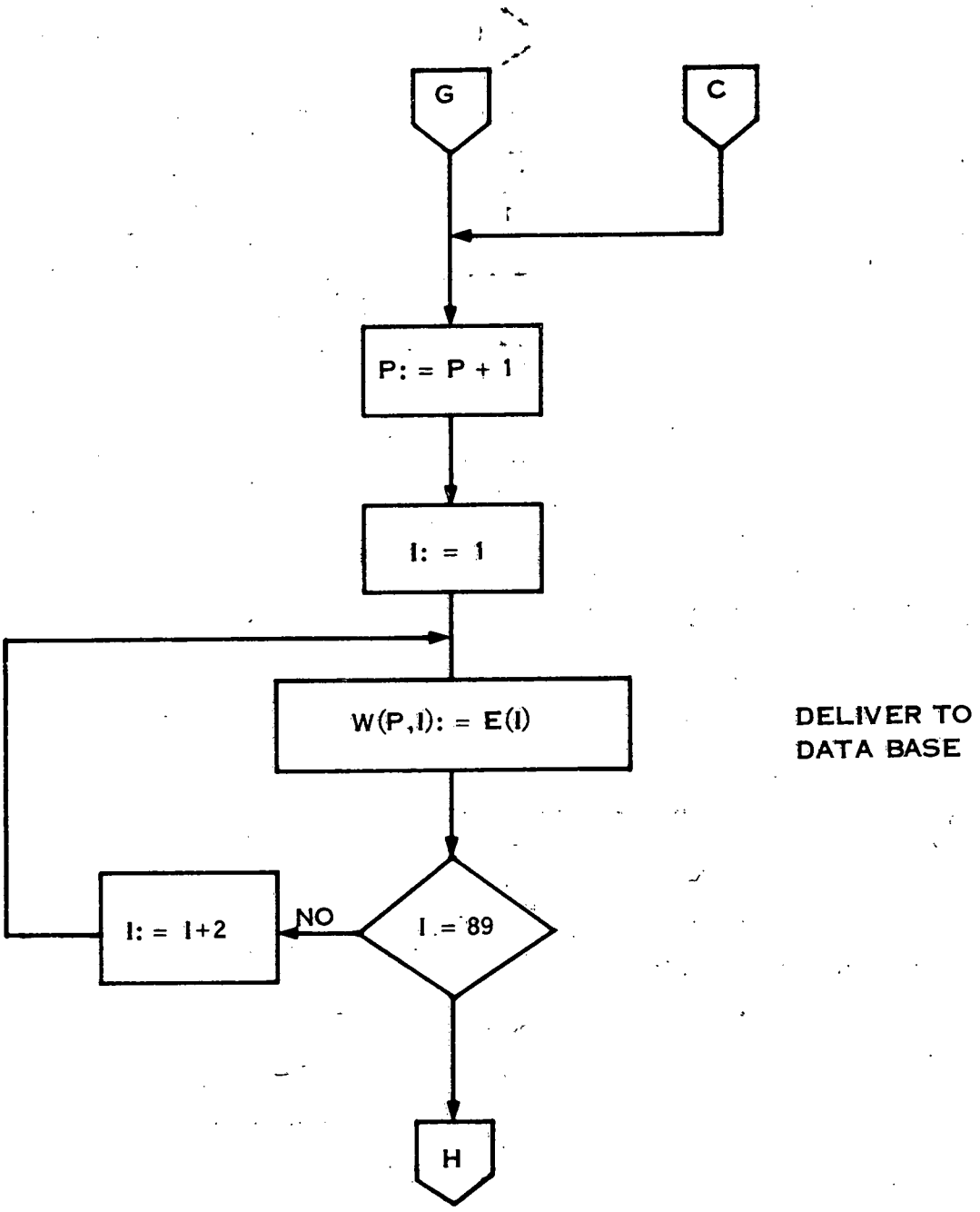

Figure A-31. Logic Flow Diagram for Subroutine REFLECT (Cont'd)

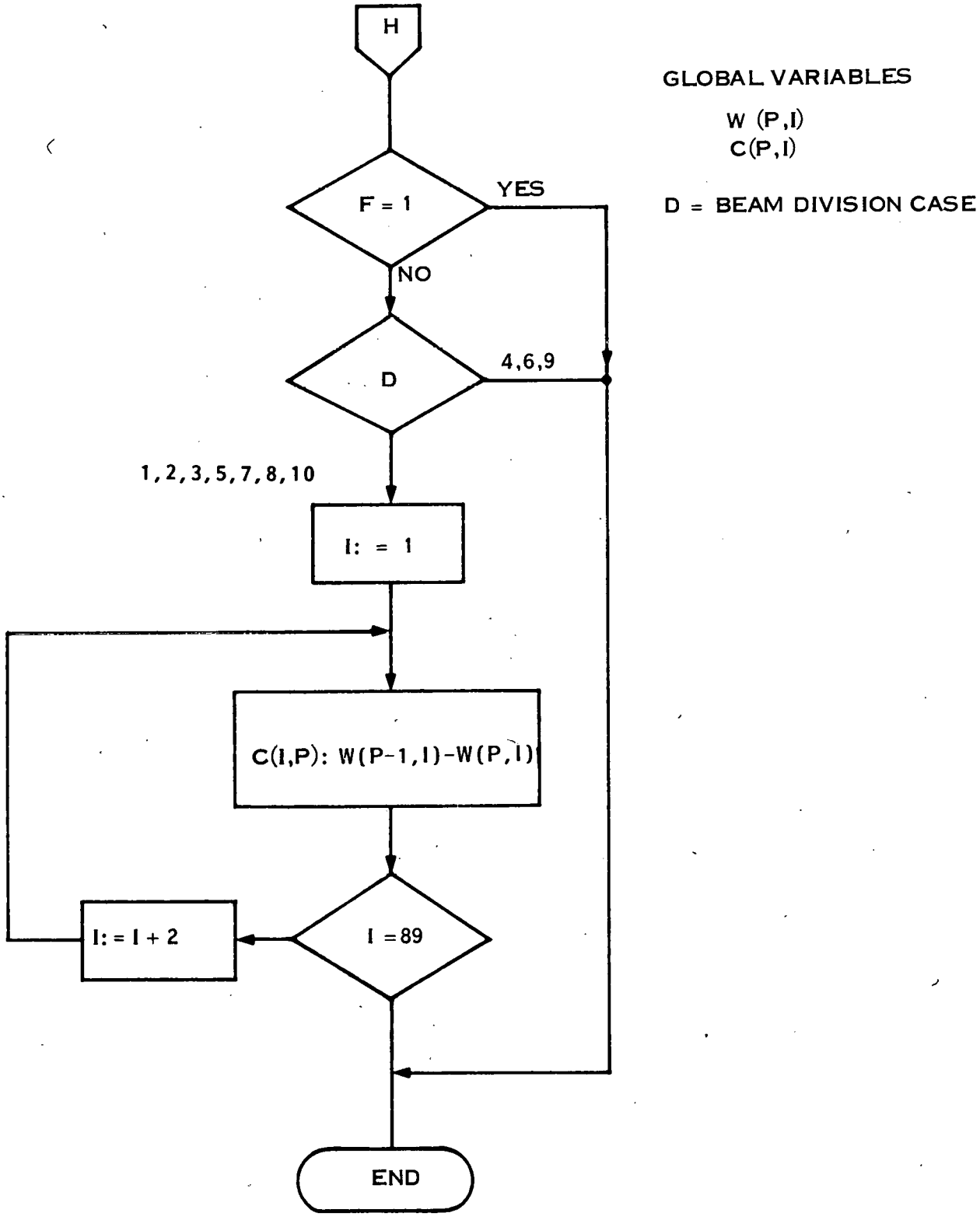

Figure A-31. Logic Flow Diagram for Subroutine REFLECT (Cont'd)

N(2) = Index of refraction for glass coverplate

N(3) = Index of refraction for cell bonding adhesive

N(4) = Index of refraction for encapsulant

The routine treats reflection at each of the interface identified by "F" by the appropriate assignment of the indices of refraction.

This routine also includes the logic for the accumulation of the collected energy on the solar cell.

A.5.3 SUBROUTINE REFRACT

Snell's Law refraction which occurs at the air-to-glass interface as the energy enters the glass (Interface F=1) is accounted for by this subroutine as shown in Figure A-32. The refraction process changes the angular boundaries of each two degree energy cell. A major portion of this procedure deals with the technique employed to redistribute the refracted energy into the originally assigned 45 angular energy cells. The refracted boundaries (A and C) for each cell are calculated and the redistribution of the energy into the original cell boundaries is carried out as shown in Figure A-33.

A.5.4 SUBROUTINE SCATTER

The SCATTER subroutine shown in Figure A-34 performs a piecewise convolution of the energy function (W) with the scattering function (S). This latter function takes the form of a set of data tables as defined in Figure A-35. For the SUNADEX glass surfaces under consideration the values for these data tables can be derived from the experimentally determined function shown in Figure A-21. Tables A-3 through A-5 give the required scattering function data tables for the four interfaces in question. Both of the embossed (or lower) interfaces will have the same scattering function table, but the matte (or upper) surface interfaces (F=1 and F=4) will be different because scattering is by refraction in one case and by reflection in the other.

A.5.5 SUBROUTINE ABSORB

The ABSORB subroutine shown in Figure A-36 accounts for the broad-band bulk absorption which occurs as the energy passes through the glass cover plate material. Table A-6 gives typical values for the broad-band bulk absorption coefficient, G, for several soda-lime glass compositions.

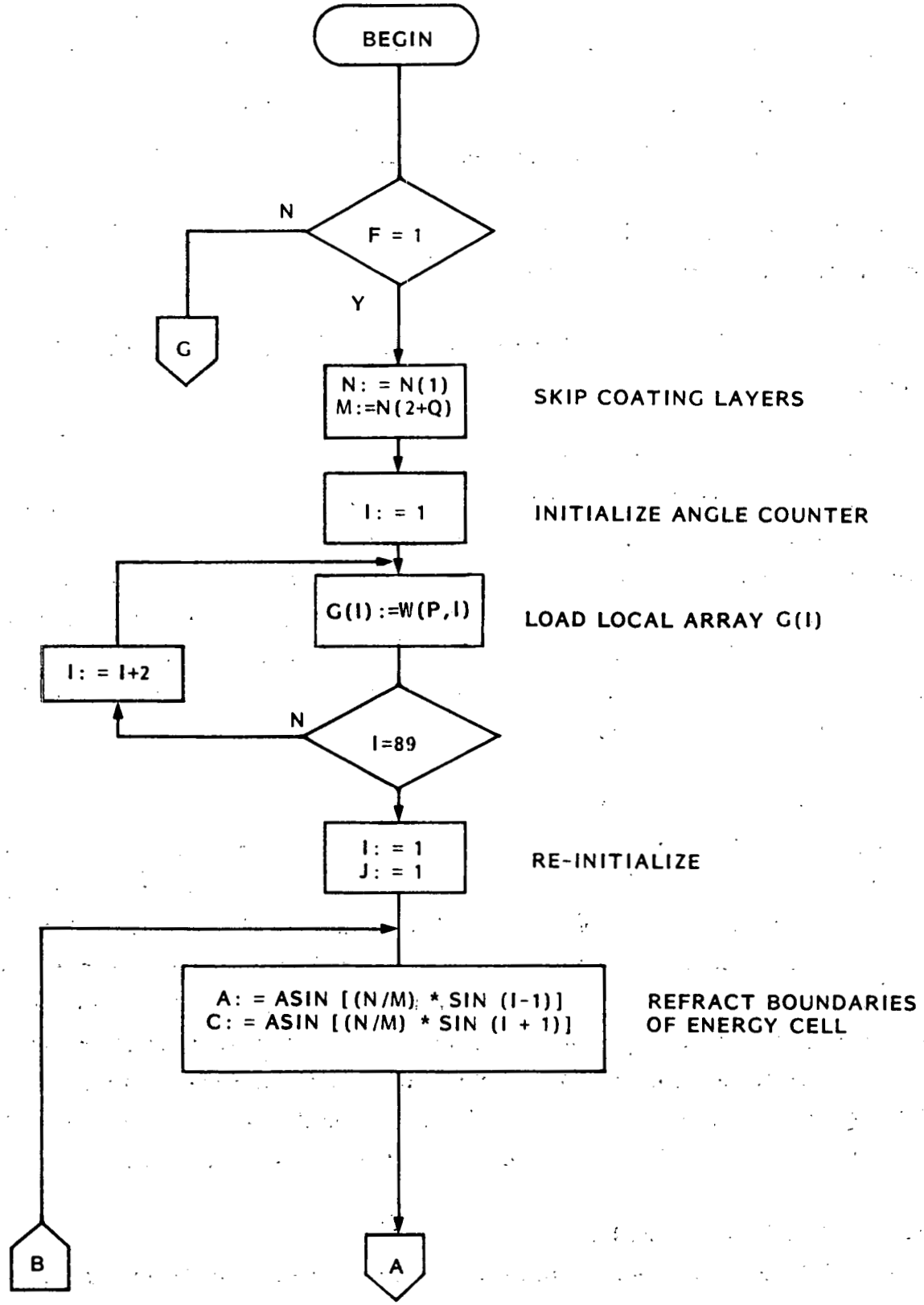

Figure A-32. Logic Flow Diagram for Subroutine REFRACT

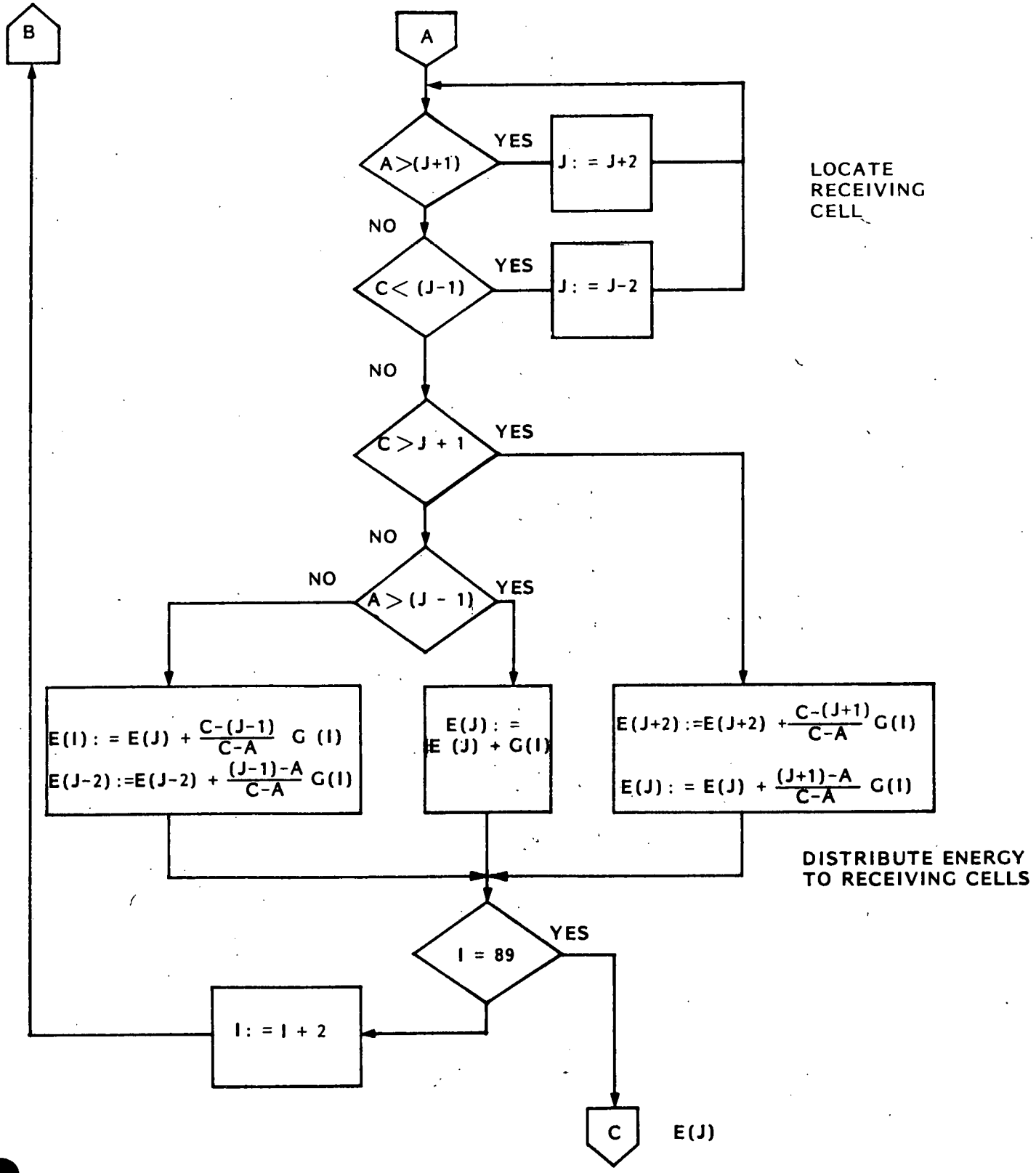

Figure A-32. Logic Flow Diagram for Subroutine REFRACT (Cont'd)

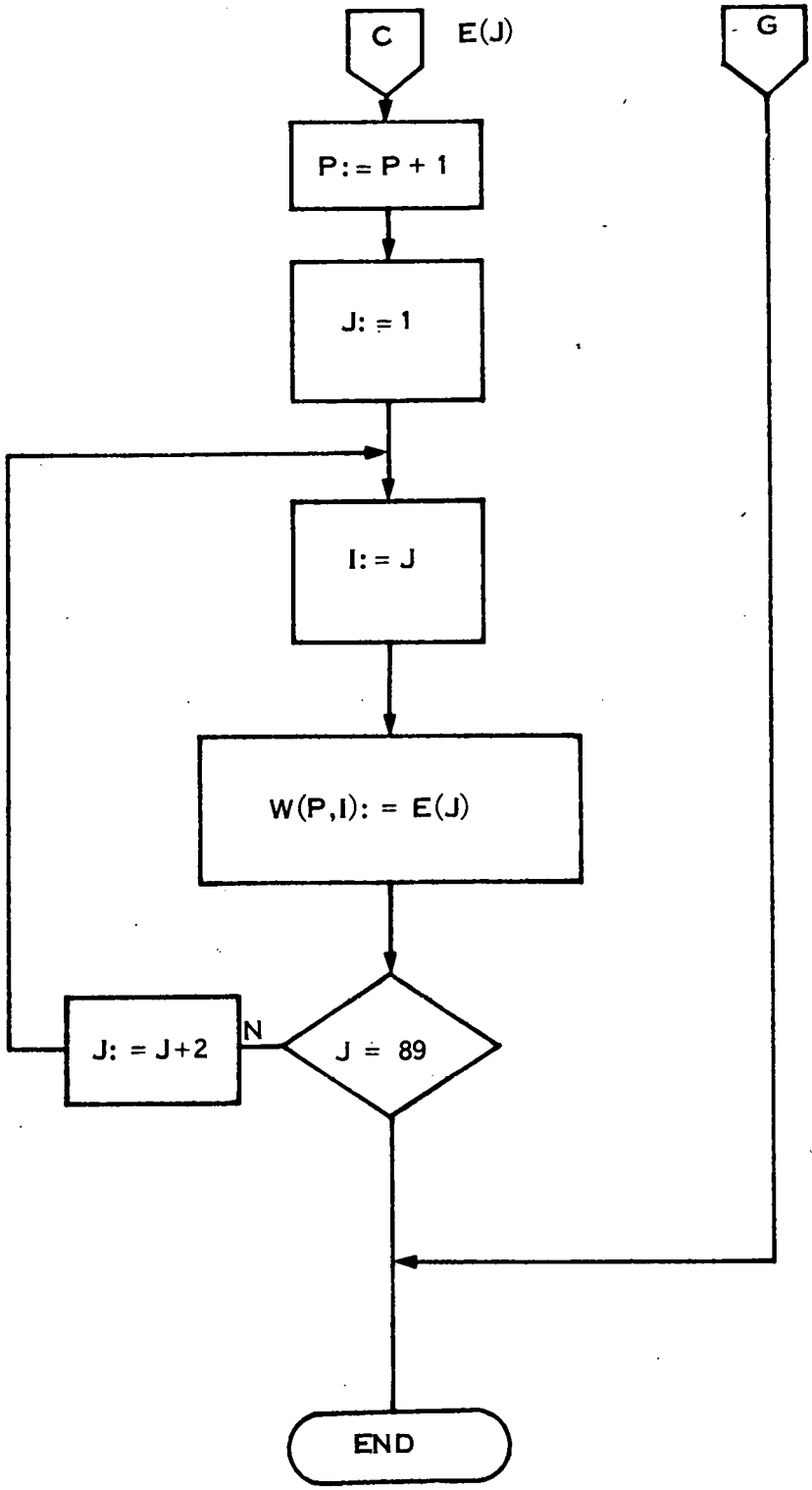

Figure A-32. Logic Flow Diagram for Subroutine REFRACT (Cont'd)

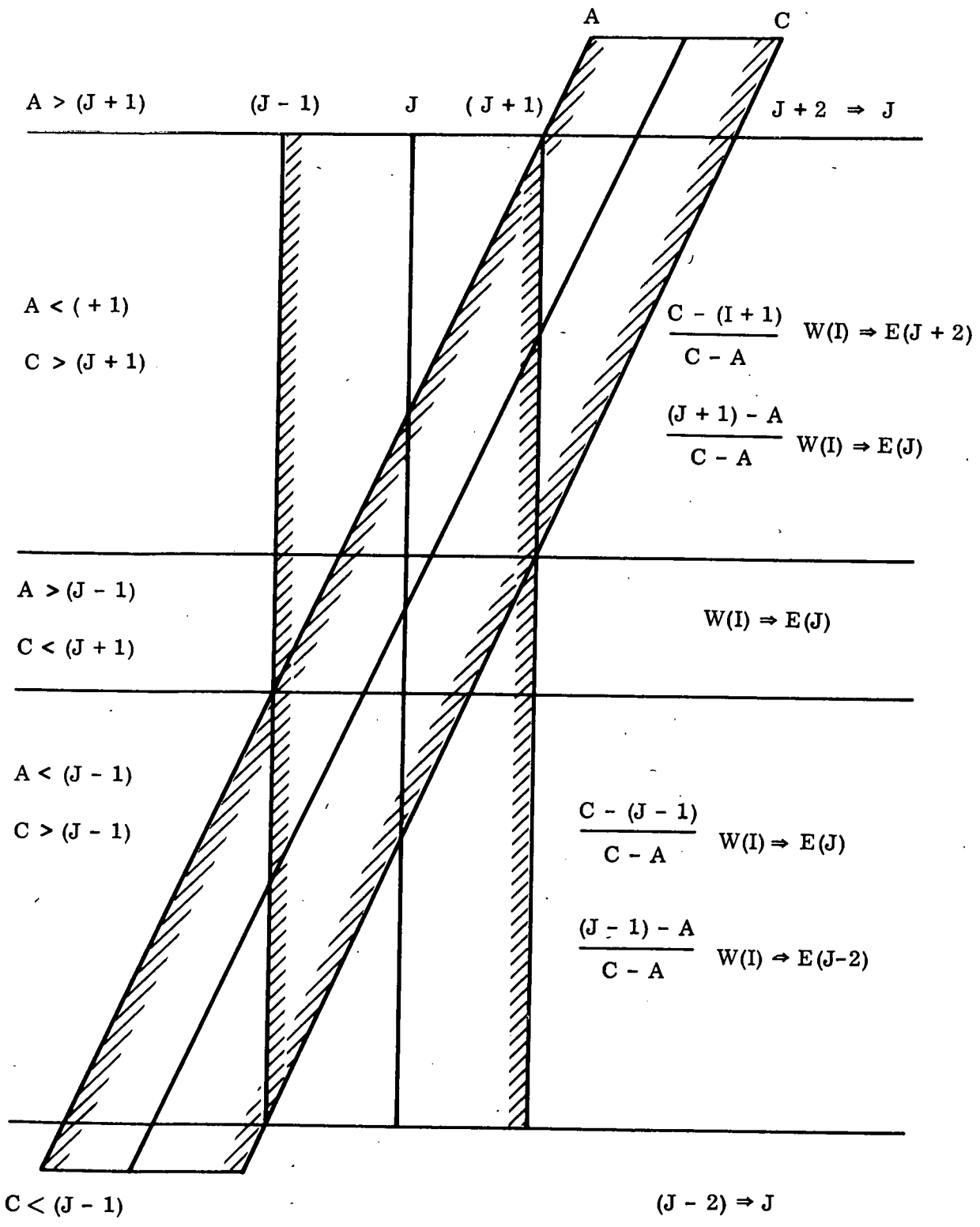

Figure A-33. Redistribution of Refracted Energy Into Original Energy Cell Boundaries

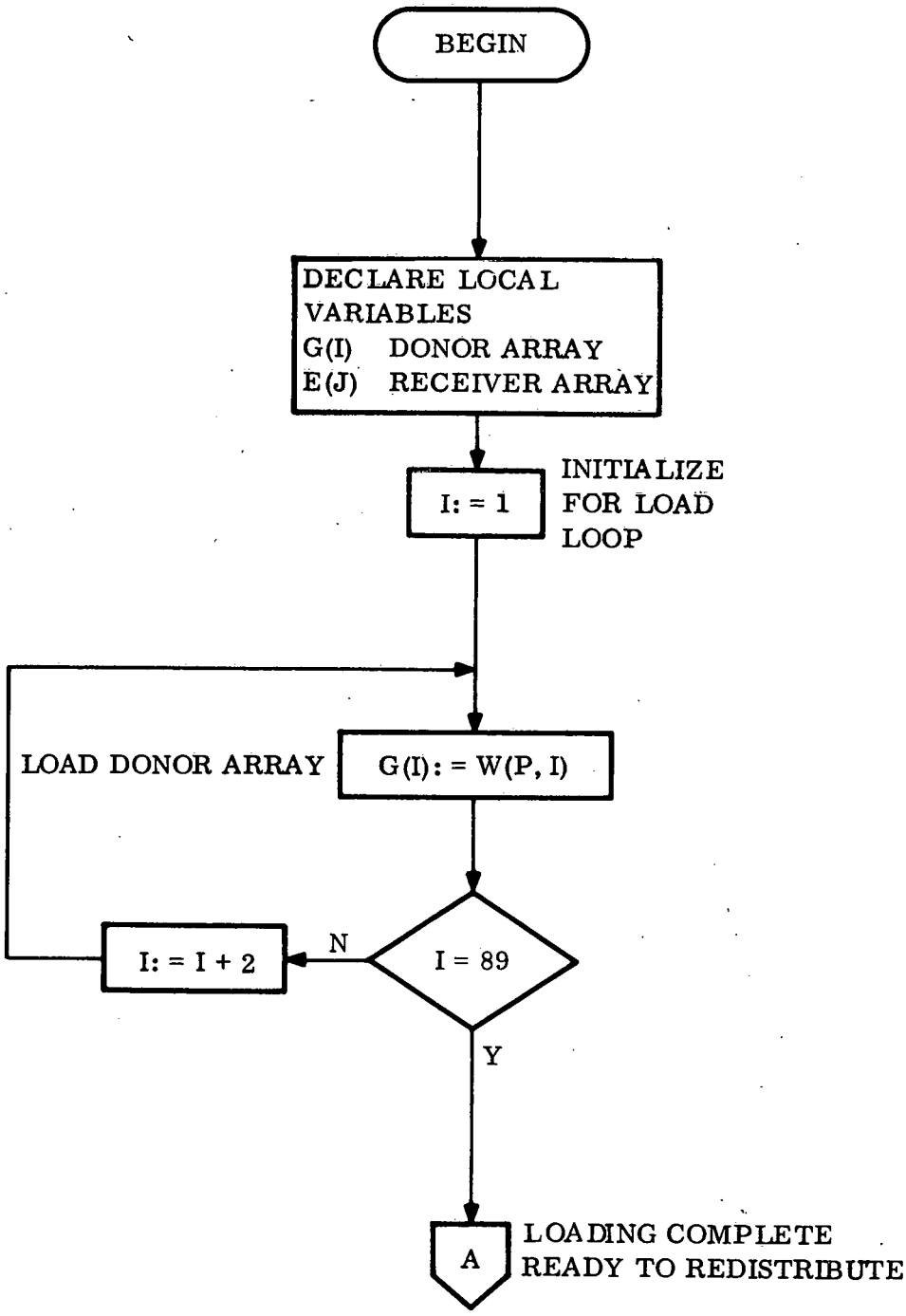

Figure A-34. Logic Flow Diagram for Subroutine SCATTER

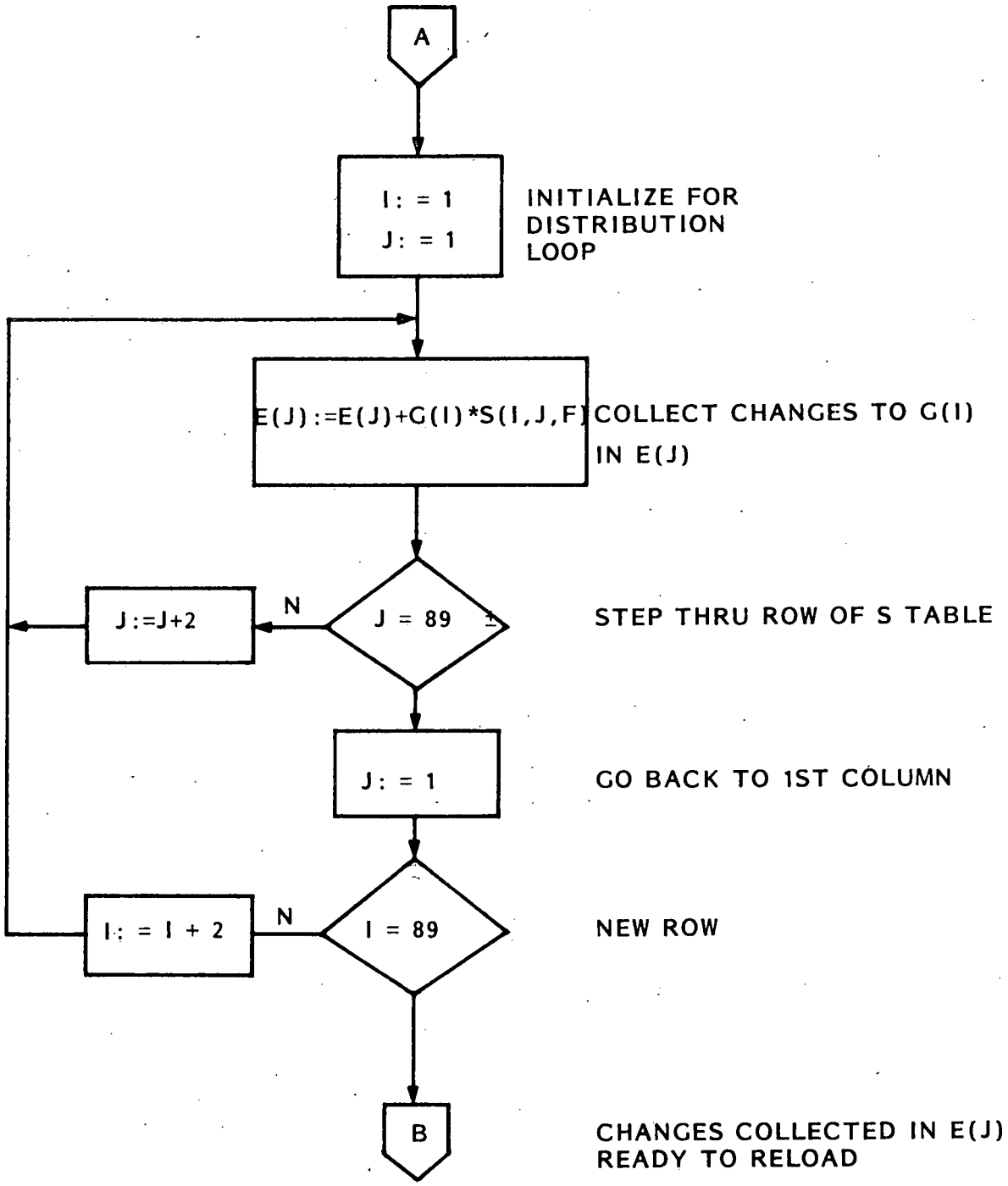

Figure A-34. Logic Flow Diagram for Subroutine SCATTER (Cont'd)

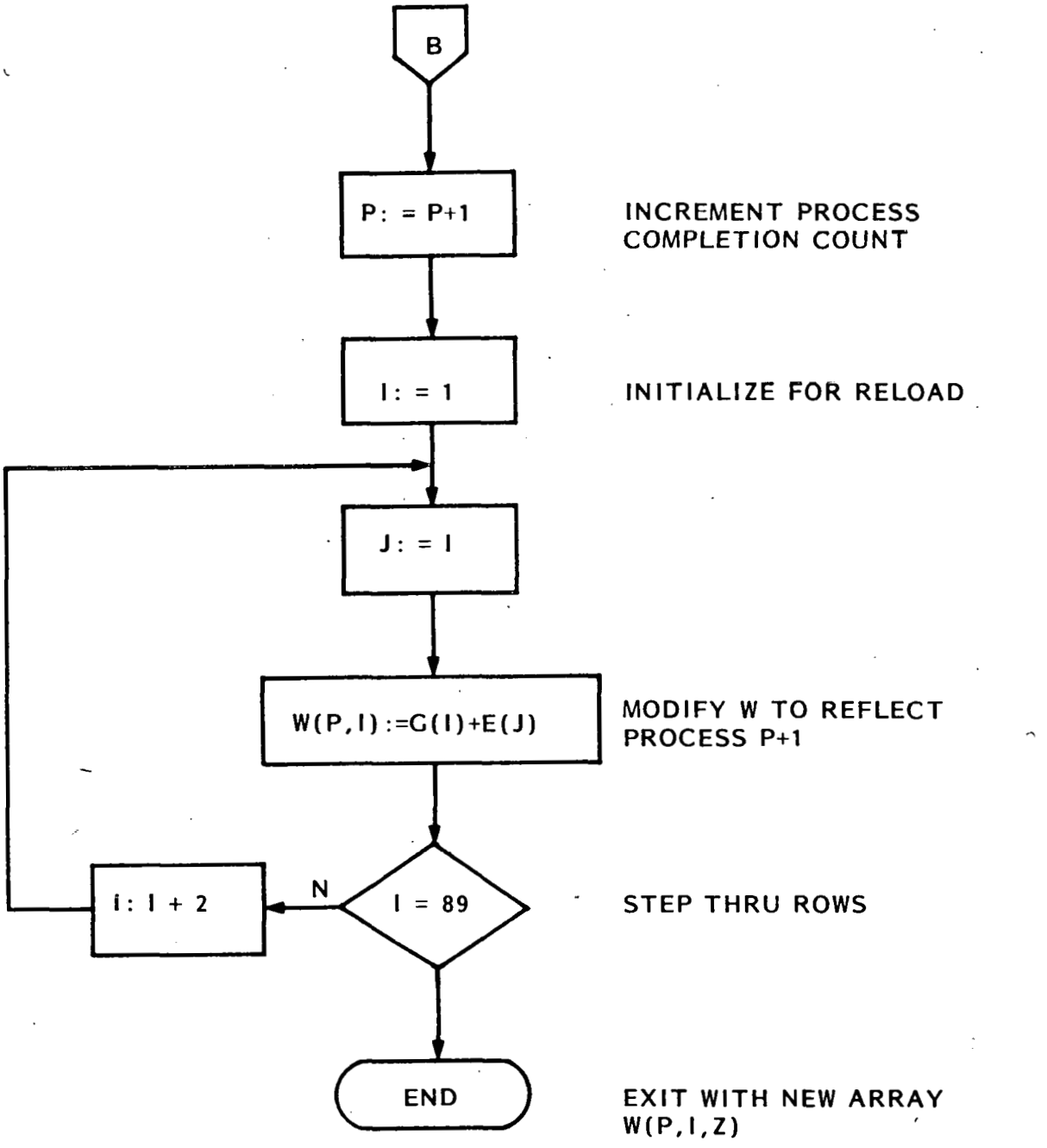

Figure A-34. Logic Flow Diagram for Subroutine SCATTER (Cont'd)

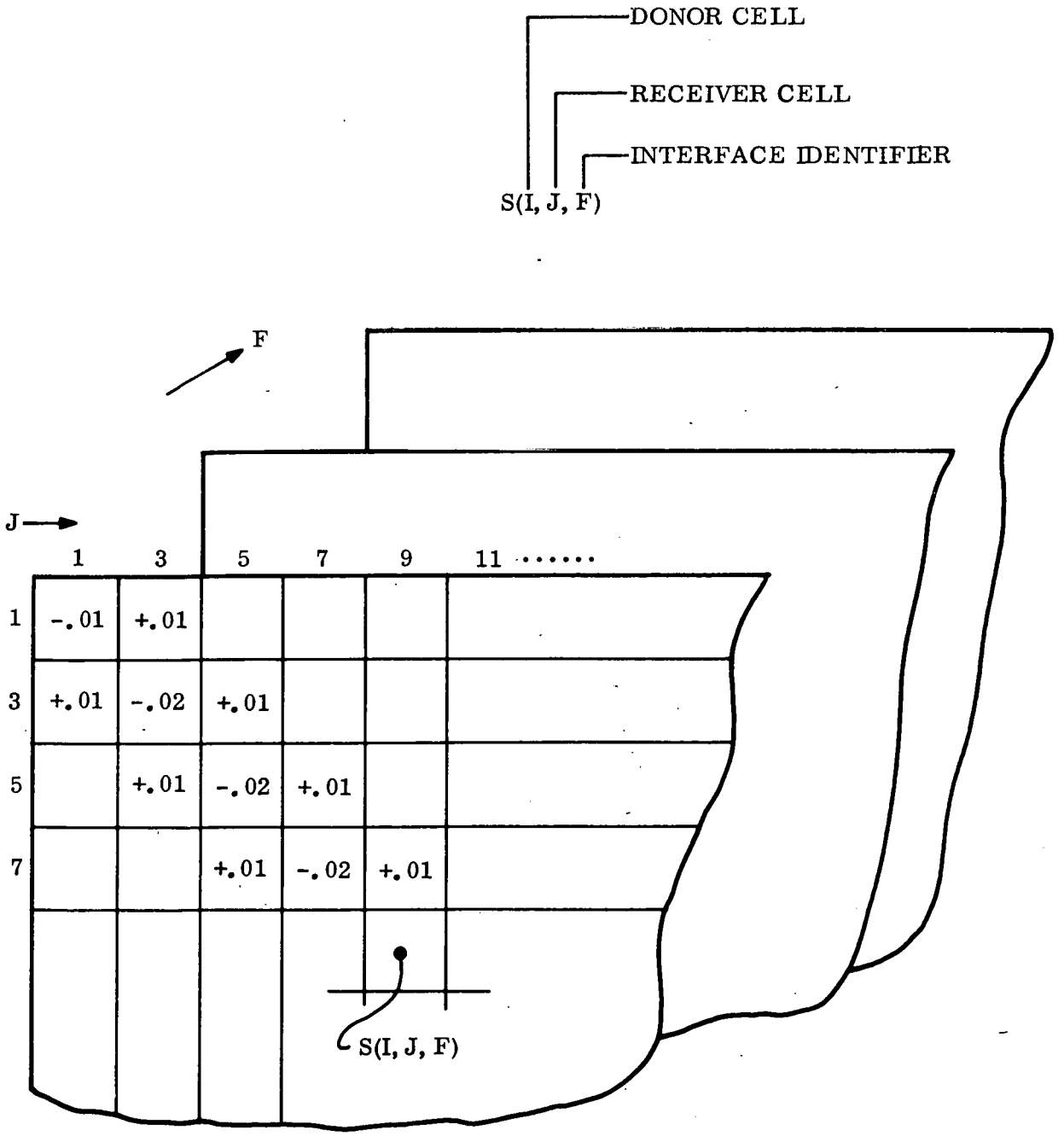

$$E(J) := E(J) + S(I, J, F) * G(I)$$

Figure A-35. Definition of Scatter Function Table

Table A-3. Scatter Function Table for SUNADEX Glass - Matte Surface (F=1)

I (Donor Cell) \ J (Receiver Cell)	1	3	5	7	9	11	13	15	17	19	• • •
1	0	0	0	0	0	0					
3	0	0	0	0	0	0					
5	0	0	0	0	0	0					
7	0	0	0	0	0	0					
9	0	0	0	0	0	0					
11											
13											
•											
•											
•											

Table A-4. Scatter Function Table for SUNADEX Glass - Matte Surface (F=4)

I (Donor Cell) \ J (Receiver Cell)	1	3	5	7	9	11	13	15	17	19	• • •
1	-.08	.04	0	0	0						
3	.04	-.08	.04	0	0						
5	0	.04	-.08	.04	0						
7	0	0	.04	-.08	.04	0					
9											
11											
13											
•											
•											
•											

Table A-5. Scatter Function Table for SUNADEX Glass - Embossed Surface (F=2 and F=3)

		J (Receiver Cell)											
		1	3	5	7	9	11	13	15	17	19	21	23
	1	-.94	.31	.34	.19	.09	.01	0	0	0	0	0	
	3	.155	-.94	.155	.34	.19	.09	.01	0	0	0	0	
I	5	.17	.155	-.94	.155	.17	.19	.09	.01	0	0	0	
	7	.095	.17	.155	-.94	.155	.17	.095	.09	.01	0	0	
(Donor	9	.045	.095	.17	.155	-.94	.155	.17	.095	.045	.01	0	
Cell)	11	.005	.045	.095	.17	.155	-.94	.155	.17	.095	.045	.005	0
	13	0	.005	.045	.095	.17	.155	-.94	.155	.17	.095	.045	.005
	15												
	17												
	•												
	•												
	•												

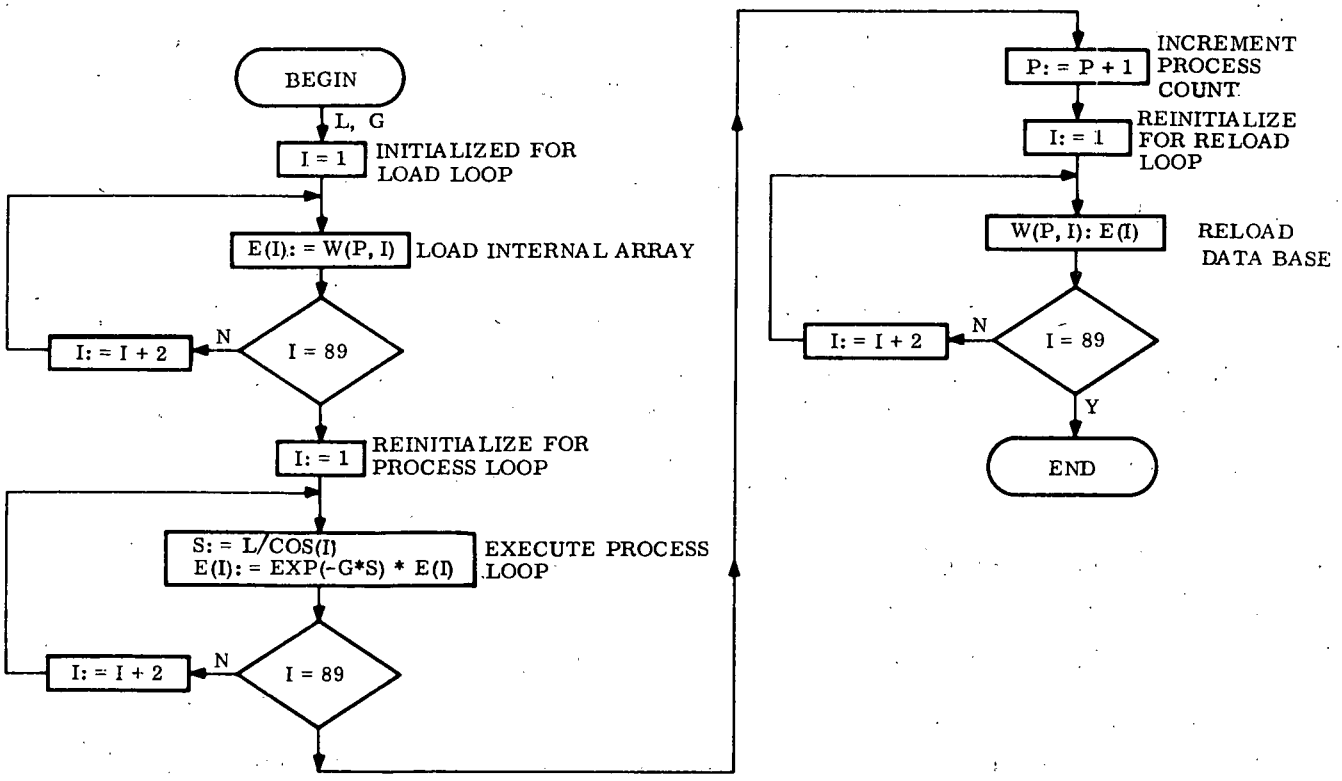

Figure A-36. Logic Flow Diagram for Subroutine ABSORB

Table A-6. Broad-band Bulk Absorption Coefficients for Several Soda-Lime Glass Compositions

Glass Identification	Iron Oxide Content (%)	G (mm^{-1})
ASG SUNADEX	0.01	0.00184
ASG LO-IRON	0.05	0.00926
AGS STARLUX	0.12	0.01933

A.5.6 SUBROUTINE DIVIDE

Figure A-37 gives the logic flow diagram for the DIVIDE subroutine which accounts for the beam division which occurs at each reflection from the lower surface of the cover plate. An empirically determined beam division function (F) is used to describe the geometric fraction of reflected area which is coincident with the solar cells. The determination of these functional relationships is described in Section A.4.2.

A.6 DESCRIPTION OF COST MODELS

The expected costs for shingle solar cell modules have been developed as a function of solar cell area, cover plate area and substrate area based on the following ground rules:

- 500 kW peak
- Late 1980 time period
- 13 percent bare cell efficiency at 28°C
- Circular solar cells packed within a hexagon shape as shown in Figure A-11. Both a 19 cell and a 7 cell configuration will be considered in the cost model.
- The shingle module configuration is as shown in Figure A-12.

The shingle module cost has been divided into three categories as described below:

1. Solar Cell Cost - The specific cost of the circular solar cells is given in Figure A-38 as a function of the total solar cell area per module and the module configuration (7 or 19 cells). This cost element includes the interconnection between cells as well as the cost of laminating the cells to the glass coverplate.

2. Encapsulation Cost - The specific cost of the encapsulation system, which includes the glass coverplate, the hard back and the solar cell encapsulation material, is given in Figure A-39 as a function of the coverplate area per module and the glass coverplate thickness.

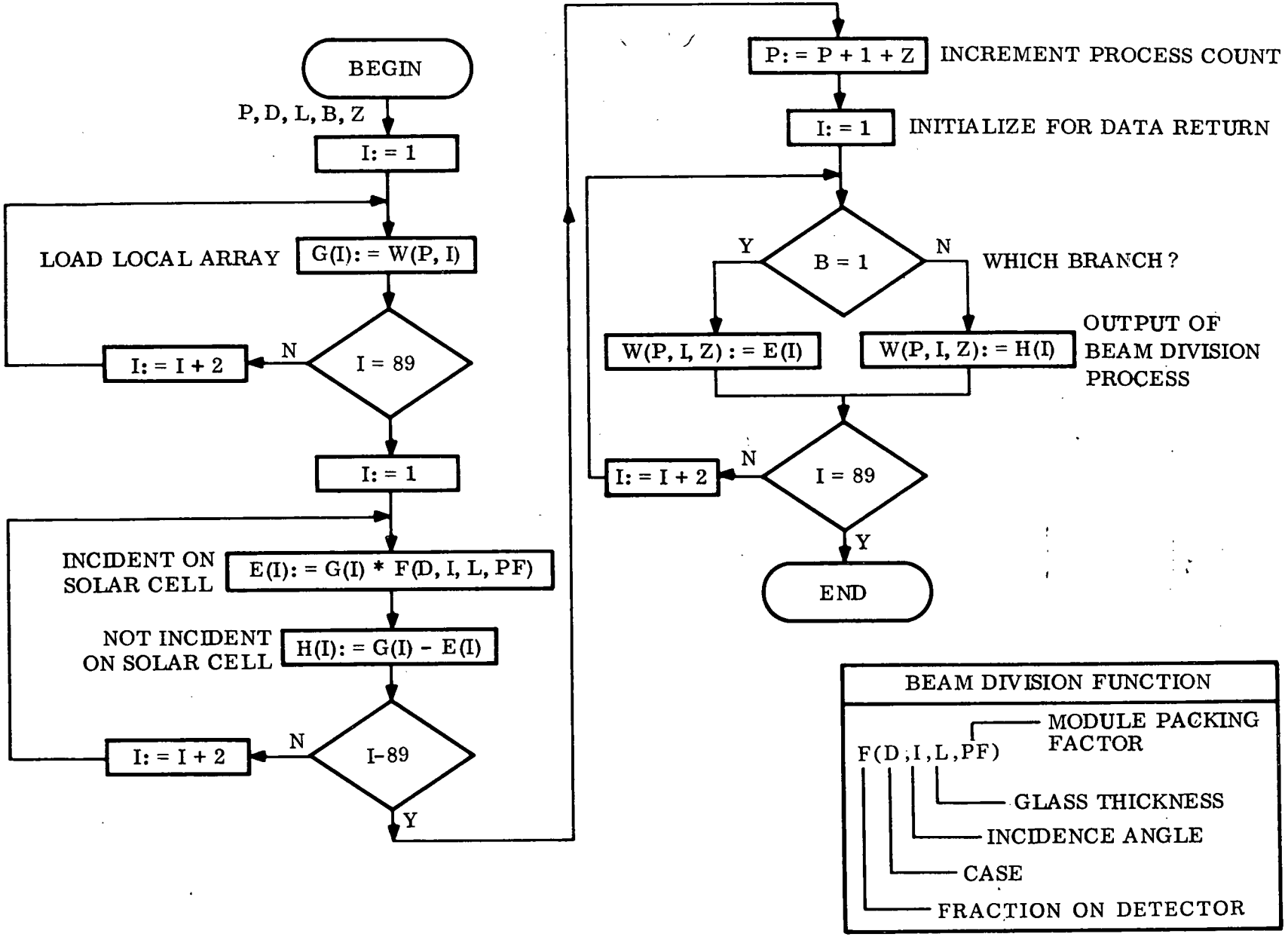

Figure A-37. Logic Flow Diagram for Subroutine DIVIDE

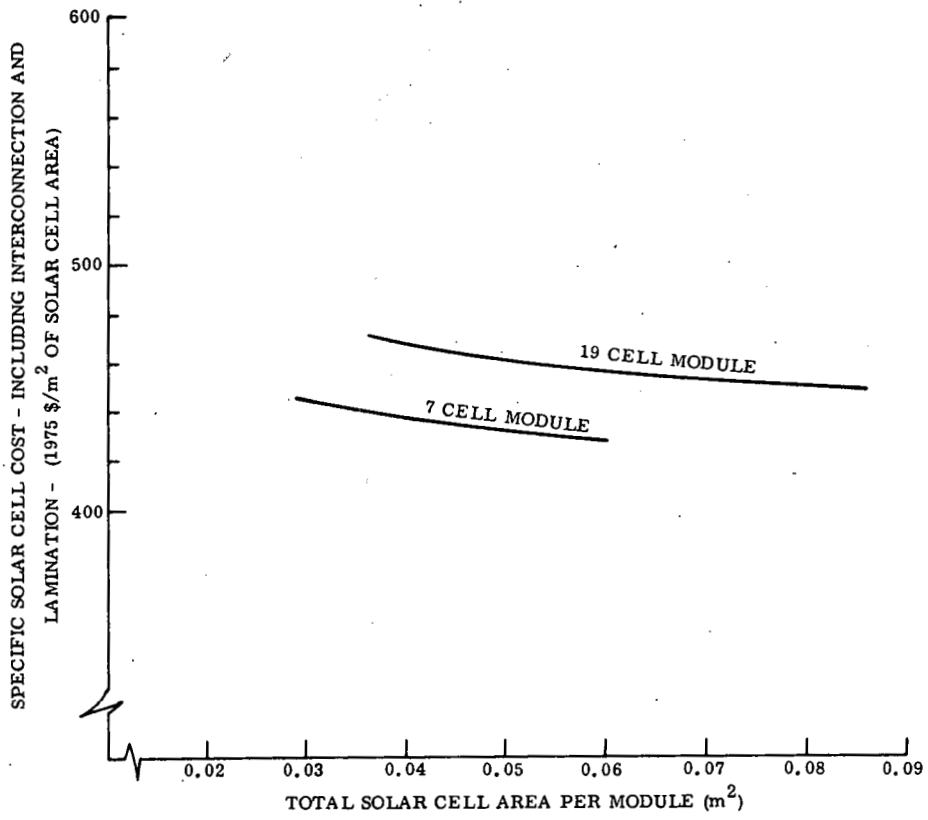

Figure A-38. Specific Solar Cell Cost

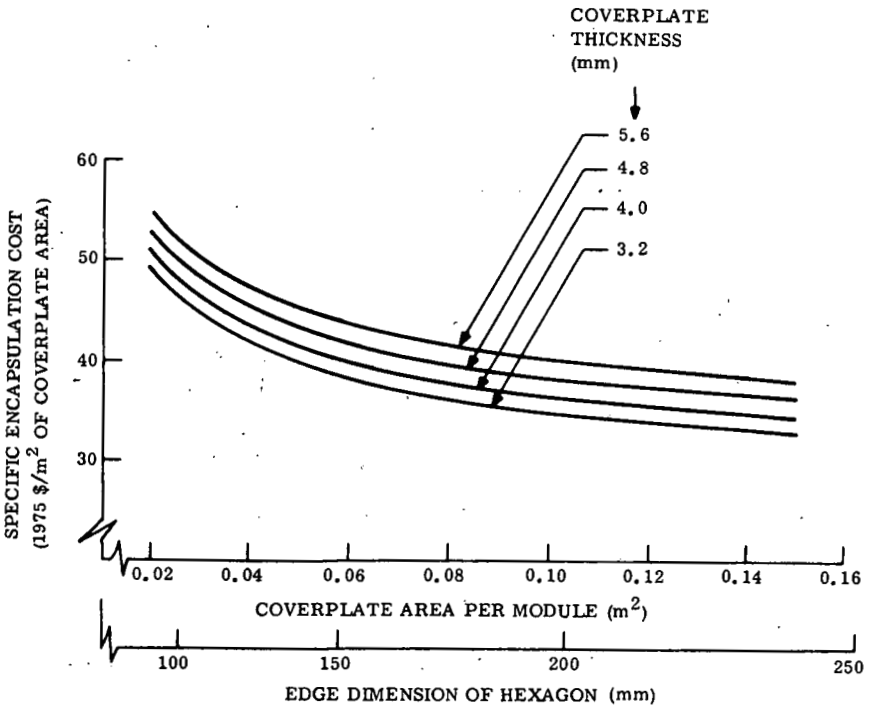

Figure A-39. Specific Encapsulation Cost

3. Substrate Cost - The specific cost of the semi-flexible shingle module substrate, which includes the flexible circuit board, the outer skins and the core material, is given in Figure A-40 as a function of the substrate area per module and the glass coverplate thickness.

Applying the cost model to the existing shingle module geometry with a cell diameter of 53 mm, a hexagon edge dimension of 139.7 mm, a cover plate area of 0.0507 m^2 and a substrate area of 0.0761 m^2 yields the results listed in Table A-7.

Table A-7. Cost Prediction Using Existing Shingle Module Geometry

Item	Cost per Module (1975 $)	Fraction of Total Cost
• Solar Cells (including interconnection and lamination)	19.53	0.834
• Encapsulation	2.03	0.087
• Substrate	1.86	0.079
Total Cost	23.42	1.000

Such a module will produce 5.88 watts using a 13.0 percent bare cell efficiency at 28°C. At the Standard Operating Conditions, which include a calculated NOCT of 61°C, this module output will be reduced to 5.03 watts. Thus, the resulting cost-to-power ratio is $4.66/peak watt.

A.7 SAMPLE CASE CALCULATIONS

A sample calculation using the optical analysis program for the zero depth concentrator is shown in Table A-8. This program has been written for time-share execution from a remote terminal. In the example given the responses required by the user have been underlined. The results of the calculation for the Phoenix distribution of incident energy as a function of angle of incidence (from Table A-1) are given as the energy collected on the solar cells in each two degree angular increment representing the angle of the refracted specular ray as it passes through the top coverplate surface. The total collected energy is calculated to be 1644.52 kWh/m^2. With an input insolation of 1853.6 kW/m^2 (from Table A-1) this result represents an overall enhancement of 16 percent for the packing factor used.

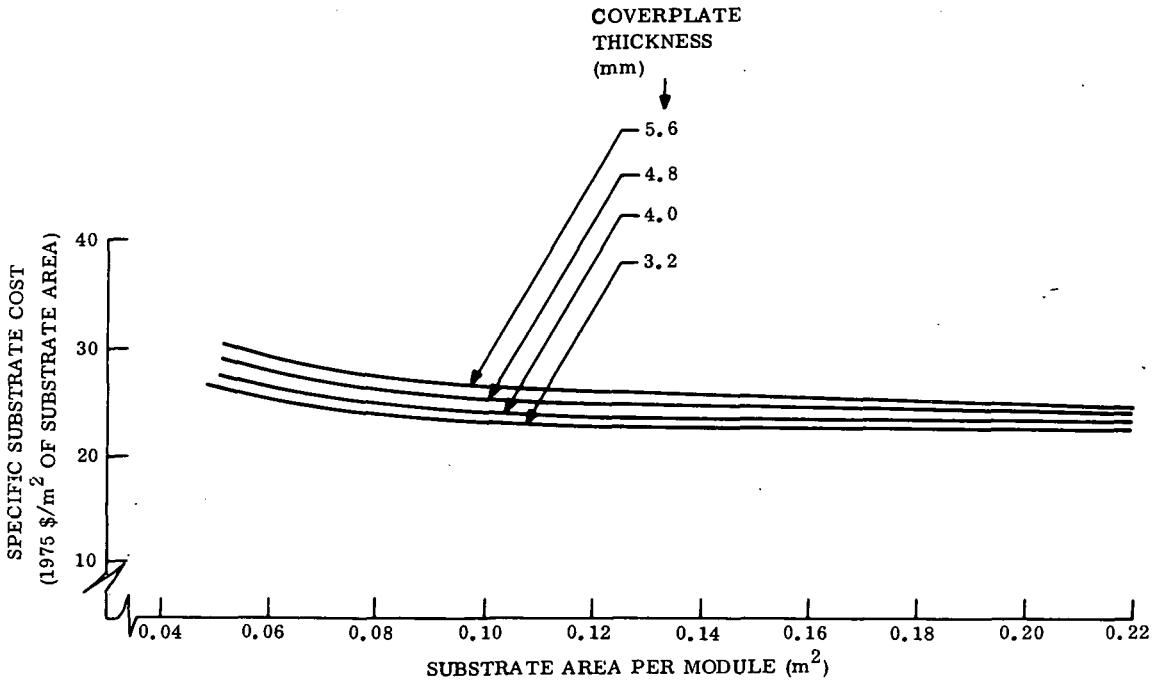

Figure A-40. Specific Substrate Cost

Table A-8. Sample Calculation Using Optical Model of Zero Depth Concentrator

```
NO. OF COATING LAYER, 1 OR 0
=0
INDEXES OF REFRACTION OF GLASS COVER, BONDING ADHESIVE & ENCAPSULANT
=1.52,1.4,1.4
MODULE PACKING FACTOR (BETWEEN .512 & .814)
=.764
GLASS THICKNESS(3.2, 4 OR 4.8MM), BULK ABSORP. COEFF.(1/MM)
=4,.00184
REFLECTANCE OF ENCAPSULANT
=.8

  0- 2     2- 4     4- 6     6- 8     8-10    10-12    12-14    14-16    16-18
 19.76    21.75    22.22    29.33    91.70   117.59    92.47    40.08    38.19

 18-20    20-22    22-24    24-26    26-28    28-30    30-32    32-34    34-36
205.19   149.28    68.26    37.14   219.25    76.16    41.66    85.89   135.06

 36-38    38-40    40-42    42-44    44-46    46-48    48-50    50-52    52-54
 37.63    98.11    14.85     1.27     0.81     0.47     0.23     0.11     0.04

 54-56    56-58    58-60    60-62    62-64    64-66    66-68    68-70    70-72
  0.01     0.00     0.00     0.00     0.00     0.00     0.       0.       0.

 72-74    74-76    76-78    78-80    80-82    82-84    84-86    86-88    88-90
  0.       0.       0.       0.       0.       0.       0.       0.       0.
TOTAL ENERGY COLLECTED=  1644.52
MAKING MORE RUNS? 1=YES, 0=NO
=0
```

The model was used to calculate the enchancement, relative to the cosine relationship, as a function of angle of incidence on the outer coverplate surface for these same conditions of module packing factor, etc. The result shown in Figure A-41 shows a significant enhancement in the performance of this type of module relative to the cosine relationship which is representative of the output of a closely-packed planar module.

A.8 FORTRAN CODE

Table A-9 is a listing of the FORTRAN code of the optical analysis program developed for the zero-depth concentrator. This program is compatible with the Honeywell L66 system but can be executed on any system with a FORTRAN compiler with minor modifications to the source statements.

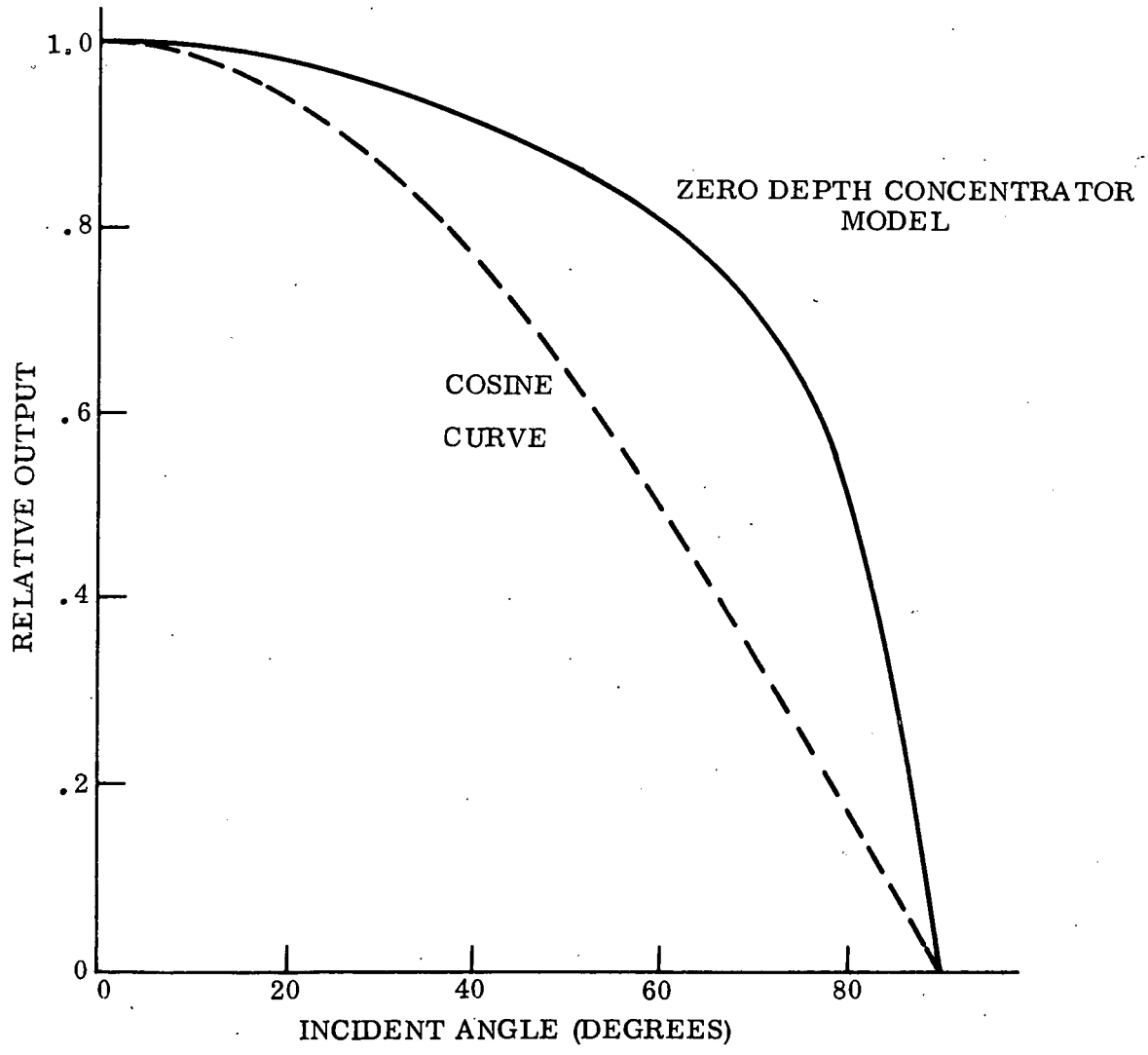

Figure A-41. Output Enhancement vs. Angle of Incidence

Table A-9. Source Listing for Optical Analysis Program

```
      COMMON/M/IPR,INTF,IBD,W(55,45),GL,IZ,NCOAT,IBRANCH,PACK          00000010
      COMMON/REFL/TRANS(45),COLL(55,45)                                00000020
      DIMENSION COLLT(45)                                              00000030
    5 CONTINUE                                                         00000031
      TOTW=0                                                           00000032
      DO 7 I=1,45                                                      00000033
      COLLT(I)=0                                                       00000034
      DO 6 K=1,55                                                      00000035
      COLL(K,I)=0                                                      00000036
    6 CONTINUE                                                         00000037
    7 CONTINUE                                                         00000038
      CALL DATAIN                                                      00000050
      CALL MAIN                                                        00000060
      DO 20 I=1,45                                                     00000070
      DO 10 J=1,55                                                     00000071
      COLLT(I)=COLLT(I)+COLL(J,I)                                      00000072
   10 CONTINUE                                                         00000074
      TOTW=TOTW+COLLT(I)                                               00000076
   20  CONTINUE                                                        00000078
      DO 30 M=18,90,18                                                 00000080
      L=M-16                                                           00000081
      MM=M/2; LL=MM-8                                                  00000082
      WRITE(6,90)(K-2,K,K=L,M,2)                                       00000083
      WRITE(6,91)(COLLT(I),I=LL,MM)                                    00000084
   30 CONTINUE                                                         00000086
      WRITE(6,92)TOTW                                                  00000088
   90 FORMAT(/,10(2X,I2,"-",I2,1X))                                    00000090
   91 FORMAT(9F8.2)                                                    00000091
   92 FORMAT("TOTAL ENERGY COLLECTED=",F9.2)                           00000092
C                                                                      00000093
      PRINT    "MAKING MORE RUNS? 1=YES, 0=NO"                        00000110
      READ,IAGAIN                                                      00000111
      IF(IAGAIN  EQ. 1)GO TO 5                                         00000112
      STOP                                                             00000113
      END                                                              00000114
C                                                                      00000130
      SUBROUTINE MAIN                                                  00000140
      COMMON/M/IPR,INTF,IBD,W(55,45),GL,IZ,NCOAT,IBRANCH,PACK          00000150
C                                                                      00000160
      IBRANCH=1                                                        00000170
      INTF=1                                                           00000180
      IBD=1                                                            00000190
      IPR=1                                                            00000200
      IZ=0                                                             00000210
      CALL ONEPASS                                                     00000220
   10 CONTINUE                                                         00000230
      IF(IBRANCH  NE. 1)GO TO 40                                       00000240
      IBD=1                                                            00000250
      INTF=2                                                           00000260
      CALL TWOPASS                                                     00000270
   20 CONTINUE                                                         00000280
      IF(IBRANCH .NE. 1)GO TO 30                                       00000290
      IBD=2                                                            00000300
      INTF=2                                                           00000310
      CALL TWOPASS                                                     00000320
      IBD=3                                                            00000330
      CALL TWOPASS                                                     00000340
      IBRANCH=0                                                        00000350
      GO TO 20                                                         00000360
```

Table A-9. Source Listing for Optical Analysis Program (Cont'd)

```
C                                                                    00000370
C                                                                    00000380
   30 CONTINUE                                                       00000390
      IPR=12                                                         00000400
      IZ=9                                                           00000410
      IBD=4                                                          00000420
      INTF=3                                                         00000430
      CALL TWOPASS                                                   00000440
      IZ=0                                                           00000450
      IBD=5                                                          00000460
      INTF=2                                                         00000470
      CALL TWOPASS                                                   00000480
      IBRANCH=0                                                      00000490
      GO TO 10                                                       00000500
C                                                                    00000510
   40 CONTINUE                                                       00000520
      IPR=5                                                          00000530
      IZ=25                                                          00000540
      IBRANCH=1                                                      00000550
      IBD=6                                                          00000560
      INTF=3                                                         00000570
      CALL TWOPASS                                                   00000580
      IZ=0                                                           00000590
   50 CONTINUE                                                       00000600
       F(IBRANCH  NE. 1)GO TO 60                                     00000610
      IBD=7                                                          00000620
      INTF=2                                                         00000630
      CALL TWOPASS                                                   00000640
      IBD=8                                                          00000650
      INTF=2                                                         00000660
      CALL TWOPASS                                                   00000670
      IBRANCH=0                                                      00000675
      GO TO 50                                                       00000680
C                                                                    00000690
   60 CONTINUE                                                       00000700
      IPR=37                                                         00000710
      IZ=9                                                           00000720
      IBD=9                                                          00000730
      INTF=3                                                         00000740
      CALL TWOPASS                                                   00000750
      IZ=0                                                           00000760
      IBD=10                                                         00000770
      INTF=2                                                         00000780
      CALL TWOPASS                                                   00000790
      RETURN                                                         00000800
      END                                                            00000810
C                                                                    00000820
C                                                                    00000830
C                                                                    00000840
      SUBROUTINE ONEPASS                                             00000850
      CALL REFLCOL                                                   00000860
      CALL REFRACT                                                   00000870
      CALL SCATTER                                                   00000880
      CALL ABSORB                                                    00000890
      RETURN                                                         00000900
      END                                                            00000910
C                                                                    00000920
C                                                                    00000930
C                                                                    00000940
      SUBROUTINE TWOPASS                                             00000950
      COMMON/M/IPR,INTF,IBD,W(55,45),GL,IZ,NCOAT,IBRANCH,PACK        00000960
```

Table A-9. Source Listing for Optical Analysis Program (Cont'd)

```
C                                                                       00000970
      CALL DIVIDE                                                       00000980
      CALL REFLCOL                                                      00000990
      GO TO (10,10,20,10,20,10,10,20,10,20),IBD                         00001000
   10 CONTINUE                                                          00001010
      CALL SCATTER                                                      00001020
      CALL ABSORB                                                       00001030
      INTF=4                                                            00001040
      CALL REFLCOL                                                      00001050
      CALL SCATTER                                                      00001060
      CALL ABSORB                                                       00001070
   20 CONTINUE                                                          00001080
      RETURN                                                            00001090
      END                                                               00001100
C                                                                       00001110
C                                                                       00001120
C                                                                       00001130
      SUBROUTINE REFLCOL                                                00001140
      COMMON/REFR/RF(5),REFF                                            00001150
      COMMON/REFL/TRANS(45),COLL(55,45)                                 00001160
      COMMON/M/IPR,INTF,IBD,W(55,45),GL,IZ,NCOAT,IBRANCH,PACK           00001170
      DIMENSION E(45),G(45)                                             00001180
C                                                                       00001190
      DTR=.0174533                                                      00001200
      GO TO (10,20,20,10),INTF                                          00001210
   10 CONTINUE                                                          00001220
      IF(NCOAT .EQ. 0)GO TO 20                                          00001230
      DO 11 I=1,45                                                      00001240
      G(I)=W(IPR,I)                                                     00001250
      E(I)=G(I)*TRANS(I)                                                00001260
   11 CONTINUE                                                          00001270
      IF(INTF .NE. 4)GO TO 60                                           00001280
      DO 12 I=1,45                                                      00001290
      E(I)=G(I)-E(I)                                                    00001300
   12 CONTINUE                                                          00001310
      GO TO 60                                                          00001320
C                                                                       00001330
   20 CONTINUE                                                          00001340
      DO 22 I=1,45                                                      00001344
   22 G(I)=W(IPR,I)                                                     00001345
      GO TO (24,25,26,27),INTF                                          00001350
   24 RFRN=RF(1)                                                        00001360
      RFRM=RF(2+NCOAT)                                                  00001370
      GO TO 28                                                          00001380
   25 RFRN=RF(2+NCOAT)                                                  00001390
      RFRM=RF(3+NCOAT)                                                  00001400
      GO TO 28                                                          00001410
   26 RFRN=RF(2+NCOAT)                                                  00001420
      RFRM=RF(4+NCOAT)                                                  00001430
      GO TO 28                                                          00001440
   27 RFRN=RF(2+NCOAT)                                                  00001450
      RFRM=RF(1)                                                        00001460
   28 CONTINUE                                                          00001470
C                                                                       00001480
      DO 50 N=1,45                                                      00001490
      I=N+N-1                                                           00001500
      R=1-((RFRN/RFRM)*SIN(I*DTR))**2                                   00001510
      IF(R .GT. 0)GO TO 30                                              00001520
      TR=0                                                              00001530
      GO TO 40                                                          00001540
   30 CONTINUE                                                          00001550
```

Table A-9. Source Listing for Optical Analysis Program (Cont'd)

```
      RP=(COS(I*DTR)-(RFRN/RFRM)*SQRT(R))/(COS(I*DTR)+                  00001560
     & (RFRN/RFRM)*SQRT(R))                                             00001570
      RS=(COS(I*DTR)*RFRN/RFRM-SQRT(R))/(COS(I*DTR)*RFRN/RFRM+          00001580
     & SQRT(R))                                                         00001590
      TR=1-(RP**2+RS**2)/2                                              00001600
      IF(TR .LE. 0)TR=0                                                 00001605
   40 CONTINUE                                                          00001610
      IF(INTF .EQ. 1)GO TO 45                                           00001620
      GO TO (41,41,41,42,41,42,41,41,42,41),IBD                         00001624
   41 TR=1-TR                                                           00001630
      GO TO 45                                                          00001632
   42 TR=1-TR+REFF*TR**2                                                00001634
   45 E(N)=G(N)*TR                                                      00001640
   50 CONTINUE                                                          00001650
   60 CONTINUE                                                          00001660
C                                                                       00001670
      IPR=IPR+1                                                         00001680
      DO 70 I=1,45                                                      00001690
      W(IPR,I)=E(I)                                                     00001700
   70 CONTINUE                                                          00001710
C                                                                       00001720
      IF(INTF .EQ. 1)GO TO 85                                           00001725
      GO TO (80,80,80,85,80,85,80,80,85,80),IBD                         00001730
   80 CONTINUE                                                          00001740
      DO 82 I=1,45                                                      00001750
      ANGI=(I+I-1)*.0174533                                             00001755
      COLL(IPR,I)=(W(IPR-1,I)-W(IPR,I))*COS(ANGI)                       00001760
   82 CONTINUE                                                          00001770
   85 RETURN                                                            00001780
      END                                                               00001790
C                                                                       00001800
C                                                                       00001810
C                                                                       00001820
      SUBROUTINE SCATTER                                                00001830
      COMMON/S/ SCAT(45,45,4)                                           00001840
      COMMON/M/IPR,INTF,IBD,W(55,45),GL,IZ,NCOAT,IBRANCH,PACK           00001850
      DIMENSION E(45),G(45)                                             00001860
      DO 10 I=1,45                                                      00001870
      G(I)=W(IPR,I)                                                     00001880
      E(I)=0                                                            00001885
   10 CONTINUE                                                          00001890
C                                                                       00001900
      DO 30 I=1,45                                                      00001910
      DO 20 J=1,45                                                      00001920
      E(J)=E(J)+G(I)*SCAT(I,J,INTF)                                     00001930
   20 CONTINUE                                                          00001940
   30 CONTINUE                                                          00001950
      IPR=IPR+1                                                         00001960
      DO 40 I=1,45                                                      00001970
      W(IPR,I)=G(I)+E(I)                                                00001980
   40 CONTINUE                                                          00001990
      RETURN                                                            00002000
      END                                                               00002010
C                                                                       00002020
C                                                                       00002030
C                                                                       00002040
      SUBROUTINE ABSORB                                                 00002050
      COMMON/ABS/ABSF                                                   00002060
      COMMON/M/IPR,INTF,IBD,W(55,45),GL,IZ,NCOAT,IBRANCH,PACK           00002070
      DIMENSION E(45)                                                   00002080
      DO 10 N=1,45                                                      00002090
```

Table A-9. Source Listing for Optical Analysis Program (Cont'd)

```
      E(N)=W(IPR,N)                                                    00002100
      I=N+N-1                                                          00002110
      S=GL/COS(I*.0174533)                                             00002120
      E(N)=EXP(-S*ABSF)*E(N)                                           00002130
   10 CONTINUE                                                         00002140
      IPR=IPR+1                                                        00002150
      DO 20 I=1,45                                                     00002160
   20 W(IPR,I)=E(I)                                                    00002170
      RETURN                                                           00002180
      END                                                              00002190
C                                                                      00002200
C                                                                      00002210
C                                                                      00002220
      SUBROUTINE REFRACT                                               00002230
      COMMON/REFR/RF(5),REFF                                           00002240
      COMMON/M/IPR,INTF,IBD,W(55,45),GL,IZ,NCOAT,IBRANCH,PACK          00002250
      DIMENSION G(45),E(45)                                            00002260
C                                                                      00002270
      IF(INTF .NE. 1) GO TO 40                                         00002280
      J=1                                                              00002290
      DO 5 I=1,45                                                      00002292
      E(I)=0                                                           00002294
    5 G(I)=W(IPR,I)                                                    00002296
      DTR=.0174533                                                     00002300
      RFRN=RF(1)                                                       00002310
      RFRM=RF(2+NCOAT)                                                 00002320
      DO 20 N=1,45                                                     00002330
      I=N+N-1                                                          00002350
      A=ARSIN(SIN((I-1)*DTR)*RFRN/RFRM)/DTR                            00002360
      C=ARSIN(SIN((I+1)*DTR)*RFRN/RFRM)/DTR                            00002370
   11 CONTINUE                                                         00002380
      IF(A .LT. J+1.)GO TO 12                                          00002390
      J=J+2                                                            00002400
      GO TO 11                                                         00002410
   12 CONTINUE                                                         00002420
      IF(C .GT. J-1.)GO TO 13                                          00002430
      J=J-2                                                            00002440
      GO TO 11                                                         00002450
   13 CONTINUE                                                         00002460
      K=(J+1)/2                                                        00002470
      IF(C .LT. J+1.)GO TO 14                                          00002480
      E(K+1)=E(K+1)+(C-J-1)*G(N)/(C-A)                                 00002490
      E(K)=E(K)+(J+1-A)*G(N)/(C-A)                                     00002500
      GO TO 20                                                         00002510
   14 CONTINUE                                                         00002520
      IF(A .GT. J-1.)GO TO 15                                          00002530
      E(K)=E(K)+(C-J+1)*G(N)/(C-A)                                     00002540
      E(K-1)=E(K-1)+(J-1-A)*G(N)/(C-A)                                 00002550
      GO TO 20                                                         00002560
   15 E(K)=E(K)+G(N)                                                   00002570
   20 CONTINUE                                                         00002580
C                                                                      00002590
      IPR=IPR+1                                                        00002600
      DO 30 K=1,45                                                     00002610
      W(IPR,K)=E(K)                                                    00002620
   30 CONTINUE                                                         00002630
   40 RETURN                                                           00002640
      END                                                              00002650
C                                                                      00002660
C                                                                      00002670
C                                                                      00002680
```

Table A-9. Source Listing for Optical Analysis Program (Cont'd)

```
      SUBROUTINE DIVIDE                                                 00002690
      COMMON/REFR/RF(5),REFF                                            00002705
      COMMON/M/IPR,INTF,IBD,W(55,45),GL,IZ,NCOAT,IBRANCH,PACK           00002710
      DIMENSION E(45),G(45),H(45)                                       00002720
C                                                                       00002730
      DO 10 I=1,45                                                      00002740
      G(I)=W(IPR,I)                                                     00002750
      IANG=I                                                            00002755
      E(I)=G(I)*CELLBDF(IBD,IANG,GL,NCOAT,PACK,RF)                      00002760
      H(I)=G(I)-E(I)                                                    00002770
   10 CONTINUE                                                          00002780
      IPR=IPR+1+IZ                                                      00002790
      IF(IBRANCH .EQ. 1)GO TO 30                                        00002800
      DO 20 I=1,45                                                      00002810
      W(IPR,I)=H(I)                                                     00002820
   20 CONTINUE                                                          00002830
      GO TO 50                                                          00002840
   30 DO 40 I=1,45                                                      00002850
      W(IPR,I)=E(I)                                                     00002860
   40 CONTINUE                                                          00002870
   50 RETURN                                                            00002880
      END                                                               00002890
C                                                                       00002900
C                                                                       00002910
C                                                                       00002920
      SUBROUTINE DATAIN                                                 00002930
      COMMON/REFL/TRANS(45),COLL(55,45)                                 00002940
      COMMON/ABS/ABSF                                                   00002950
      COMMON/REFR/RF(5),REFF                                            00002960
      COMMON/M/IPR,INTF,IBD,W(55,45),GL,IZ,NCOAT,IBRANCH,PACK           00002980
      COMMON/S/SCAT(45,45,4)                                            00002990
      DIMENSION FSCAT(5),SOLAR(45)                                      00003000
      DATA FSCAT/.155,.17,.095,.045,.005/                               00003010
C                                                                       00003020
C   INSOLATION FOR PHOENIX 1953                                         00003030
      DATA SOLAR/16.7,20.1,19.3,19.3,20.5,26.2,43.1,130.2,90.9,         00003040
     & 101.1,54.1,29.4,27.4,30.,144.8,173.,101.9,68.,35.,21.6,          00003050
     & 24.2,106.2,176.7,24.6,21.4,17.9,20.1,26.5,38.1,103.9,19.3,       00003060
     & 11.4,9.1,11.7,4.5,12.5,33.3,12.1,2.5,.8,.4,.0,1.7,1.7,.5/        00003070
C                                                                       00003080
C    SCATTERING FUNCTION LOADING                                        00003090
C                                                                       00003100
      DO 10 I=1,45                                                      00003110
      SCAT(I,I,1)=0.                                                    00003120
      SCAT(I,I,2)=-.94                                                  00003130
      SCAT(I,I,3)=-.94                                                  00003140
      SCAT(I,I,4)=-.08                                                  00003150
   10 CONTINUE                                                          00003160
      DO 20 I=1,44                                                      00003170
      SCAT(I+1,I,4)=.04                                                 00003180
      SCAT(I,I+1,4)=.04                                                 00003190
   20 CONTINUE                                                          00003200
      DO 40 J=1,5                                                       00003210
      K=45-J                                                            00003220
      FK=FSCAT(J)                                                       00003230
      DO 30 I=1,K                                                       00003240
      FK1=FK                                                            00003244
      IF(I .LE. 5 .AND. I+J .GE. 2*I)FK1=2*FK                           00003245
      SCAT(I+J,I,2)=FK                                                  00003250
      SCAT(I,I+J,2)=FK1                                                 00003260
      SCAT(I+J,I,3)=FK                                                  00003270
```

Table A-9. Source Listing for Optical Analysis Program (Cont'd)

```
      SCAT(I,I+J,3)=FK1                                                  00003280
   30 CONTINUE                                                           00003290
   40 CONTINUE                                                           00003300
C                                                                        00003310
C    INSOLATION DATA LOADING                                             00003320
      DO 45 J=1,45                                                       00003330
      ANGI=(J+J-1)*.017453                                               00003335
   45 W(1,J)=SOLAR(J)/COS(ANGI)                                          00003340
C                                                                        00003350
      PRINT    "NO. OF COATING LAYER, 1 OR 0"                            00003360
      READ,NCOAT                                                         00003370
      IF(NCOAT .EQ. 0)GO TO 60                                           00003380
C                                                                        00003390
      PRINT    "COATING INDEX OF REFRACTION"                             00003400
      READ,RF(2)                                                         00003410
      PRINT    "COATING THICKNESS & WAVELENGTH (MUST HAVE SAME UNITS)"   00003420
      READ,COATL,WAVEL                                                   00003450
   60 CONTINUE                                                           00003460
      RF(1)=1                                                            00003470
      PRINT    "INDEXES OF REFRACTION OF GLASS COVER, BONDING ADHESIVE & 0003480
     &ENCALSULANT"                                                       00003490
      READ,(RF(J+NCOAT),J=2,4)                                           00003510
      PRINT    "MODULE PACKING FACTOR (BETWEEN ,512 & ,814)"             00003520
      READ,PACK                                                          00003530
      PRINT    "GLASS THICKNESS(3.2, 4 OR 4.8MM), BULK ABSORP. COEFF.(1/MM)"3540
      READ,GL,ABSF                                                       00003560
      PRINT    "REFLECTANCE OF ENCALSULANT"                              00003562
      READ,REFF                                                          00003564
C                                                                        00003570
C  CALCULATION OF TRANSMISSIVITY FOR ONE LAYER COATING                   00003580
C                                                                        00003590
      IF(NCOAT .EQ. 0)GO TO 80                                           00003600
      DTR=.017453                                                        00003610
      DO 70 N=1,45                                                       00003620
      I=N+N-1                                                            00003630
C                                                                        00003640
C                                                                        00003650
C  INCIDENCE ANGLES IN MEDIA FROM SNELL'S LAW                            00003660
C                                                                        00003670
      ANG1=I*DTR                                                         00003680
      ANG2=ARSIN((RF(1)/RF(2))*SIN(ANG1))                                00003690
      ANG3=ARSIN((RF(1)/RF(3))*SIN(ANG1))                                00003700
C                                                                        00003710
C                                                                        00003720
C  EFFECTIVE INDEXES FOR NON-NORMAL INCIDENCE                            00003730
C                                                                        00003740
      RF1S=RF(1)*COS(ANG1)                                               00003750
      RF2S=RF(2)*COS(ANG2)                                               00003760
      RF3S=RF(3)*COS(ANG3)                                               00003770
      RF1P=RF(1)/COS(ANG1)                                               00003780
      RF2P=RF(2)/COS(ANG2)                                               00003790
      RF3P=RF(3)/COS(ANG3)                                               00003800
C                                                                        00003810
C  PHASE ANGLE BETWEEN AMPLITUDE VECTORS                                 00003820
      PHS=(4*3.1416*COATL/WAVEL)*RF2S                                    00003830
C                                                                        00003840
C  AMPLITUDE REFLECTANCE S & P COMPONENTS                                00003850
      R1S=(RF2S-RF1S)/(RF2S+RF1S)                                        00003860
      R2S=(RF3S-RF2S)/(RF3S+RF2S)                                        00003870
      R1P=(RF2P-RF1P)/(RF2P+RF1P)                                        00003880
      R2P=(RF3P-RF2P)/(RF3P+RF2P)                                        00003890
```

Table A-9. Source Listing for Optical Analysis Program (Cont'd)

```
C                                                                       00003900
C  INTENSITY REFLECTIVITIES                                             00003910
      RS=R1S**2+R2S**2+2*R1S*R2S*COS(PHS)                               00003920
      RP=R1P**2+R2P**2+2*R1P*R2P*COS(PHS)                               00003930
C                                                                       00003940
C  AVERAGE FOR POLORIZED LIGHT                                          00003950
      R=(RS+RP)/2.                                                      00003960
      TRANS(N)=1-R                                                      00003970
   70 CONTINUE                                                          00003980
   80 CONTINUE                                                          00003990
      RETURN                                                            00004200
      END                                                               00004210
      FUNCTION CELLBDF(IBD,I,GL,NCOAT,PACK,RF)                          00004250
      DIMENSION RSHIFT2(10),RSHIFT1(10),FPACK(4),RF(5)                  00004260
      DIMENSION DD(10,4),DND(10,4),NDD(10,4),NDND(10,4),DDD(10,4),      00004270
     &DNDD(10,4),NDDD(10,4),NDNDD(10,4)                                 00004280
      REAL NDD,NDND,NDDD,NDNDD                                          00004283
C                                                                       00004285
      DATA RSHIFT1/0.,.01,.02,.03,.04,.05,.06,.07,.08,.1/               00004290
      DATA RSHIFT2/.0,.02,.04,.06,.08,.1,.12,.16,.18,.2/                00004300
      DATA FPACK/.512,.658,.782,.814/                                   00004310
C                                                                       00004315
      DATA DD/1.,.994,.98,.965,.951,.936,.922,.907,.893,.868,           00004320
     &1.,.994,.98,.965,.951,.936,.922,.907,.893,.868,                   00004330
     &1.,.994,.98,.965,.951,.936,.922,.907,.893,.868,                   00004340
     &1.,.994,.98,.965,.951,.936,.922,.907,.893,.868/                   00004350
C                                                                       00004355
      DATA DDD/1.,.992,.965,.934,.895,.846,.8,.705,.66,.63,             00004360
     &1.,.992,.965,.934,.895,.846,.8,.705,.66,.63,                      00004370
     &1.,.992,.965,.934,.9,.873,.845,.79,.763,.736,                     00004380
     &1.,.992,.965,.934,.9,.873,.845,.79,.763,.736/                     00004390
C                                                                       00004395
      DATA DND/0.,.006,.021,.042,.061,.082,.1,.117,.134,.15,            00004400
     &0.,.008,.027,.048,.071,.094,.116,.139,.161,.183,                  00004410
     &.0,.008,.027,.048,.065,.081,.1,.117,.134,.15,                     00004420
     &.0,.006,.02,.036,.051,.064,.075,.09,.102,.115/                    00004430
C                                                                       00004435
      DATA DNDD/0.,0.,0.,0.,0.,0.,0.,0.,0.,0.,                          00004440
     &0.,0.,0.,0.,.001,.0054,.0156,.0156,.0156,.0156,                   00004450
     &0.,0.,.0012,.006,.0122,.02,.0296,.0296,.0296,.0296,               00004460
     &0.,.0014,.0048,.0096,.0158,.023,.032,.032,.032,.032/              00004470
C                                                                       00004475
      DATA NDD/0.,.008,.025,.046,.07,.096,.124,.124,.124,.124,          00004480
     &0.,.016,.044,.08,.12,.164,.208,.208,.208,.208,                    00004490
     &0.,.025,.076,.133,.19,.24,.29,.29,.29,.29,                        00004500
     &0.,.025,.076,.133,.19,.24,.29,.29,.29,.29/                        00004502
C                                                                       00004505
      DATA NDDD/0.,.012,.033,.057,.081,.105,.105,.105,.105,.105,        00004510
     &0.,.012,.042,.079,.116,.153,.153,.153,.153,.153,                  00004520
     &.0,.012,.06,.118,.172,.24,.24,.24,.24,.24,                        00004530
     &0.,.012,.06,.118,.172,.24,.24,.24,.24,.24/                        00004540
C                                                                       00004545
      DATA NDND/1.,.99,.967,.94,.912,.88,.855,.855,.855,.855,           00004550
     &1.,.986,.945,.892,.84,.798,.767,.767,.767,.767,                   00004560
     &1.,.962,.88,.79,.71,.64,.585,.585,.585,.585,                      00004570
     &1.,.97,.897,.81,.725,.656,.605,.605,.605,.605/                    00004580
C                                                                       00004585
      DATA NDNDD/0.,.01,.028,.051,.076,.101,.101,.101,.101,.101,        00004590
     &0.,.018,.051,.078,.098,.108,.108,.108,.108,.108,                  00004600
     &0.,.018,.051,.08,.094,.105,.105,.105,.105,.105,                   00004610
     &0.,.025,.058,.082,.095,.105,.105,.105,.105,.105/                  00004620
```

Table A-9. Source Listing for Optical Analysis Program (Cont'd)

```
C                                                                       00004625
      AI=(I+I-1)*.017453                                                00004630
      RFM=RF(2)                                                         00004640
      IF(NCOAT .EQ. 1)RFM=RF(3)                                         00004650
      ANGS=ARSIN(SIN(AI)/RFM)                                           00004660
      S=2*GL*TAN(ANGS)/5.9545/25.4                                      00004670
      GO TO (10,12,14,16,18,20,22,24,26,28),IBD                         00004680
   10 CELLBDF=PACK                                                      00004690
      GO TO 35                                                          00004700
   12 CELLBDF=TNT2(S,PACK,10,4,RSHIFT1,FPACK,DD,I1,I2,10)               00004710
      GO TO 35                                                          00004720
   14 S=S*2                                                             00004730
      CELLBDF=TNT2(2,PACK,10,4,RSHIFT2,FPACK,DDD,I3,I4,10)              00004740
      GO TO 35                                                          00004750
   16  CELLBDF=TNT2(S,PACK,10,4,RSHIFT1,FPACK,DND,I5,I6,10)             00004760
      GO TO 35                                                          00004770
   18  S=S*2                                                            00004780
      CELLBDF=TNT2(S,PACK,10,4,RSHIFT2,FPACK,DNDD,I7,I8,10)             00004790
      GO TO 35                                                          00004800
   20  CELLBDF=1-PACK                                                   00004810
      GO TO 35                                                          00004820
   22 CELLBDF=TNT2(S,PACK,10,4,RSHIFT1,FPACK,NDD,I9,I10,10)             00004830
      GO TO 35                                                          00004840
   24  S=S*2                                                            00004850
      CELLBDF=TNT2(S,PACK,10,4,RSHIFT2,FPACK,NDDD,J1,J2,10)             00004860
      GO TO 35                                                          00004870
   26  CELLBDF=TNT2(S,PACK,10,4,RSHIFT1,FPACK,NDND,J3,J4,10)            00004880
      GO TO 35                                                          00004890
   28  S=S*2                                                            00004900
      CELLBDF=TNT2(S,PACK,10,4,RSHIFT2,FPACK,NDNDD,J5,J6,10)            00004910
   35  CONTINUE                                                         00004920
      RETURN                                                            00004930
      END                                                               00004940
```


☆U.S. GOVERNMENT PRINTING OFFICE: 1979-640-092/ 1255